University of Pannonia

DOCTORAL (PhD) THESIS

BALÁZS REIDER

VESZPRÉM

2022.

University of Pannonia

Research Institute of Biomolecular and Chemical Engineering
Translational Glycomics Research Group

DEVELOPMENT OF AN *N*-GLYCAN PROFILE-BASED PROSTATE CANCER DIAGNOSTIC METHOD

DOCTORAL (PhD) THESIS

Balazs Reider

Supervisor:

Gabor Jarvas, PhD, research associate

Doctoral School of Chemical Engineering and Material Sciences

2022

Development of an *N*-glycan profile-based prostate cancer diagnostic method

Thesis for obtaining a PhD degree in the Doctoral School of Chemical Engineering and Material Sciences of the University of Pannonia

in the branch of Bio-, Environmental and Chemical Engineering Sciences

Written by Balazs Reider
Supervisor: Gabor Jarvas

propose acceptance (yes / no)

(supervisor)

As reviewer, I propose acceptance of the thesis:

Name of Reviewer: .... yes / no

(reviewer)

Name of Reviewer: .... yes / no

(reviewer)

The PhD-candidate has achieved .... % at the public discussion.

Veszprém, ...

(Chairman of the Committee)

The grade of the PhD Diploma .... (.............. %)

Veszprém, ...

(Chairman of UDHC)

Abstract

Development of an *N*-glycan profile-based prostate cancer diagnostic method

Prostate cancer represents the second highest frequent rate in men regarding all cancer diagnoses worldwide. The development and progression of prostate cancer is not completely understood yet at molecular level, but it is suggested that *N*-glycosylation changes occur during tumor genesis. In my PhD thesis I present the development, implementation and optimization processes of a high-throughput capillary electrophoresis based *N*-glycan analysis workflow for urinary prostate-specific antigen (PSA) analysis. The technology utilized a selective, high yield single domain antibody based PSA immunoprecipitation, followed by a novel, evaporative process based glycan labeling protocol in an open vial format during the tagging reaction to maximize the derivatization yields. The labeled *N*-glycan pool was analyzed by capillary electrophoresis coupled with laser-induced fluorescence detection, resulting in high resolution *N*-glycan profiles. Urinary PSA glycan profiles were compared to a commercially available PSA standard revealing differences in α2,3- and α2,6-sialylated isomers, proving the applicability of the suggested workflow. Sialylation classification plays important role in the differentiation between indolent, significant and aggressive forms of prostate cancer. Therefore, this technology can become a new base for a fast, non-invasive and sensitive diagnostic tool for the detection and classification of prostate cancer.

Kivonat

N-glikán profil alapú prosztatarák diagnosztikai módszer fejlesztése

A világ összes rákdiagnózisát tekintve a prosztatarák a második leggyakoribb daganatos megbetegedés a férfiaknál. A prosztatarák kialakulása és progressziója molekuláris szinten még nem teljesen tisztázott, de számos bizonyíték van rá, hogy a tumor genezise során *N*-glikozilációs változások következnek be. Doktori értekezésemben egy kapilláris elektroforézis alapú *N*-glikánanalízis munkafolyamat fejlesztését, megvalósítását és optimalizálási folyamatait mutatom be vizeletből izolált prosztata-specifikus antigén (PSA) vizsgálatára. A technológia alapja egy szelektív, nagy hozamú, egydoménes antitest alapú PSA immunprecipitáció, amelyet egy új, glikánjelölési protokoll követ, amely nyitott fiolákat használ, hogy a folyamatosan párolgó oldószer maximalizálja a hozamot a jelölési reakció során. A jelölt *N*-glikánok lézer indukált fluoreszcencia detektálással kapcsolt kapilláris elektroforézis vizsgálata nagy felbontású *N*-glikán profilokat eredményezett, amely képes volt az α2,3- és α2,6-szialilált izomerek elválasztására is, mely formák kulcsszerepet játszhatnak a prosztatarák indolens és agresszív formáinak megkülönböztetéseben. A vizeleti PSA glikánprofilja egybevágott a kereskedelmi forgalomban kapható PSA standard profiljával, bizonyítva, hogy a javasolt munkafolyamat képes nyomon követni a vizeleti PSA-ban mutatkozó változásokat. Ezért ez a technológia szilárd alapjává válhat egy gyors, nem invazív és érzékeny diagnosztikai eszköznek a prosztatarák kimutatására és klasszifikálására.

Auszug

Entwicklung eines auf *N*-Glykanprofilen basierenden Diagnoseverfahrens für Prostatakrebs

Prostatakrebs ist bei Männern die zweithäufigste Krebsdiagnose weltweit. Die Entwicklung und das Fortschreiten von Prostatakrebs ist auf molekularer Ebene noch nicht vollständig geklärt, aber es wird vermutet, dass während der Tumorentstehung Veränderungen der *N*-Glykosylierung auftreten. In meiner Doktorarbeit präsentiere ich die Entwicklung, Implementierung und Optimierung eines auf Kapillarelektrophorese basierenden Hochdurchsatz-Workflows zur Analyse von *N*-Glykanen im Urin für prostataspezifisches Antigen (PSA). Die Technologie nutzte eine selektive, hoch ergiebige PSA-Immunpräzipitation auf der Basis von Single-Domain-Antikörpern, gefolgt von einem neuartigen, auf einem Verdampfungsprozess basierenden Glykan-Markierungsprotokoll in einem offenen Vial Format während der Markierungsreaktion, um die Derivatisierungsausbeute zu maximieren. Der markierte *N*-Glykan-Pool wurde durch Kapillarelektrophorese in Verbindung mit laserinduzierter Fluoreszenzdetektion analysiert, was zu hochauflösenden *N*-Glykanprofilen führte. Die PSA-Glykanprofile im Urin wurden mit einem handelsüblichen PSA-Standard verglichen, wobei Unterschiede bei den α2,3- und α2,6-sialylierten Isomeren festgestellt wurden, was die Anwendbarkeit des vorgeschlagenen Arbeitsablaufs beweist. Die Klassifizierung der Sialylierung spielt eine wichtige Rolle bei der Unterscheidung zwischen indolenten, signifikanten und aggressiven Formen von Prostatakrebs. Daher kann diese Technologie eine neue Grundlage für ein schnelles, nicht-invasives und empfindliches Diagnoseinstrument für die Erkennung und Klassifizierung von Prostatakrebs werden.

Contents

1 List of Abbreviations

2-AB	2-aminobenzamide
A	*N*-Acetyl-D-glucosamine
ABRF	Association of Biomolecular Resource Facilities
aPSA	anti-Prostate specific antigen
ANTS	8-aminonaphthalene-1,3,6-trisulfonic
APTS	8-aminopyrene-1,3,6-trisulphonic acid
BPH	Benign prostate hyperplasia
CE	Capillary electrophoresis
CGE	Capillary gel electrophoresis
ChIP	Chromatin immunoprecipitation
CoIP	Co-immunoprecipitation
Con A	Concanavalin A
CTOS	Cancer tissue-originated spheroids
DP2	Maltose
DP15	Maltopentadecaose
DTT	Dithiothreitol
EDTA	Ethylenediaminetetraacetic acid
ELISA	Standard enzyme-linked immunosorbent assay
EPS	Expressed prostatic secretions
ESI	Electrospray ionization
F	L-Fucose
G	D-Galactose
GS	Gleason score
GU	Glucose unit
HEPES	4-(2-hydroxyethyl)-1-piperazineethanesulfonic acid
hIgG	Human immunoglobulin G
HILIC	Hydrophilic interaction liquid chromatography
HPLC	High performance liquid chromatography
HV	Healthy volunteers
IMAC	Immobilized metal affinity chromatography
IMS	Imaging MS
IP	Immunoprecipitation
LIF	Laser-induced fluorescent detection
LoD	Limit of detection
M	D-Mannose
mAb	Monoclonal antibody
MALDI	Matrix-assisted laser desorption/ionization
MeCN	Acetonitrile
MRM	Multiple reaction monitoring
NAG	*N*-Acetyl-D-galactosamine
PA	Pyridylamin
PCa	Prostate cancer
PDAM	1-pyrenyldiazomethane
pI	Isoelectric point
PAGE	polyacrylamide gel electrophoresis
PEG	Polyethylene glycol
PSA	Prostate specific antigen
QIT	Quadrupole ion trap
RP	Reversed-phase
S	Sialic acid
sdAb	Single-domain antibody
SDS	Sodium dodecyl sulfate
SPE	Solid phase extraction
SRM	Selective reaction monitoring
THF	Tetrahydrofuran
TMT	Tandem-mass-tag

2   Introduction and objective

Cancer is one of the worst, still undefeated disease of our time. All around the world, huge efforts and resources are being invested to control this illness, and yet, only minor victories have been won. However, there is reason to be optimistic, as it can be seen that this field of science has developed very rapidly over the last 20-30 years. As our knowledge of the disease expanded, it became visible that, alongside increasing the effectiveness of treatments, early diagnosis can offer the best prospects for the survival of the patients. This effort raised a huge demand for biomarkers, which can predict cancer in early stage or help to distinguish malignant and indolent tumors. Such alterations were detected in certain glycoproteins due to various cancer types, which made glycosylation a widely researched area for novel biomarker candidates [1].

The Translational Glycomics Research Group at University of Pannonia also actively took part in several research aiming to observe cancer related changes in different glycoproteins. As a part of the group, I got involved in an analytical method development in prostate cancer (PCa) glycobiomarkers. In my doctoral dissertation, a novel workflow for the analysis of the glycosylation of urinary prostate specific antigen (PSA) is presented. PSA is a commonly used PCa biomarker for years, and the alterations in its glycosylation were also associated with the disease. Our research team had many years of experience in the instrumental analysis of glycans and glycoproteins, which greatly contributed to the process design. In my thesis work, I introduce the development of an analytical workflow for *an N*-glycan profile-based prostate cancer diagnostic tool, which could be a solid base for future use. My first aim was to optimize the reaction conditions for the fluorophore labeling of released glycans for the analysis by capillary electrophoresis coupled with laser-induced fluorescent detection (CE-LIF). My main principle was to lower the overnight incubation time without significant decrease (or preferably increase) in derivatization yields. Equally importantly, the preservation of sensitive sugar structures was also crucial as they can present essential therapeutic information. To facilitate that, a novel, open vial based approach was utilized in which the continuously evaporating solvent helps to reach the optimal reaction conditions for most glycan structures in the mixture. The second objective was to determine the glycan structures of standard PSA linked carbohydrates by exoglycosidase mediated sequencing and comparison to GU databases. As direct PSA analysis from urine or semen was not feasible. The third goal was the development of a selective PSA capture method from

biological matrices. High selectivity separation was necessary due to interfering glycoproteins from the matrix, but facilitation of the future implementation as a diagnostic tool was also considered. To accomplish that, a novel nanobody based PSA immunoprecipitation (IP) approach was implemented, which was appropriately selective, but did not increase costs drastically. The final objective was to merge all pieces into a single workflow for the *N*-glycan analysis of urinary PSA.

3 Theoretical background

According to the WHO report, PCa was the most commonly diagnosed cancer in men in Hungary in 2020 [2]. 6 234 cases were registered, accounting for 18.5% of all new cases. Globally, it was ranked second with 1 414 259 cases, representing 14.1% of all cases, only 0.2% behind lung cancer, which accounted for the highest proportion. PCa is a highly heterogeneous disease, which can be indolent or very aggressive, often metastasizing to bone and other organs, with a significant increase in morbidity and mortality [3]. One of the major clinical challenges is that current diagnostic tests, including prostate-specific antigen (PSA) screening and histological grading, are unable to distinguish between aggressive and indolent tumors [4]. Serum PSA levels have been used as a biomarker for PCa for more than 25 years and PSA screening has revolutionized the clinical management of the disease [5], but this period has also highlighted the limitations of the test, mainly due to lack of specificity, which often leads to overdiagnosis and overtreatment. In light of this, intensive efforts are now underway to find alternative PCa biomarkers, particularly those that can predict disease aggressiveness and better support treatment decisions [6].

3.1 Prostate specific antigen

PSA, also known as human kallikrein 3 (KLK3 or hK3), is an organ-specific glycoprotein, exclusively produced as a proenzyme by the prostate epithelial cells. It is an androgen-regulated serine protease, coded on chromosome 19q13.4 [7] and a member of the tissue kallikrein family [8] among hK2 and hK4 [7]. The precursor PSA is secreted into the lumen of the prostate gland and activated by proteolytic release of 7 amino acids at a monobasic site resulting PSA [9]. In the semen, PSA exists predominantly in free form [10] and plays an important role in its liquefaction after ejaculation by cleaving semenogelin and fibronectin, the proteins forming the seminal clot [9]. A fraction of this active PSA can diffuse into the circulation, where its either bound by protease inhibitors such as α1-antichymotrypsin and α2-macroglobulin or circulates as free PSA if unbound. In PCa, loss of basal cells and the fragmentation of basement membrane result in a relative increase of unbound and precursor PSA in the serum [11]. Semen, blood, and urine are the most common biological sources of PSA. Standard, commercially available PSA is obtained from human semen, as it contains PSA in the highest concentration (approximately 1.3 mg/ml) [12], but semen usage in clinical analysis is very limited.

Blood is much easier to collect (even though it is an invasive procedure), therefore it is frequently applied as a viable sample source. Unfortunately, the PSA concentration in blood is usually very low (<10 ng/ml), which can make extensive qualitative analysis problematic. Urine contains PSA in a higher dose (~100 ng/ml [13]), but its concentration can change on a very large scale. Urine has another upside, compared to blood and semen, that its matrix possesses a lower overall protein content, which otherwise could interfere with certain analysis.

3.2 Prostate cancer biomarkers

According to the National Cancer Institute (NCI) definition, a "biomarker" is a biological molecule found in blood, other body fluids or tissues that can be objectively measured and evaluated as an indicator of a normal/abnormal biological process and a pathogenic condition/disease. A biomarker can be used for screening purposes, disease diagnosis and prognosis, assessment of disease susceptibility and prediction or monitoring of responses to various therapeutic interventions [14]. The ideal diagnostic biomarker has high specificity (test can correctly identify those without disease; true negative rate), high sensitivity (test can correctly identify those with disease; true positive rate), simplicity, ease of use, reproducibility, clear readability for clinicians, cost-effectiveness and quantifiable metrics that can be easily obtained from biological fluid or specimens [6]. PSA is the most widely used prostate cancer biomarker. However, more recent studies have shown that the test result not always reliable, especially at PSA levels of 4-10 ng/ml are considered a 'grey zone' because this is where the test result is most uncertain as to whether or not further biopsy is needed. The reason is, although PSA is organ-specific, it is not cancer-specific, and serum PSA levels are often elevated in conditions that disrupt the basal epithelial cells of the prostate, such as prostatitis, benign prostate hyperplasia (BPH), prostate biopsy and surgery [4]. Due to these shortcomings, extensive PSA screening has led to overdiagnosis and overtreatment of low-risk prostate cancer, and created the need for more precise biomarkers.

PSA velocity (PSAV) [15], PSA density (PSAD) [16], free PSA score (% fPSA) [17], benign PSA score (BPSA) [18], [-2] proPSA score (p2PSA) [19], prostate health index (*phi*) [20] or 4KScore [21] are statistical or mathematical models based on the serum level of PSA or any other PSA related subform with the aims to improve PSA screening for more accurate and earlier PCa diagnosis. Other, urine-based test like Progensa [22],

Prostate cancer angiten 3 gen (PCA3), TMPRS22:ERG score [23], Mi prostate score (MiPS) [24], SelectMDx [25], ExoDx prostate intelliscore (EPI) [26] and Prostarix [27] are screening the expression of certain gene sequences related to PCa. These tests usually used to define PCa aggressiveness or the necessity of biopsy or proctectomy. Tissue-based test like ConfirmMDx [28], OncotypeDX genomic prostate score (GPS) [29], ProMark [30], Polaris or Decipher [31] were developed to improve the evaluation of tissue samples from biopsies or help monitoring the progress of prostate cancer in patients undergoing medical treatment.

Glycan-based biomarkers also showed a lot of potential in PCa diagnosis. Alterations in protein glycosylation are a universal feature of cancer cells, and cancer-associated glycans have been detected in almost every cancer types [32,33]. The altered glycosylation state of cancer cells can be monitored from sugars and proteins secreted by cancer cells, which may hold enormous biomarker potential for early diagnosis or to aid in a more accurate prognosis. Several glycosylation changes in PSA and other proteins have also been observed due to prostate cancer. Among these, the most abundantly reported alterations were the increase of $\alpha2,3$ sialylation at the expense of $\alpha2,6$ form, appearance of tetra-antennary tetra-sialylated, tri-antennary, tri-galactosylated, tri-galactosylated and tri-sialylated, tri-sialylated with and without fucose residues, sialylated glycoforms containing GalNAc moieties, core or antennary fucosylation and LacdiNAc pattern. These changes have been summarized in several publications, like in a recent, very thorough and extensive study by Anna Kałuża and her colleagues [34] or focusing on specific proteins by dos Santos Silva et al. [35]. The various analytical procedures applied for monitoring changes in PSA glycosylation were also summarized in my work [36]. These glycan-related alterations could help to distinguish high-risk PCa from indolent disease, which is key information for helping the doctors to find the most successful treatment and avoid the unnecessary invasive procedures.

3.3   Separation based characterization methods for PSA *N*-glycosylation

The three main analytical strategies currently used in instrumental analysis of protein *N*-glycosylation are as follows: 1) top-down at the intact glycoprotein level, 2) bottom-up at the glycopeptide level, and the 3) released glycan approach (Figure 1). Modern analytical instrumentation offers a wide variety of techniques and equipment to fulfill these tasks. In the past decades, mass spectroscopy, liquid chromatography, CE, nuclear magnetic

resonance spectroscopy or their combinations were applied for glycan biomarker research, excellently summarized by Rudd and coworkers [37]. In their paper special attention is paid to separation based techniques applied for PSA *N*-glycosylation analysis. Additionally, released glycan approaches are often combined with exoglycosidase sequencing, e.g. it was utilized in an automated fashion [38]. Shortly, the released *N*-glycans were consequently digested by monomer and anomericity specific exoglycosidase enzymes such as Sialidase A, β-Galactosidase and β-*N*-Acetyl Hexosaminidase. Native, i.e., undigested and all digested pools can be analyzed separately and the structural information was derived from the changes of the analytical signal of the individual structures as the result of the consecutive exoglycosidase treatments [39].
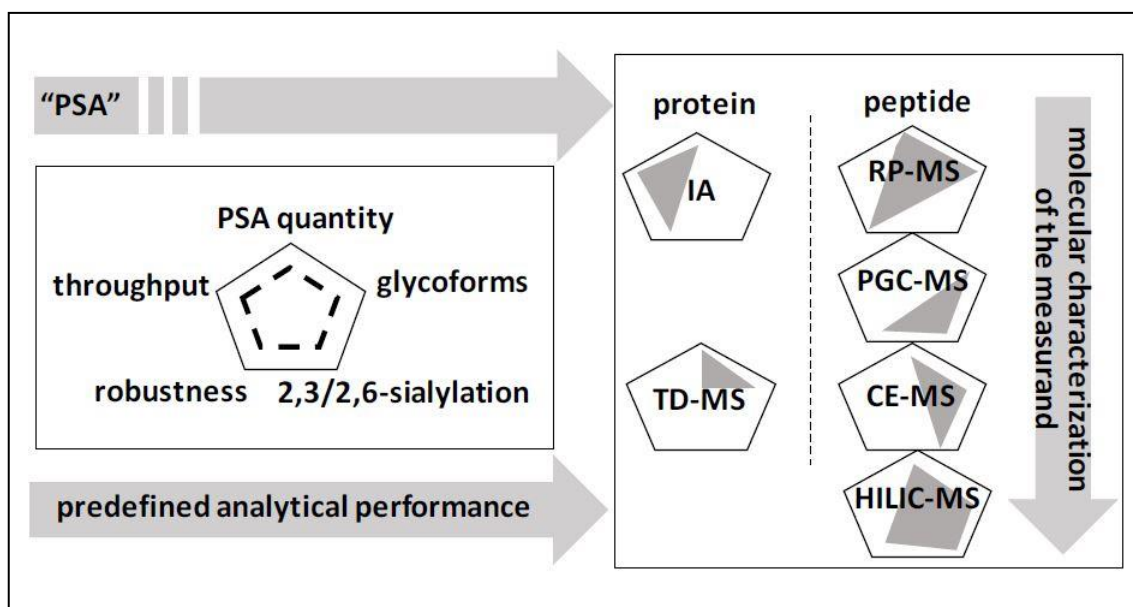
Figure 1. Top-down and bottom-up strategies for PSA glycosylation analysis. The approaches were evaluated based on their ability for absolute quantitation, throughput, robustness, glycoform profiling and sialic acid linkage analysis. IA = immunoassay, TD-MS = Top-Down mass spectrometry, RP-MS = reversed phase LC-MS, PGC-MS = porous graphitized carbon LC-MS, CE-MS = capillary electrophoresis coupled to MS and HILIC-MS = hydrophilic interaction liquid chromatography coupled to MS. With permission from [40].

3.3.1 Liquid chromatography and LC-MS

High-pressure liquid chromatography is predominantly used in the biomedical and biopharmaceutical fields for the analysis of a large variety of analytes. Its robustness and high reproducibility made HPLC one of the instrumental choices for the separation of glycoproteins, glycopeptides and even released glycans [41]. A large variety of LC modes

has been employed in carbohydrate separation, e.g., reversed-phase (RP) chromatography [42], hydrophilic interaction liquid chromatography (HILIC), high-pH anion-exchange chromatography [43] and porous graphitized carbon chromatography [44,45]. The analysis of released *N*-glycans usually requires derivatization with such reagents as 2-aminobenzamide (2-AB), 2-aminobenzoic acid (2-AA), etc., to provide the necessary hydrophobicity for the separation [46] and fluorophore groups for high sensitivity detection [47]. Although RP-LC is the most commonly used general chromatographic technique today, HILIC is the preferred method for sugar separation. Considered as a part of normal phase LC, the retention mechanism in HILIC is primary based on the hydrophilicity of the solute molecules, may also be affected by other properties such as size, charge, composition, structure, linkage and oligosaccharide branching.

N-glycosylation changes in PSA and prostatic acid phosphatase from pooled seminal plasma of PCa, BPH and control groups were analyzed by HILIC by the Drake group [48]. Thirteen different glycan structures were identified from PSA samples [49], but no significant differences were found between the patient groups examined. The *N*-glycome of pooled expressed prostatic secretions (EPS) of patients having high (Gleason score (GS) $\geq$8) and low (GS <8) grade PCa and from non-cancerous samples were also investigated with HILIC [50]. Prior to the separation, the *N*-glycans from EPS urine samples were enzymatically released and labeled with 2-AB [51]. Glycan identification was carried out with exoglycosidase digestions and GU value based database search [49]. The results showed a linear increase of bisecting GlcNAc containing biantennary structures as the aggressiveness of PCa increased. Also, a decrease in fucosylation was observed in aggressive EPS urinary glycans.

The importance of PSA sialylation linkage in PCa was also proposed [52]. HILIC was applied with a combination of weak anion exchange chromatography, this latter to partition the glycans according to their sialylation level, to investigate the serum *N*-glycome of BPH and PCa (both GS=5 and GS=7) patient groups [53]. The α2,3 and α2,6 sialylated structures were distinguished with selective sialidase digestion. The results showed significant increase in core-fucosylated biantennary glycans also carrying α2,3-linked sialic acids in cancerous samples. Furthermore, a decrease in triantennary trigalactosylated glycans and tetraantennary tetrasialylated glycans with outer arm fucosylation and an increase in tetraantennary tetrasialylated glycans were detected in more aggressive (GS=7) PCa, compared to its non-aggressive form. In another example,

HILIC was used to analyze *N*-glycans from the bound and unbound fractions of *Sambucus Nigra* lectin immunoaffinity column [54]. Their linkage type was confirmed with selective sialidase digestion, and a significant increase in α2,3-sialylation was observed in high-risk PCa compared to other samples.

Peracaula et al. prepared five PSA subforms (F1-F5) with different isoelectric points (pI) by 2D gel electrophoresis and analyzed with HILIC [55]. The quantitative measurement of these subforms from serum of BPH and PCa patients revealed significant differences in their relative distribution between the disease groups [56]. The F1, F2 and F3 subforms resulted in similar glycoprofiles with mainly mono- and disialylated complex biantennary structures [55]. F4 contained mainly monosialylated complex biantennary glycans, while F5 was not glycosylated. Further investigation of sialylation and fucosylation of F3 revealed a significant elevation of α2,3-sialylation and a decrease of core fucosylation in cancerous samples compared to control.

Though HILIC is considered as a preferred separation approach for hydrophilic and uncharged species, such as glycans, RP-LC has also been utilized for carbohydrate analysis. In RP, acidic glycans elute earlier than neutral glycans, however, the quantitation of individual sialic acid-containing glycans is difficult [57]. Compared with HILIC, the injection volume limit of aqueous samples allows higher detection sensitivity, especially if connected to MS. RP-LC coupled with fluorescent detection revealed four different glycoforms of pyridylamin (PA) labeled *N*-glycans originated from a commercially available PSA standard [58].

RP-HPLC-MS analysis of intact PSA of both normal and high pI isoforms utilizing the top-down approach identified 38 individual glycoforms in the normal and 23 in the high pI group [59]. PSA samples were directly injected without derivatization. Using an in-house developed script, the isotopic distribution patterns were calculated, which allowed identification and relative quantification of all glycoforms.

Locating all possible glycosylation sites and characterizing site-specific *N*-glycan microheterogeneity are of also high importance. The investigation of ArgC digested core and antennary fucosylation of standard PSA by nano LC-MS/MS revealed that the fucosylation site could be identified by low energy collision-induced dissociation spectra of the glycopeptides [60]. It was also shown, that the occasionally occurring fucose migration may lead to false fragmentation information. A multiple reaction monitoring

(MRM) MS method combined with a novel energy-resolved oxonium-ion monitoring technique was also applied to examine the glycosylation of monoclonal antibodies (mAbs) [61]. This procedure provided very high sensitivity and linear quantitative range
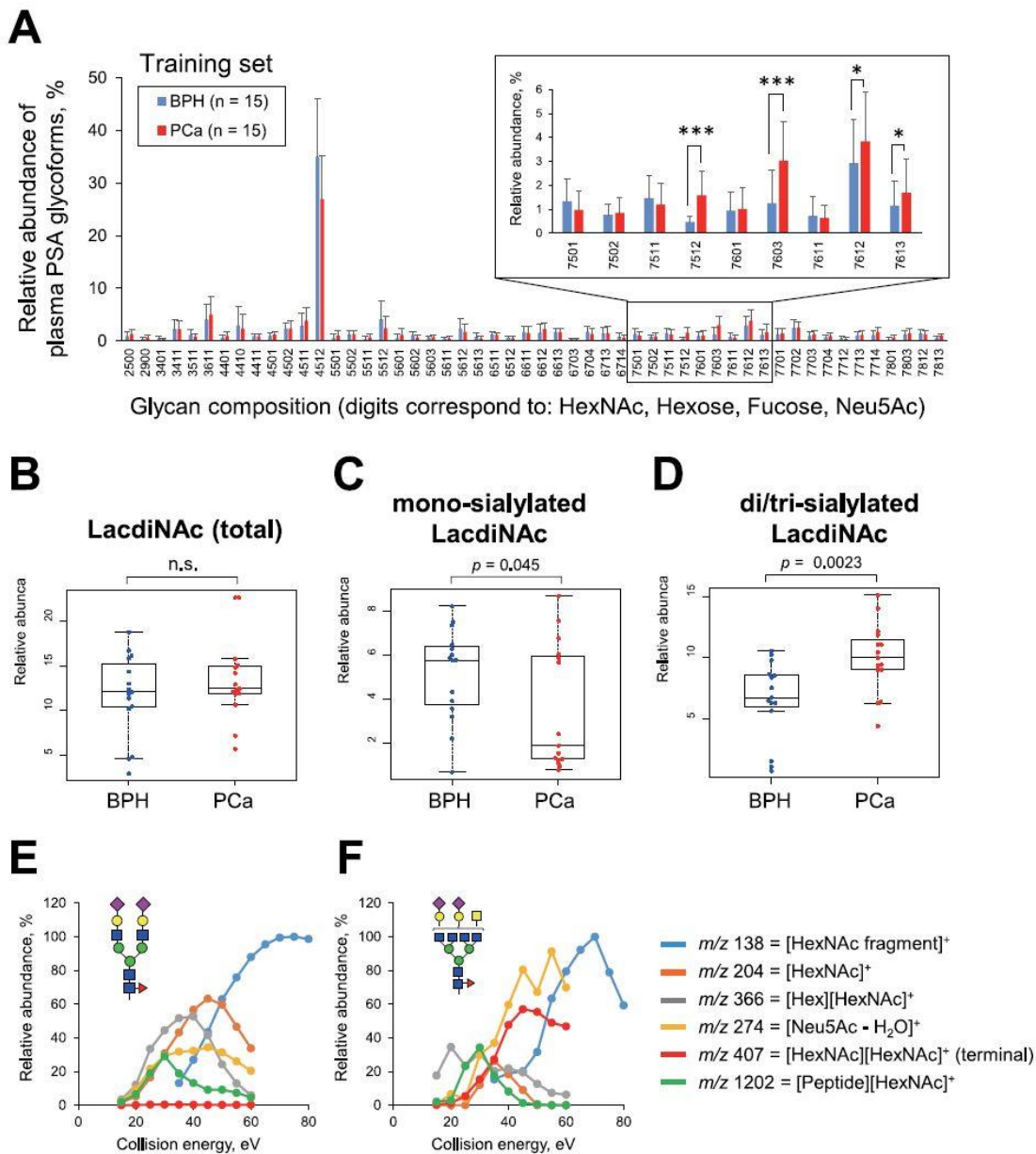
Figure 2. Determination of multisialylated LacdiNAc structures by LC-MS on PSA as PCa-specific glycan signatures. (A) A comparative overview of 52 PSA glycoforms in BPH (n = 15, blue bars) or PCa (n = 15, red bars) from patient serum samples. The data represent the means ± SD of the training sample set. *p < 0.05 or ***p < 0.001 by Student's t test. (B−D) Boxplots represent the relative abundance of LacdiNAc-containing (B), monosialylated LacdiNAc-containing (C), or di/trisialylated LacdiNAc-containing (D) PSA glycopeptides of the training sample set. (E, F) The Erexim curves of representative PSA glycopeptides (Glycan ID: 4521 in (E) or 7521 in (F)) in PCa patient sera. With permission from [62].

of glycopeptides from 30 amol to 30 fmol making possible to differentiate isomeric structures without the need of additional exoglycosidase digestion. Standard PSA as well as PSA from serum samples of PCa and BPH patients were also investigated [62]. The PSA was captured from the medium using antiPSA monoclonal antibodies immobilized to Protein G Sepharose beads. The partitioned proteins were reduced, alkylated, and trypsin digested, followed by glycopeptide enrichment and LC-MS analysis. 67 N-glycan structures were identified and quantified from standard PSA and 52 of that were quantified from both of PCa and BPH samples. Comparison of the two patient groups revealed a significant increase in multisialylated LacdiNAc-containing glycan structures in case of PCa but not in BPH (Figure 2). Based on these differences, a new diagnostic algorithm was created referred to as the 'PSA G-index', which was tested on clinical samples. The PSA G-index showed close to 100% sensitivity and specificity compared to total PSA or PSA free/total ratio, which resulted only 80.0% sensitivity with 33.3% specificity and 73.3% sensitivity with 60.0% specificity, respectively. The authors also found that multisialylated LacdiNAc structures correlated positively with Gleason scores, while simpler glycoforms showed negative correlation.

The degree of PSA fucosylation (both total and core) was also extensively studied [63] as its decrease was associated with high-risk PCa [54]. PSA was spiked into human serum and captured by biotinylated anti-PSA antibody immobilized to streptavidin-coated magnetic particles, followed by on-bead partial deglycosylation and proteolytic digestion. Core-fucosylation was determined by the glycopeptide N(GlcNAc+Fuc)K ratio to the total glycopeptide level. HILIC was applied to separate the core fucosylated structures and the results were linear in the concentration range of 0.5 to 60 ng mL^{-1} total PSA covering even the grey zones of clinical PCa diagnostic testing range (4 -10 ng mL^{-1}). Searching for a correlation between the level of core-fucosylation in PSA glycans and tumor aggressiveness, 150 serum samples from PCa and BPH patients were analyzed [64]. Despite of the high number of samples in the study, %-fuc-PSA standardized to total PSA values did not provide significantly better diagnostic differentiation between aggressive and non-aggressive PCa compared to the standard free- and total PSA tests.

The fucosylation of the proteome originated from non-aggressive and aggressive PCa cell lines was also investigated by nanoLC-MS/MS [65]. The extracted proteins were tryptic digested and the fucosylated glycopeptides were enriched with specific lectins and solid phase extraction (SPE). Prior to nanoLC-MS/MS analysis, the peptides were tandem-

mass-tag (TMT) labeled. A total of 973 fucoslyated glycopeptides from 252 proteins were discovered, in which 51 glycopeptides from 26 proteins showed differences between the aggressive and non-aggressive PCa forms. The glycosylation changes caused by PCa were also investigated by selective reaction monitoring (SRM) MS [66]. Malignant and benign tissues were digested by collagenase to the single cell level and the cell-free supernatant was used for analysis [67]. After tryptic digestion, the glycopeptides were isolated by streptavidin affinity partitioning [68] followed by HPLC-SRM-MS analysis. Albeit, the results did not reveal any correlation between the relative abundance of either glycosylated or sialylated PSA isoforms and total PSA protein levels, significantly increased sialylation was found in cancer tissues compared to non-cancerous ones.

Besides serum and tissue samples, urine has also been extensively studied in PCa biomarker research. Whole urinary *N*- and *O*-glycoproteome analysis was carried out using LC-MS/MS by Kawahara et al. [69]. The samples from PCa and BPH patients were subject to a multistep sample preparation process, in which the urine was concentrated, urinary proteins were extracted and trypsin digested. The peptides were TMT tagged and selectively enriched by SPE. The resulting fractions were analyzed either directly or after simultaneous endo- and exoglycosidase treatments. A remarkable amount of 1,310 de-*N*-glycosylated peptides, 954 intact *N*-glycopeptides and 887 desialylated but otherwise intact *O*-glycopeptides belonging to a total of 788 glycoproteins were identified. Based on these results, a panel of 56 intact *N*-glycopeptides were suggested to distinguish PCa from BPH. The panel reached very high specificity and sensitivity in differentiating the diseases, also revealed a number of new glycobiomarker candidates for further investigations. The glycosylation of individual urinary proteins, like PSA, also showed a great potential in biomarker research. Hsiao et al. analyzed urinary PSA glycosylation from BPH and PCa patients [70]. From concentrated urine, PSA was captured by anti-PSA mAbs immobilized to protein G magnetic beads. The partitioned proteins were separated by sodium dodecyl sulfate–polyacrylamide gel electrophoresis (SDS-PAGE) and in-gel digested by chymotrypsin [71]. The resulting glycopeptides were identified by an in-house developed software based on their mass spectra and confirmed by MS^2 of the oxonium and Y1 ions. LC peak areas were used for quantitation. Eight PSA glycoforms including high-mannose and complex types were identified from pooled urinary PSA samples. The individual analysis of clinical samples revealed significant differences between the two disease groups. According to the results, the relative abundance of the H5N4S1F1 and H6N3S1 glycoforms showed noticeable alterations. The grouped

glycoforms (monosialylated, nonfucosylated, and total) also displayed different expression levels. These changes resulted in higher sensitivity (87.5%) and specificity (60%) for PCa identification than that of serum PSA concentration. Even though, the normal PSA concentration in urine is higher compared to serum, *N*-glycosylation analysis often requires pre-concentration. Biotinylated antihuman PSA antibodies coupled to streptavidin coated magnetic beads were applied to capture standard PSA spiked into pooled human urine by Ruhaak and coworkers [40]. The pre-concentrated PSA was subject to trypsin and ArgC digestion [72] and analyzed by HILIC-MRM-MS. Both the HILIC separation and the MRM-MS separation conditions were optimized considering several aspects. In the first case, the effect of different HILIC columns, eluent compositions, pHs and ammonium formate concentrations were fine tuned for optimal separation. Collision energies, MS source and ion transfer parameters were also optimized. These conditions allowed to distinguish α2,3- and α2,6-silalylated structures at the glycopeptide level parallel to absolute quantitation of PSA through proteotypic peptides in the same analysis. For the identification of sialic acid linkage, selective sialidase digestion was used with Sialidase A, which cleaves both α2,3- and α2,6-linked terminal sialic acids, and with Sialidase S, which specifically catalyzes the hydrolysis of α2,3- linked sialic acids, but leaves α2,6-linked sialic acids unaffected.

Immunopurification with the combination of SDS-PAGE was also used to enrich PSA from EPS urine [73]. PSA was in-gel PNGase F digested and the released glycans were fluorescently labeled. 62 samples from BPH and PCa patients were then analyzed by UPLC-MS. While no significant differences were found in total fucosylation or sialylation between the two diseases, a remarkable increase was detected in the relative abundance of the FA2 glycan in high-risk (GS≥8) PCa compared to low-risk PCa or BPH.

3.3.2 Capillary electrophoresis and CE-MS

Featuring high resolution, excellent sensitivity and very low required sample volumes, CE is a more and more often applied technique for the analysis of biologically important oligomers [74,75]. Numerous CE-based approaches have been published for the separation and analysis of DNA [76], proteins and peptides [77] in the past decades. Techniques for glycan analysis have also been developed rapidly [78].

CE is often combined with laser-induced fluorescent detection (LIF) offering the limit of detection (LoD) in the femtomolar range, which is ideal for the characterization of released glycans especially from low volume body fluids in the field of biomarker

discovery [79]. Because carbohydrates usually do not possess charges and chromophore/fluorophore groups, derivatization with tags such as 8-aminopyrene-1,3,6-trisulphonic acid (APTS) is required to accommodate their electric field driven separation and high sensitivity detection. In the study of Vermassen et al., the tPSA concentration in urine was raised more than 170 times with prostate massage prior to sampling, which made direct CE-LIF based *N*-glycan profiling possible [80]. The results correlated with the findings of a previous study [81] i.e., showing a decrease in triantennary structures and core fucosylation in PCa samples compared to BPH and healthy volunteers (HV).

CE-MS coupling is challenging due to the nanoliter per minute flow rates required to minimize ion suppression and increase sensitivity [82]. A few interfaces to accommodate these requirements are commercially available mainly using electrospray ionization (ESI), but other types such as matrix-assisted laser desorption/ionization (MALDI) have also been reported [83]. The potential of CE-MS has been demonstrated as a useful tool for high-resolution molecular level analysis, predominantly applied for the analysis of proteins, peptides and metabolites [84]. In terms of glycosylation, both intact glycoproteins or digested glycopeptides can be investigated by this hyphenated method. Intact standard PSA was analyzed under both denaturing and native conditions by CE-ESI-MS, revealing 202 proteoforms with 36 glycoforms and 236 proteoforms with 38 glycoforms, respectively [85]. The overall separation profiles under native and denaturing conditions were very similar, strongly suggesting that this separation was based on the hydrodynamic volume to charge ratio represented by the protein isotope envelope. More interestingly, no sample preparation was required other than dilution of the commercial protein standard.

In another study, CE-ESI-MS analysis of trypsin digested PSA glycopeptides resulted in base-line separation between α2,3- and α2,6-sialylated structures with no derivatization requirement [86]. The results were confirmed by selective exoglycosidase digestion and MALDI-TOF-MS analysis of released PSA glycans as well. With selective preliminary PSA capture, the approach was applied to urine samples of PCa and non-PCa patients [87]. 41 glycopeptides were identified from the control pool (Figure 3), while 67 different glycan structures from the pooled patient sample. While large variation (~50% average RSD) was discovered between the glycan profiles of the patient samples, no significant differences were found between the PCa and non-PCa sample groups. However, the low sample count (13 PCa and 10 non-PCa) did not support adequate statistical calculations.
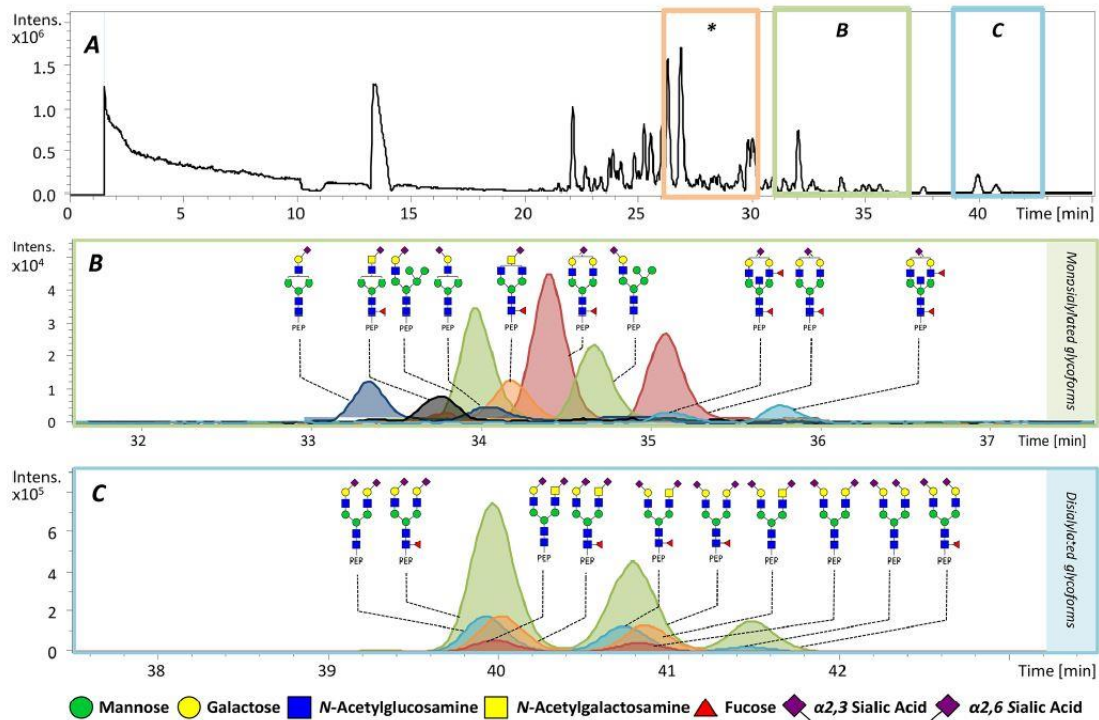
Figure 3. CE-ESI-MS analysis of tryptic (glyco)peptides from PSA standard (A), extracted ion electropherograms for mono- (B) and disialylated *N*-glycopeptides (C) of PSA. Each color represents an individual glycopeptide in its isomeric form (multiple peaks). With permission from [87].

3.3.3   Other mass spectrometry based methodologies

One of the prominent and popular techniques in the area of glycobiomarker research is mass spectrometry via ESI-MS or tandem MS can provide detailed molecular level information, but by itself only do not deliver comprehensive characterization of isomeric glycan structures due to their isobaric properties. High order tandem MS, in some cases, is capable of complete elucidation of one or a few structures, yet high concentrations are required, which is not often available in biological samples. Chromatographic separation of those isomers can alleviate this handicap and significantly increases MS sensitivity as well [42]. Mild ionization conditions can be key to preserve unstable, especially sialylated glycan structures and not to miss valuable structural information [88]. ESI is a low energy ionization method usually yielding multiple charged parent molecules, which is optimal for high molecular mass biomolecules such as peptides or proteins [89].

In the Association of Biomolecular Resource Facilities (ABRF) Glycoprotein Research Multi-Institutional Study at 2012, the *N*-glycosylation of both PSA and its high pI isoform were characterized in different laboratories worldwide by mass spectrometry [90]. Several analytical strategies were applied, including bottom-up glycopeptide analysis,

top-down MS and tandem MS measurements as well as the analysis of PNGase F released glycans. The results were evaluated considering 1) sample integrity, 2) qualitative-, and 3) differential-quantitative aspects. Possible degradation of the sample protein was investigated by two different laboratories with two PSA isoforms separately (samples were kept at 6°C during shipping and storing) within different time rates (almost a week difference). Almost all of the laboratories identified Asn-69 as the position of *N*-glycosylation and four laboratories found an additional site of Ans-78 carrying mainly high-mannose type glycosylation. Based on the glycopeptide sequences, this was considered to be originated from KLK2, with ~77% sequence homology to PSA. An *O*-glycosylation site was also reported on Ser-23 on the PSA high pI isoform. A total of 61 glycoforms were identified altogether from both PSA isoforms. Comparing all the approaches, top-down and released glycan methods were more efficient in detecting the major and intermediate compositions than that of the bottom-up methods. One of the bottom-up approaches of the ABRF study of trypsin digested glycopeptides from the two isoforms of PSA and high pI PSA identified 56 and 57 *N*-glycans, respectively, in which 46 were overlapping structures [91]. The results showed increased core-fucosylation, sialylation, GalNAc residues and highly branched structures in the high pI PSA.

MALDI is another common ionization technique besides ESI and frequently used in MS analysis of *N*-glycosylation. MALDI requires low sample volume, which is a great advantage for the analysis of biological samples with limited quantities. As a soft ionization technique, it can preserve unstable structures, e.g. sialic acid residues, which could degrade during harsher ionization techniques [92]. As PSA glycans are predominately sialylated, using mild conditions like MALDI-MS is very useful not to lose valuable structural information. With MALDI Fourier transformation - ion cyclotron resonance mass spectrometry (MALDI-FT-ICR-MS), a total number of 24 glycan structures were identified from released PSA *N*-glycans by de Leoz et al. [93]. PSA was originated from two PCa patient groups, before and after prostatectomy, respectively. Seven structures showed significant difference between the two sample groups and suggested as a potential biomarker panel.

MALDI-MS is also useful for carbohydrate analysis at the glycopeptide level. The glycosylation of both free and complex forms of PSA obtained from blood samples of PCa patients were investigated and compared to seminal plasma. The PSA was first captured using an anti-PSA IgG column, then separated by SDS-PAGE. The SDS-PAGE

separated bands were subject to in-gel *S*-aminoethylation, lysylendopeptidase, and in some cases neuraminidase digestion. The resulted peptides were separated by RP-LC, followed by both MALDI-linear-TOF-MS and MALDI-quadrupole ion trap (QIT)-TOF-MS/MS analysis. The results were identical for both free and α1-antichymotrypsin (ACT) complex PSA, suggesting that these forms were probably the same [94].

Direct analysis of glycans in clinically derived formalin-fixed paraffin-embedded (FFPE) prostate tissues was carried out by MALDI imaging MS (MALDI-IMS) [95]. This approach effectively visualized and evaluated the *N*-glycan localization in tissue sections. Human prostate tissue blocks containing both tumor and non-tumor gland regions were on-tissue PNGase F treated, permethylated and analyzed by MALDI-IMS. A heterogeneous *N*-glycan distribution was observed with the overlay of two glycan sets, that helped to distinguish between prostate stroma and glands.

Microarrays, thankfully for their high sensitivity and specificity, represent another alternative approach for the detection of low level glycan biomarkers. Immobilized lectins and carbohydrate-binding antibodies with various carbohydrate-binding specificity can be used for partitioning based glycosylation analysis. A huge advantage of these microarrays is the direct analysis option of even crude samples containing glycoproteins, without the need to release or derivatize the glycans. These techniques were reviewed in detail by Hirabayashi et al. [96] and Tkac and coworkers [97]. This latter group thoroughly discussed an extensive list of lectin-based microarrays utilized for PSA glycosylation analysis [98].

3.4   Concentration and selective isolation of proteins from biological matrices

The production, analysis and utilization of proteins often require to increase their concentration in their solution, moreover selectively isolate the target from the other matrix components in the process. Several methods have been developed for concentrating proteins, e.g. by precipitation with salts, organic solvents, organic polymers etc. [99], SDS-PAGE [100], three-phase partitioning [101], centrifugation, affinity chromatography [102] and several other techniques, summarized by Goldring [103]. Among these methods, IP is particularly prominent for the selective capture of target proteins even from complex biological matrices [104]. The procedure is based on the participation of target antigen protein by the addition of its specific antibody. The approach is usually referred to as individual protein IP. The IP of intact protein complexes

is known as co-immunoprecipitation (CoIP) [105], which is utilized by selecting an antibody that targets a known protein that is believed to be a member of a larger protein complex. By targeting the known member, it may become possible to isolate the entire protein complex including the unknown members as well. Chromatin IP (ChIP) is used to determine the location of DNA binding sites on the genome for a particular protein [106]. This technique provides insight into the protein–DNA interactions that occur inside the nucleus of living cells or tissues. Similarly to ChIP, Ribonucleoprotein IP (RNP-IP or RIP) targets ribonucleoproteins resulting isolated RNA-protein complexes from which RNA can be harvested [107]. IP methods are usually built up by the same basic steps:

1. Preparation of sample for immunoprecipitation.
2. Pre-clear the sample by introducing the sample to untreated beads or treated by irrelevant antibody to extract any proteins that non-specifically bind to the IP components.
3. Mix and incubate sample with the antibody. Antibody can be immobilized beforehand (direct method) or after (indirect method).
4. Removal of immunocomplex.
5. Washing step for the removal of non-specific contaminants.
6. Elution of immunocomplex.
7. Analyze complex or antigen alone.

The classical IP and CoIP approaches utilize a solid phase support, typically immobilized Protein A or Protein G crosslinked agarose beads for the capture of the formed immune complexes and the beads can be separated by centrifugation [108]. The highest disadvantage of the approach is the contamination of the sample with the IP antibody. To avoid the elution of the IP antibody, oriented IP applies crosslinker molecules to bind IP mAb to Protein A or Protein G, but the crosslinker usually decrease the affinity. To eliminate the need of Protein A or Protein G, direct immobilization approaches utilize activated surfaces to bind mAbs, but the random orientation can also lead to the loss of affinity. The conventional agarose beads can also be replaced by paramagnetic beads to facilitate the easier removal and washing off of sample matrix [109].

MAbs are commonly used capturing agents [110], but their accessibility can limit their application and they are glycoproteins, therefore their removal from the sample prior to analysis is often necessary to avoid any possible interference. Single domain antibodies (sdAbs) (or nanobodies) can alleviate this drawback [111]. Nanobodies are single-domain

antibody fragments derived from camelid heavy-chain antibodies. Their small size, straightforward production, easy tailoring, high affinity, specificity, stability and solubility have been exploited in various biotechnological applications [112]. Antigen-specific nanobodies can be produced through immune-, naïve-, or synthetic libraries [113]. After selection by phage surface display, mRNA/cDNA display, or MS spectrometric identification the subsequent amplification of the encoding sequence can be facilitated by PCR. Then, utilizing restriction enzyme sites, the different fragments are inserted into a phagemid cloning vector [114]. The selection of the most suitable nanobodies can be performed using in vitro assays, like phage ELISA.
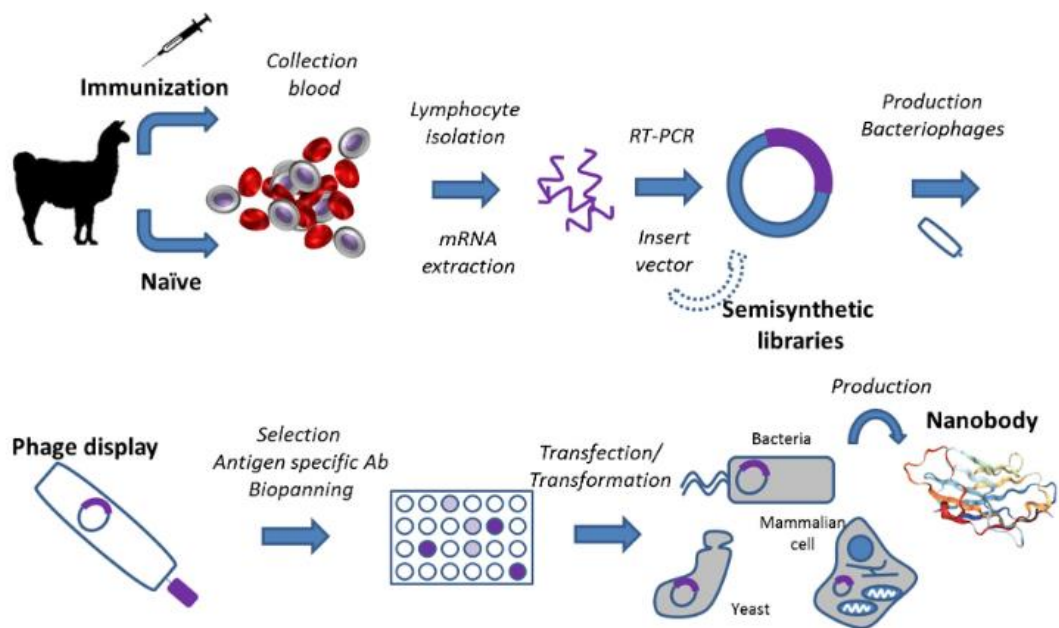
Figure 4. Nanobody production scheme using a phage display library. The genetic information can be obtained by active immunization using an immunogen or using non-immunized animals by collection of blood, which contains the lymphocytes. Increasing the diversity using semisynthetic libraries and randomly introducing amino acids in the complementarity-determining region is possible in order to improve the binding capabilities. After the insertion of the plasmid in a bacterophage, the phagemid library is ready for this selection. Phage ELISA is the usual way to perform the biopanning [115]. After the best candidate is selected, the nanobody can be expressed in bacteria, yeast, or mammalian cells in production scale through its corresponding expression vector (With permission from [114]).

The most widely used expression system is Escherichia coli, which expresses proteins in different cellular compartments. As E. Coli cannot provide post-translational modifications, sdAbs do not contain sugar moieties, which otherwise could interfere with glycosylation analysis (as in case of mAbs). Also, different linker tags (e.g., 6-histidine or Avi tag) can be attached to them, not just to facilitate the purification of sdAbs by

immobilized metal affinity chromatography or gel filtration [116] but also realize their immobilization to various surfaces while providing preferable orientation as well [117]. All these advantages make nanobodies a perfect alternative for mAbs as capturing agent for IP methods.

3.5   Glycan derivatization for released glycan approaches

Carbohydrates do not possess fluorophore or chromophore groups, thus derivatization methods like fluorophore labeling are commonly used to accommodate their analysis in liquid phase separation methods such as CE and LC with UV/VIS or fluorescent detection. Derivatization can also be applied to link charged or hydrophobic groups at the reducing end to enhance glycan separation and mass-spectrometric detection. One of the most generally used techniques to release *N*-linked oligosaccharides is via enzymatic cleavage by either PNGase A or F (peptide-N4-[*N*-acetyl-beta-glucosaminyl] asparagine-amidase A or F) digestion, due to its reliable and specific cleavage capability and moderate reaction conditions [118]. As a result of continuous developments, the traditional protocol of overnight PNGase F digestion at 37°C has been successfully accelerated by microwave irradiation [119], pressure cycling technology [120], or with the utilization of immobilized PNGase F microreactors [121,122].

The released carbohydrates can be tagged at their reductive ends in various ways, such as by Michael-type addition [123] or hydrazine labeling [124], but the most commonly used method is reductive amination in a two-step-reaction. During the first step a Schiff-base is formed in the presence of an acid catalyst, followed by reduction to form a stable conjugate in the second step. An advantage of this labeling approach is the stoichiometric attachment of one label per glycan, allowing a direct quantitation based on fluorescence or UV-absorbance intensity. In most instances sodium-cyanoborohydride ($NaBH_3CN$) is used as a reductive agent [125], but other methods utilizing sodium-triacetoxyborohydride ($NaBH(O_2CCH_3)_3$) [126], borane-diethylamine (($CH_3)_2NHBH_3$) [127], 2-picoline-borane (pic-BH_3) [128] or by the recently introduced transfer hydrogenation [129] have also been reported. The reaction speed and yield of this acid-catalyzed labeling reaction is greatly influenced by the amount and type of acid used. Organic acids with low pK_a, such as acetic acid (pK_a = 4.75), malonic acid (pK_{a1} = 2.83) or citric acid (pK_{a1} = 3.15), are commonly used to accelerate glycan labeling [130]. Studies showed that stronger acids were able to increase derivatization yield [131], but

their use was associated with higher sialic acid loss [132]. The most widely applied sugar labeling dyes are 2-AB, 2-AA, PA, APTS [79] and 8-aminonaphthalene-1,3,6-trisulfonic acid (ANTS) [133], often available in commercial labeling kits, providing all the necessary chemicals for sample preparation. 2-AB and PA lack negative charges, therefore, their application is limited mostly for chromatographic analysis. However, extensive databases have been developed based on the elution positions of 2-AB-labeled glycans in HILIC separation [134]. On the other hand, the one negative charge holding 2-AA makes it a very flexible labeling candidate. It is used in HPLC and capillary electrophoresis (CE) separations as well as in positive-mode and negative-mode matrix-assisted laser desorption/ionization (MALDI) analysis, allowing detection of both neutral and sialylated glycan species [43]. APTS and ANTS both have three negative charges, which makes them very suitable for CE or CGE as the labeling dye carries the necessary charges for the electrophoretic separation, which otherwise oligosaccharides mostly lack. MALDI analysis of APTS-labeled glycans were also reported [135].

Procedures reported in the literature apply comparable but not unified reaction conditions and volumes for fluorescent labeling [43], most of them suggesting overnight labeling at 37°C [131,136] or several hours of reaction times at higher temperatures (50°C) [137]. Recently introduced rapid labeling approaches required only 20 minutes reaction time, but at 60°C [138]. Practically all but this latter method used sealed vials to prohibit evaporation of the reaction mixture components and the labeling reaction volumes have been varied from several microliters up to tens of microliters.

4   Materials and Methods

4.1   Chemicals and Reagents

Human immunoglobulin G (hIgG), water (HPLC grade), acetic acid (glacial), acetonitrile (MeCN), tetrahydrofuran (THF), sodium cyanoborohydride (1M in THF), sodium chloride, imidazole, 4-(2-hydroxyethyl)-1-piperazineethanesulfonic acid (HEPES) and DTT (dithiothreitol) were obtained from Sigma Aldrich (St. Louis, MO, USA). SDS and Nonidet P-40 were from VWR (West Chester, PA, USA). The Fast Glycan Labeling and Analysis Kit was from Bio-Science Kft. (Budapest, Hungary) including the tagging dye of APTS, magnetic beads for excess dye removal, HR-NCHO separation gel-buffer system, the bracketing standards of maltose (DP2) and maltopentadecaose (DP15). The exoglycosidase enzymes of Sialidase A (Arthrobacter ureafaciens), β-Galactosidase (Jack bean) and β-*N*-Acetyl Hexosaminidase (Jack bean) were from ProZyme (Hayward, CA, USA). The endoglycosidase PNGase F was from UD Genomed (Debrecen, Hungary) and from Asparia Glycomics, (San Sebastian, Spain). 20 ml volume 10 kDa cut-off spinfilters were from Pall (New York, NY, USA), 500 µl ml volume 10 kDa cut-off spinfilters were from VWR. PhyTip Nickel Immobilized Metal Affinity Chromatography (Ni-IMAC) microcolumns (40 µl) were provided by PhyNexus (San Jose, CA). Buffer 'A': 100 mM HEPES, 500 mM NaCl, 50 mM imidazole, pH=8.0. Buffer 'B': 100 mM HEPES, 500 mM NaCl, 500 mM imidazole, pH=8.0. Denaturation solution: mixture of 0.5% Nonidet P-40,100 mM DTT and 5.0% SDS in the ratio of 6:1:1 respectively. Digestion solution: 75 µUnit/µl of PNGase F in 16.7 mM ammonium acetate. Labeling solution: 5.7 mM of APTS in the mixture of H_2O:AcOH:THF:$NaBH_3CN$ (1 M in THF) = 5:5:8:2. Magnetic bead solution: the solvent was removed from 200 µl of magnetic bead suspension from Fast Glycan Labeling and Analysis Kit on a magnetic stand, the beads were resuspended in 200 µl of water and the solvent was removed again on a magnetic stand, the beads were resuspended again in 20 µl of water.

4.2   Sample Preparation

4.2.1   Evaporative labeling sample preparation

Sample preparation started with the addition of 5.0 µl of denaturation solution from the Fast Glycan Labeling and Analysis Kit to 10 µl of 10 mg/ml aqueous hIgG1 (test protein) and etanercept (target protein) solutions. The denaturation step proceeded for 8 minutes at 60°C, followed by the addition of 15 µL of water and 1.0 µL of PNGase F (2.5 mU) to

the mixture and incubation at 50°C for 60 minutes. The released *N*-linked carbohydrate samples were aliquoted and dried at 60°C under reduced pressure (SpeedVac; 2,500 rpm) followed by mixing with 3.0 μl of 40 mM APTS in 20% acetic acid and 2.0 μl of NaBH$_3$CN (1M in THF). The effects of additional 20% acetic acid and THF were evaluated as specified later. The reaction mixtures were incubated in a heating block at 40°C, 50°C and 60°C with closed (no evaporation) or open lid (evaporative labeling) vials. After the labeling step, the samples were magnetic bead purified and analyzed by CGE-LIF.

4.2.2   PSA capture sample preparation

The sample preparation process was identical for all captured PSA, control and standard PSA (150 μg/ml) samples. 2 μl of denaturation solution was added to 10 μl sample, heated up from 30°C to 80°C in 8 min 20 sec and incubated at 80°C for 1 min 40 sec. Then 20 μl of digestion solution was added and the sample was heated up from 40°C to 60°C in 20 min. After that, the labeling solution was added and sample was incubated at 37°C overnight in an open cap vial to let the solvent evaporate. The dried sample was then resolved in 20 μl of magnetic bead suspension, then 185 μl of MeCN was added and solvent was removed from the magnetic beads on a magnetic stand. The beads were suspended in 20 μl of water, 185 μl of MeCN was added and the solvent was removed from the magnetic beads on a magnetic stand again. This step was repeated two additional times (total of 4 washes with the first one adding the beads). Finally, beads were diluted with 60 μl of water and, on a magnetic stand, 50 μl of sample was transferred into a new vial to CGE-LIF analysis.

4.3   Gene construction

Two antiPSA (aPSA) coding polypeptide sequences, N7 and C9 were taken from [139], back translated and codon optimized for *E. coli* and the genes with flanking 5'-NdeI and 3'-XhoI cleavage sites were synthetized by Genscript (Piscataway, New Jersey, United States). After amplification both genes were cloned into pET23b (Novagen, Merck, Darmstadt, Germany) between its NdeI and XhoI sites, thus fusing a *C*-terminal 6-histidine coding sequence to the gene of aPSA. Proper incorporation of the insert into the plasmid was verified by sequencing (Macrogen Europe B.V., Amsterdam, The Netherlands).

4.4 Protein expression and purification

For protein expression Shuffle T7 Express *E. coli* (New England Biolabs, Ipswich, Massachusetts, US) cells were transformed with the N7-aPSA-pET23b and C9-aPSA-pET23b plasmids, according to the supplier's protocol. 5 mL sterile Luria Broth (LB) media containing 100 µg/mL Ampicillin (Amp) was inoculated from a freshly prepared LB/Amp plate and grown at 30°C with vigorous shaking until OD600 was between 0.4-0.6 and kept at 4°C overnight. The cells were then separated from the supernatant by centrifugation, resuspended in 5 mL freshly prepared LB and 2 mL of it was used to inoculate 1 L LB/Amp. Cell culture was grown at 37°C for two hours and then at 30°, 140 rpm in baffled flask until OD600 fell into 0.6 – 1.0 and then the temperature was decreased to 22°C. After 15 min of cooling, protein expression was induced by the addition of 0.5 mM isopropyl β-D-1-thiogalactopyranoside (IPTG, final concentration) and further incubated overnight. Cells were harvested by centrifugation at 6,000g for 30 min, washed with buffer 'A' and centrifuged again at 10,000g for 30 min. Cells were resuspended again on ice in 20 ml buffer 'A' containing two EDTA-free Mini Complete protease inhibitor tablets (Roche, Basel, Switzerland) and disrupted by sonication (10 x 30 s, 50% amplitude). The suspension was centrifuged at 30,000g and the supernatant filtered through a 0.45 µm syringe filter. The sample was loaded on a pre-equilibrated 5 ml HiTrap Chelating (GE Healthcare, Chicago, Illinois, US) nickel saturated column, purified using isocratic elution and the pure protein was eluted at 50% 'B' buffer. In order to get rid of the high salt and imidazole content of the protein solution, it was dialyzed against a buffer solution. The purity of aPSA was confirmed on 15% SDS-PAGE gels and protein concentration calculated using the following parameters given by ProtParam [140]: N7-aPSA-6His, 14.5 kDa, 27,180 $cm^{-1}M^{-1}$ and C9-aPSA-6His, 14.3 kDa, 21,555 $cm^{-1}M^{-1}$, respectively.

4.5 Biological specimens

Urine samples were collected with the appropriate Ethical Permissions (approval number: 23580-1/2015/EKU (0180/15)) and Informed Patient Consents in the Semmelweis Hospital (Miskolc, Hungary). Samples were taken from male and female (blind control) healthy volunteers (population of seven Caucasian, age average: 28.3, age median 27) and kept at 4 °C until processing.

4.6   PSA quantitation in urine

All standard enzyme-linked immunosorbent assays (ELISA) tests were carried out in a UniCel DxI 800 Access Immunoassay System, kindly provided by the central laboratory of Csolnoky Ferenc Hospital (Veszprem, Hungary). Urine samples were analyzed directly, without any sample preparation.

4.7   PSA capture from urine

300 ml of male urine was cooled to room temperature and it was concentrated to 500 µl by 20 ml volume 10 kDa cut-off spinfilters (13,500g for 30 min at 6°C for each consecutive 20 ml concentration). The concentrated urine was diluted and centrifuged (13,500g for 10 min at 6°C) twice with 3-3 ml of buffer 'A' then it was transferred to an Eppendorf vial. The filter was washed two times with 250 µl buffer 'A' each and both were added to the transferred urine. The final, 1 ml mixture was vortexed and divided into 500-500 µl, one for PSA capture and one for control, respectively. Two Ni-IMAC microcolumns were washed with 200 µl buffer 'A' for 5 min, by connecting the tips to an automated pipette and the buffer was continuously aspirated and dispensed through the tips with the flow rate of 2 ml/min. In the next step, the tips were washed by 50 µg/ml C9 sdAb in 100 µl buffer 'A' for 10 min. A NanoDrop 2000 Microvolume Spectrophotometer (Thermo Scientific, Waltham, Massachusetts, US) was used for the monitoring of nanobody concentration. For the control sample, 100 µl buffer 'A' without sdAb was used instead. Both of the tips were washed again by 200 µl buffer 'A' for 5 min. Then, the tips were washed by 500-500 µl concentrated urine samples for 10 min. After that, the tips were washed again 3 times with 200 µl of buffer 'A', 5 min each, then washed by 100 µl buffer 'B' for 5 min. The eluted buffers were transferred onto 500 µl volume 10 kDa cut-off spinfilters and the solvent was centrifuged (13,500g for 10 min at 6°C). The filter was washed twice by 400 µl of water, both times the water was centrifuged out (13,500g for 10 min at 6°C). The samples were taken up into 80 µl water (washing the filter twice with 40-40 µl of water), transferred into an Eppendorf vial, then they were dried in a SpeedVac under reduced pressure at 70°C for 15 min. The dried sample was resolved again in 10 µl of water.

4.8 Glycan structure identification

Structural elucidation of separated, asparagine linked PSA glycans was utilized by direct mining of GU database entries (GUcal.hu), exoglycosidase digestion based carbohydrate sequencing and some earlier published literature data on the same subject matter [87,141]. Exoglycosidase sequencing was utilized by Sialidase A, β-Galactosidase and β-*N*-Acetyl Hexosaminidase digestions. Native and all digested pools were then analyzed by CE-LIF and the structural information was derived from the GU value shifts of the individual peaks.

4.9 Capillary gel electrophoresis

A PA800 Plus Pharmaceutical Analysis System (Beckman Coulter, Brea, CA) with laser induced fluorescence detection (λ_{ex}=488 nm / λ_{em}=520 nm) was used for all capillary gel electrophoresis separations employing the HR-NCHO separation gel buffer in a 20 cm effective length (30 cm total length, 50 µm ID) bare fused silica capillary for evaporative labeling and captured urinary PSA separation, 40 cm effective length (50 cm total length, 50 µm ID) bare fused silica capillary for standard PSA separation and sequencing. The applied electric field strength was 30 kV in reversed polarity mode (cathode at the injection side, anode at the detection side). The separation temperature was set to 30°C. A three-step electrokinetic sample injection was applied: at 30 cm capillary length 1) 3.0 psi for 5.0 sec water pre-injection, 2) 1.0 kV for 1.0 sec sample injection and 3) 1.0 kV for 1.0 sec bracketing standard (BST, DP2 and DP15) and at 50 cm capillary length 1) 5.0 psi for 5.0 sec water pre-injection, 2) 5.0 kV for 2.0 sec sample injection and 3) 5.0 kV for 2.0 sec bracketing standard (BST, DP2 and DP15). The 32Karat (version 10.1) software package (Beckman Coulter) was used for data acquisition and interpretation.

5 Results and Discussion

In my doctoral thesis, the development of an analytical procedure, which could be applied for the analysis of the urinary PSA glycanprofile, is presented. As shown previously in the theoretical background part, this chemical data can be vital for the diagnosis or monitoring of PCa, as well as providing key information of the aggressiveness of cancer, which can contribute to enabling doctors and medical experts to make the best therapeutic decisions. The first step of this work was laying down the most important parameters, which should be kept in mind during the development process. The criterion of a practical and widely useable diagnostical tool is offering the most precise results on the shortest time for the lowest price. To fulfill these requirements the diagnostic tool must be based on a selective and sensitive analytical method, which can provide sufficient structural information of the PSA glycosylation even from biological samples with especially low target protein concentrations. The sensitivity of CE-LIF is known to be very potent, and the initial tests resulted in 0.1 mg/ml LoD for standard PSA. Unfortunately, PSA concentration can vary in a high scale in different body fluids, and only semen's PSA concentration range is above the limit. Also, the traditional sample preparation methods for CE-LIF glycan analysis suggest overnight digestion and/or labeling steps, which makes its application in diagnostic rather unwanted as it requires too much time to complete. Often harsher reaction conditions are applied to reduce the reaction times, but that can affect sensitive chemical structures, like sialic acids, for which, preservation is critical to acquire the most accurate diagnostic information. In order to compensate for the disadvantages, the conventional methods had to be revised and the LoD of PSA lowered to the concentration of biological sample sources, which are more relevant and available in medical diagnostics (e.g., blood or urine). Hereby presented the development of an optimized and shortened sample preparation workflow, paired with a novel selective capturing technique to preconcentrate PSA from low concentration media. Parallel, the glycosylation of standard PSA was identified by CE-LIF combined with glycan sequencing techniques, identifying 30 individual glycan structures. Finally, these techniques were assembled into a novel workflow being able to map urinary PSA *N*-glycan patterns with the preservation of sensitive sialylated structures.

5.1   Evaporative labeling

The acceleration of certain organic reactions by the evaporation of solvents was already reported in several studies [142]. The explanation of this phenomenon is usually the remarkable enhancement of molecule-to-molecule contacts between reactants by the continuous concentration of the solution due the removal of the solvent. This effect is even more significant in microscale reactions, where mechanical mixing of the solvent is usually challenging because of the low volumes. CE-LIF sample requirement is also incredibly low, which lead to the idea to try to benefit from the evaporation effect during sample preparation. The reductive amination based fluorophore labeling of sugars is one of the key steps in the process, which reaction is usually performed only in several microliters, where proper mixing cannot be usually solved.

The effect of continuous evaporation was evaluated in an open vial format to let the solvent evaporate and it was compared to the conventional method using the exact same reaction parameters with closed vials. The value of analytical signal, the reaction time and the preservation of sialic structures were the main parameters according to which the results were evaluated. Human IgG1 was chosen as reference protein due to its availability and well characterized *N*-glycan structures. Three different reaction temperatures were studied (40°C, 50°C and 60°C) with the addition of zero, 4.0 µl and 8.0 µl of 20% extra acetic acid to the 3.0 µl 20% acetic acid containing APTS solution of the labeling mixture (total reaction volumes were 5.0, 9.0 and 13 µl, respectively) to ensure properly extended evaporation times (i.e., dryness only at the end of the process) in all instances. To obtain the same derivatization efficiency at lower temperatures and higher reaction volumes required longer labeling times as summarized in Table 1. In all instances, the maximum derivatization time was defined by the drying time of the open vial method, e.g., 40 min for the no extra acetic acid containing reaction mixture at 40°C (first line in Table 1). Identical reaction conditions were used for the closed-vial labeling method and the resulting total peak areas, as well as for the subset of peaks representing the sialylated glycans are all compared in Table 1. Standard deviation was calculated from three parallel analysis at each point. As one can observe in Figure 4, up to four times higher detection signal was obtained with the use of the evaporative labeling protocol (50°C; and the addition of 4.0 µl of 20% acetic acid). The highest peak areas were obtained at 60°C labeling temperature with the addition of extra 8.0 µl of 20% acetic acid to the reaction mixture (total reaction volume: 13 µl). Equally importantly, the peak area

percentages of the sialylated glycan representing peaks were between 14-21% using the closed-vial method, while were preserved significantly better using the open-vial labeling approach (20-24%), suggesting greater stability of the latter. The lowest sialic acid loss was observed at 40°C labeling temperature without any additional acetic acid in the reaction mixture (total reaction volume: 5.0 µl). Therefore, to accommodate the two important labeling requirements, i.e., the highest possible peak areas and the lowest sialic acid loss, 50°C reaction temperature with the addition of extra 4.0 µl of 20% acetic acid (total reaction volume: 9.0 µl) with 60 min incubation time is recommended (Figure 4, trace a). However, if minimizing the sialic acid loss is top priority, the same extra 4.0 µl of 20% acetic acid addition, but at 40°C reaction temperature for 90 minutes is endorsed.
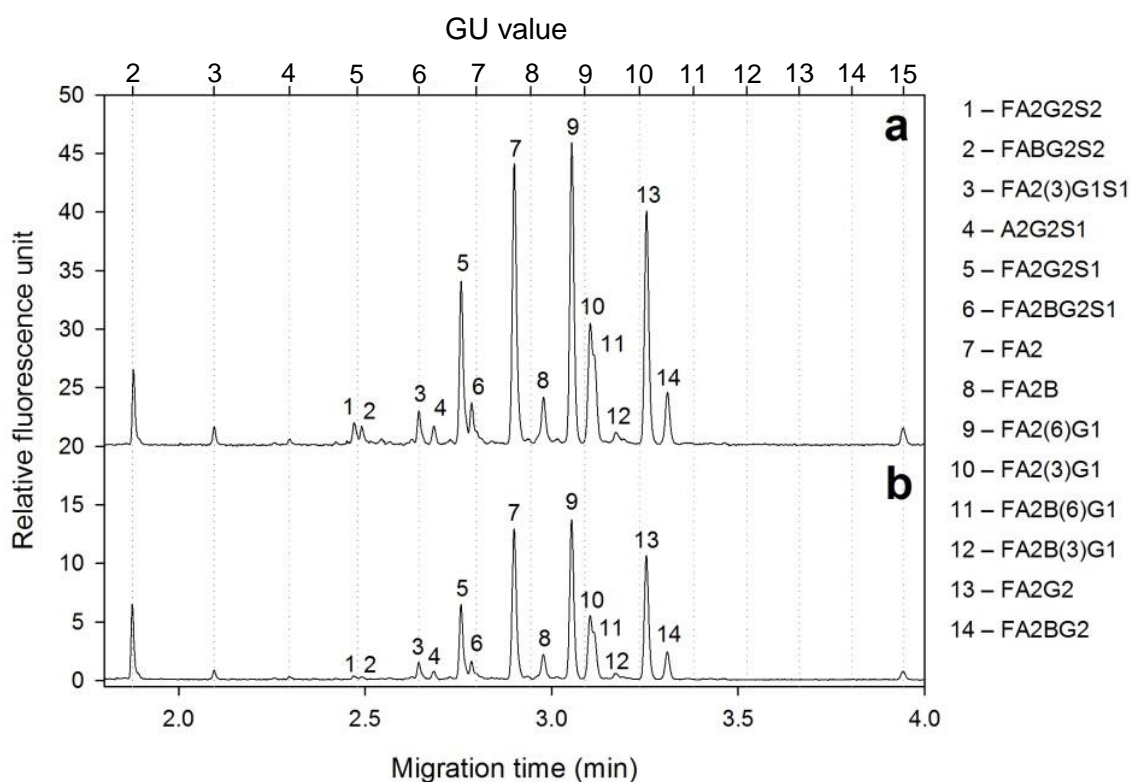
Figure 5. Comparison of the evaporative (trace a, open vial) and conventional (trace b, closed vial) APTS labeling of PNGase F released hIgG1 glycans. Labeling conditions: 50°C for 60 minutes with the addition of extra 4.0 µl 20% acetic acid catalyst to the reaction mixture. Separation conditions: 20 cm effective length (30 cm total), 50 µm ID bare fused silica capillary; 30 kV separation voltage. Injection: preinjection of water for 3.0 sec at 5.0 psi was followed by 1.0 kV/1.0 sec sample and 1.0 kV/1.0 sec bracketing standard (BST. DP2 and DP15) injection.

Table 1. Comparison of total peak areas and the sialoform subset of the hIgG1 *N*-glycan structures using evaporative and conventional (closed vial based) reductive amination based fluorophore labeling. The comparative study included three different reaction temperatures (40°C, 50°C and 60°C) with different volumes of extra catalyst added (none, 4.0 µl and 8.0 µl of 20% acetic acid, total reaction volumes 5.0, 9.0 and 13 µl, respectively). Reaction times were defined by reaching complete dryness for the open vial reactions.

Temperature and additional catalyst (20% acetic acid) volume	Reaction time (min)	Format	Total peak area	Sialylated peak area	Sialylated %
40°C; +0.0 µl 20% acetic acid	40	Open vial	23.37 ± 0.47	5.61 ± 0.17	24.26 ± 1.69
		Closed vial	16.37 ± 0.99	3.01 ± 0.11	18.77 ± 1.02
40°C; +4.0 µl 20% acetic acid	90	Open vial	32.48 ± 0.99	7.87 ± 0.19	24.02 ± 0.39
		Closed vial	29.61 ± 1.52	5.25 ± 0.43	18.11 ± 0.78
40°C; +8.0 µl 20% acetic acid	230	Open vial	49.50 ± 2.21	11.40 ± 0.40	23.53 ± 0.54
		Closed vial	33.73 ± 1.24	4.87 ± 0.07	14.78 ± 0.30
50°C; +0.0 µl 20% acetic acid	30	Open vial	78.17 ± 1.84	17.91 ± 0.36	23.23 ± 0.61
		Closed vial	25.12 ± 1.30	5.29 ± 0.13	21.03 ± 1.09
50°C; +4.0 µl 20% acetic acid	60	Open vial	89.50 ± 1.81	18.54 ± 0.50	21.88 ± 0.23
		Closed vial	19.68 ± 0.19	3.40 ± 0.04	17.13 ± 0.49
50°C; +8.0 µl 20% acetic acid	120	Open vial	93.67 ± 3.69	20.93 ± 0.86	22.02 ± 1.04
		Closed vial	39.91 ± 2.01	5.94 ± 0.35	15.75 ± 0.37
60°C; +0.0 µl 20% acetic acid	20	Open vial	57.49 ± 3.02	12.80 ± 0.65	22.21 ± 0.29
		Closed vial	18.20 ± 0.59	3.46 ± 0.07	19.15 ± 0.45
60°C; +4.0 µl 20% acetic acid	40	Open vial	113.75 ± 5.28	22.23 ± 0.67	20.76 ± 1.20
		Closed vial	38.29 ± 1.78	6.13 ± 0.12	16.31 ± 0.29
60°C; +8.0 µl 20% acetic acid	75	Open vial	121.81 ± 3.84	24.71 ± 0.87	20.11 ± 0.67
		Closed vial	52.14 ± 0.64	7.30 ± 0.34	14.22 ± 0.28

Evaporative labeling was also applied on tagging the PNGase F released *N*-glycans from 100 µg of etanercept target glycoprotein and compared to the conventional closed lid derivatization method. One-hour incubation was used in both instances for the labeling process. Similar to the hIgG1 sample, evaporative labeling showed increased peak areas and decreased sialic acid loss. In this case, a total of 13.75% increment was observed in percent values of the sialylated structures. The ratio of core and non-core fucosylated

sialic acid containing glycans was also investigated to determine if there were any alterations caused by the evaporative labeling approach, compared to the traditional closed lid method. Negligible differences were found between core fucosylated and non-core fucosylated sialylated area % ratios using the two different labeling protocols as shown by the results with the peak evaluation table inset in Figure 5.

Vaue	Trace	
	a	b
Total peak area	266.38	449.82
Sialylated %	28.88	42.62
Non core fucosilated sialylated %	7.09	10.93
Core fucosilated sialylated %	21.79	31.69
Core fuc. / Non core fuc. sial. % ratio	3.07	2.90

1 – A2G2S2
2 – FA2G2S2
3 – FA2(3)G1S1
4 – A2G2S1
5 – A2
6 – Man5
7 – FA2G2S1
8 – FA2
9 – FA2(6)G1
10 – FA2(3)G1
11 – A2G2
12 – FA2G2
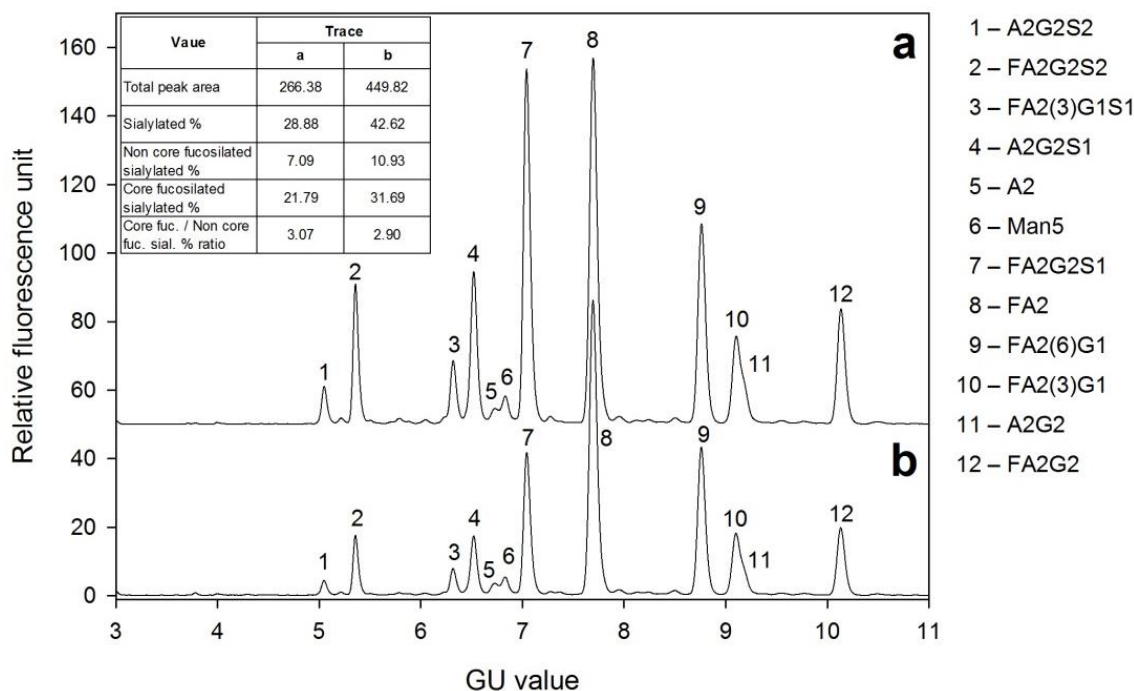
Figure 6. Comparison of the evaporative (trace a, open vial) and conventional (trace b, closed vial) based labeling protocols using Etanercept sample. The inset depicts the actual labeling efficiency in both instances. Labeling, separation and injection parameters were the same as in Figure 4.

Finally, the evaporative labeling technique was compared to the traditional overnight labeling method at 37°C to evaluate the overall performance and the sialylated peak area % values. hIgG1 samples were labeled at 50°C for one hour with the lid open and closed, as well as at 37°C overnight (16 hours). Furthermore, a combination of the closed and open lid method was also carried out by applying 50°C for one hour with the lid closed, then 50°C for one hour with the lid open. The labeling efficiency was only 16% at 50°C for one hour labeling with the lid closed, but by applying the open lid based evaporative labeling approach, it resulted in 71% compared to the reference overnight labeling at 37°C with the lid closed. Pointing out, that the reaction time using the evaporative labeling method took only one hour, instead of overnight (16 h) with 3.03% higher sialylated peak area %. More interestingly, combination of the traditional closed lid method with the evaporative labeling approach (open lid) outperformed the overnight reference method,

both in overall performance (total peak areas) and in preserving the sialylated glycan structures but at a cost of an additional hour of the process. By all means in every instance, the evaporative labeling approach resulted in higher derivatization yield and greater sialylated peak area % values compared to the closed lid methods, as shown in Table 2.

Table 2. Effect of the different APTS labeling approaches of hIgG1 released *N*-linked glycans on overall fluorophore labeling performance (total peak area) and sialylated peak area % values compared to the traditional overnight 37°C labeling method. Separation and injection parameters were the same as in Figure 4.

Labeling method	Total peak area	Total peak area relative to reference	Sialylated peak area %	Sialylated peak area % relative to reference
1.0 h / 50°C; closed lid	19.79 ± 0.85	0.16	17.01 ± 0.22	0.95
1.0 h / 50°C; opened lid	89.90 ± .067	0.71	20.97 ± 0.31	1.17
Overnight (16 h) / 37°C; closed lid*	127.43 ± 1.02*	1.00*	17.94 ± 0.42*	1.00*
1.0 h / 50°C; closed lid. then 1.0 h / 50°C; open lid	163.67 ± 0.56	1.28	20.57 ± 0.40	1.14

* Reference values

Mechanically dispensing dry samples with very low reagent volumes (several microliters) is a challenging step in reductive amination based sugar labeling. Frequently used current protocols suggest the addition of 4.0 µl – 6.0 µl labeling mixture per reaction, making it difficult to uniformly mix the reactants in the microvials, leading to possible losses. To alleviate this issue, extra tetrahydrofuran (THF) was added to the labeling reaction to increase the reaction volume. THF was a practical choice as it is usually the solvent of the reducing agent (e.g., sodium cyanoborohydride) in the reaction mixture, thus, readily miscible with the labeling solution, not affecting the reaction. The increased volume could alter or prolong the reaction but fortunately THF have a low boiling point (66°C) supporting rapid evaporation during evaporative labeling. A comparative study was executed by using the evaporative open vial labeling method with the addition of zero, 5.0 and 10 µl THF to the reaction mixtures (total reaction volumes were 5.0, 10 and 15 µl, respectively). This extra THF greatly accommodated uniform sample uptake by providing the sufficient volume for proper mixing (e.g., by vortexing), which can be especially favorable for the automation of sample preparation. Importantly, the same

reaction times could be used as delineated in Table 1, due to the rapid evaporation of THF from the reaction mixture in the open vial labeling protocol. The results are shown in Table 3, featuring more than doubled peak areas, when 10 µl of extra THF was added to the labeling solution (total reaction volume was 15 µl). Notably, standard deviation was calculated from triplicates at each point, as before. Since neither the reaction time nor any other conditions were changed, sialic acid loss was also minimized.

Table 3. Peak area comparison using the open vial labeling approach of dry sugar samples with the addition of none (0 µl), 5 µl and 10 µl extra THF (total reaction volumes were 5, 10 and 15 µl, respectively). Labeling conditions: 60°C for 20 minutes with no extra 20% acetic acid added.

Extra THF (µl)	Total peak area	Sialylated peak area subset
0	25.13 ± 0.67	5.13 ± 0.18
5.0	26.28 ± 0.87	5.64 ± 0.32
10	57.72 ± 0.54	12.30 ± 0.42

5.2 Identification of the glycanprofile of standard PSA

The global *N*-glycosylation profile of standard PSA was analyzed in order to establish a reference point for the workflow development process. 40 cm effective length capillary was utilized to achieve high resolution glycan profile as depicted in Figure 6, wherein the 30 most relevant peaks are annotated. The name, structure, migration time and GU values of all identified glycans are listed in Table 4. The exoglycosidase based glycan sequencing process is shown in Figure 7, utilizing Sialidase A, β-Galactosidase and β-*N*-Acetyl Hexosaminidase, depicted by the corresponding traces. Sequence information was derived from the GU value shifts of the individual peaks as the result of the consecutive exoglycosidase treatments in [38]. Structures marked with '*' were suspected to contain NAG instead of G on either of their branches. These structures were identified only by their GU values, because no specific enzyme was available to digest NAG selectively. During the identification, the '*' peaks were compared to structures with G on both of their branches. Peak 37 had 0.5 higher GU value than peak 35 (A2G2) and peak 40 was similarly 0.5 GU higher compared to peak 38 (F(6)A2G2). After β-Galactosidase digestion peak 35 moved into peak 44 (A2G2→A2) and 38 into 45 (F(6)A2G2→F(6)A2) while peak 37 into 48 (A2G1NAG1→A2NAG1) and 40 into 49 (F(6)A2G1NAG1→F(6)A2NAG1). Due to the digestion the GU value decreased 2.3 times more in case of G2 structures compared to their G1NAG1 counterparts. The exact
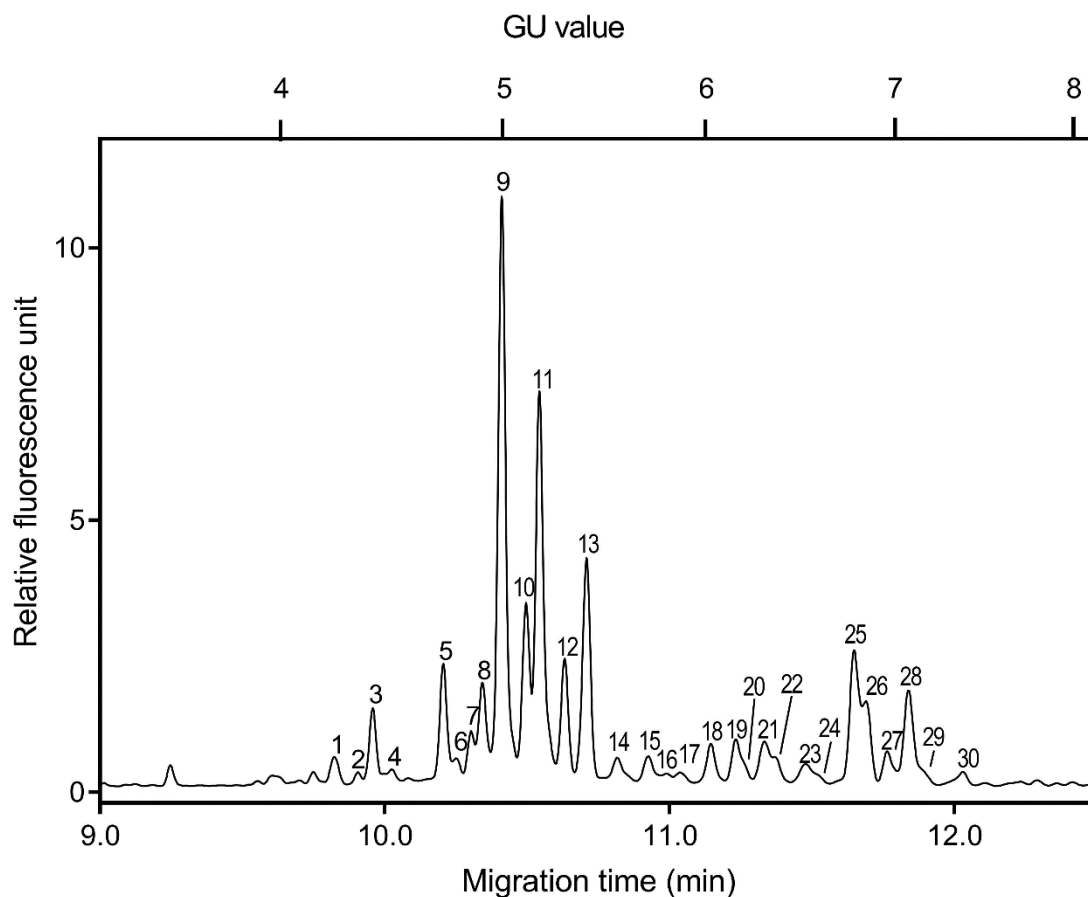
Figure 7. CE separation of the APTS-labeled standard PSA *N*-glycome. Separation conditions: 50 cm total (40 cm effective) length, 50 μm i.d. bare fused silica capillary with HR-NCHO gel buffer. Voltage: 30 kV (0.5 min ramp); Temperature: 25°C; Injection: 5 psi/5 sec water pre-injection followed by 5 kV/2 sec sample. Structures corresponding to peaks are listed in Table 4.

same ratio could be observed in the GU value change after β-*N*-Acetyl Hexosaminidase digestion between the two groups. The difference implied, that, while both branches were digested at structures containing G2, only one branch was digested from the G1NAG1 counterparts and the NAG containing branch stayed intact. Notably, comparing the sialylated G2 structures to their G1NAG1 counterparts (peak 5↔7, 9↔10, 11↔12, 13↔14, 19↔20, 22↔23, 25↔27, 28↔30) the GU difference was relatively similar in all instances. Also, as one can observe, all of the identified structures on the standard PSA sample were sialylated, emphasizing the advantage of CE-LIF as a gentle analytical technique being able to preserve sensitive glycan isomers. Orthogonal techniques, like MS often leads to de-sialylation due to in-source degradation [86]. Furthermore, the high resolution of CE-LIF was capable to readily differentiate the α2,3- and α2,6-sialylated isomers on mono- or multi-sialylated structures, which could be key for cancer diagnosis. Other PCa related alterations, like the degree of core fucosylation or branching could also

be traceable, especially after exoglycosidase sequencing. Both, the number of identified glycans as well as the high resolution separation with reliably trackable ratios of the given structures proved the high potential of this workflow as a possible PCa diagnostic tool.
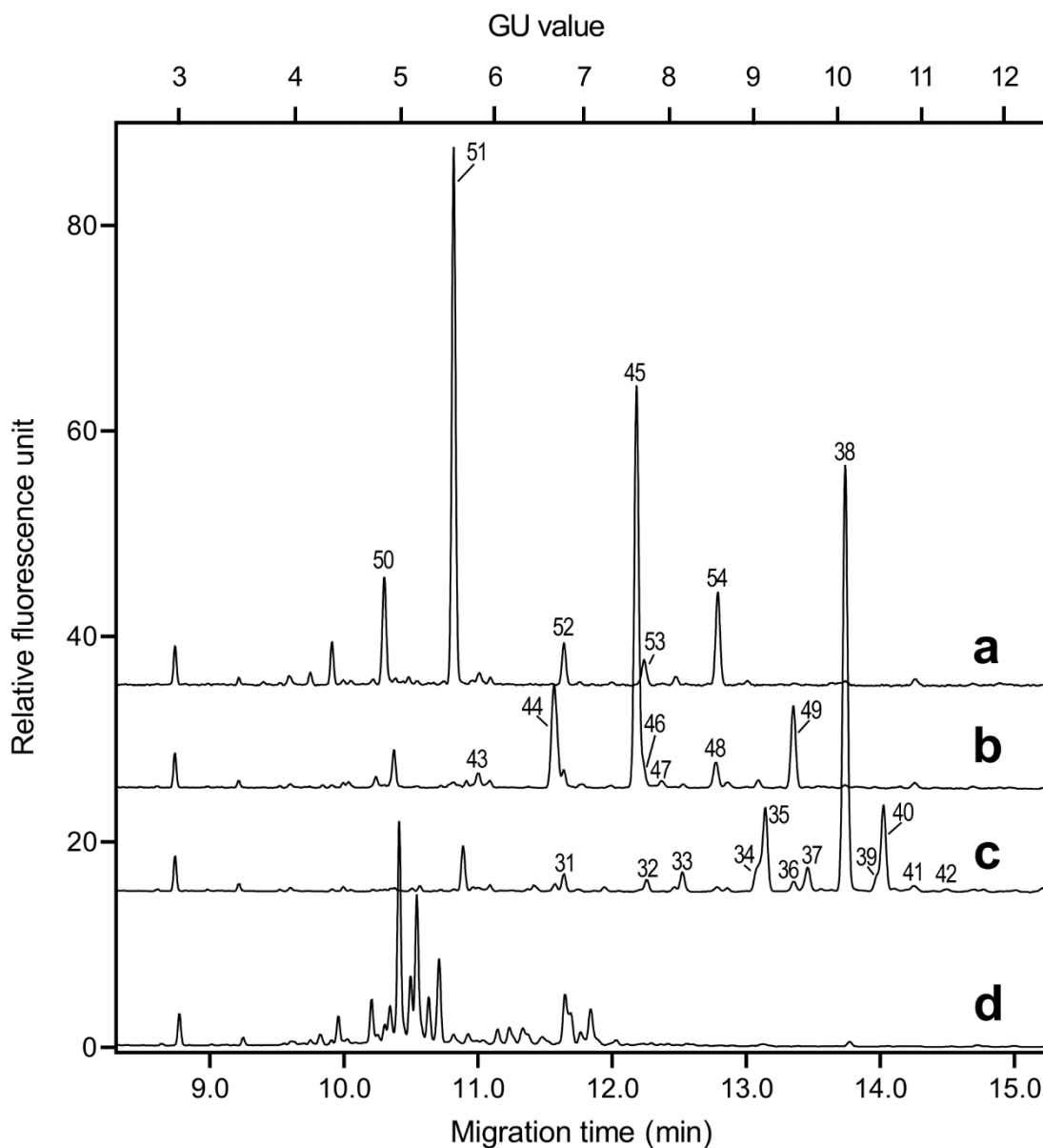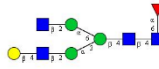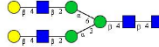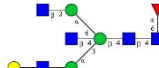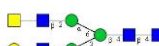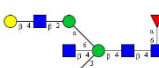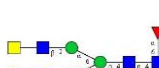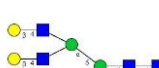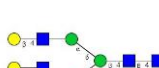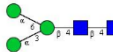
Figure 8. Exoglycosidase based sequencing of the *N*-glycome of the PSA standard. Standard PSA after Sialidase A, β-Galactosidase and β-*N*-Acetyl Hexosaminidase digestion (a) after Sialidase A, β-Galactosidase digestion (b) after Sialidase A digestion (c) and without digestion (d). Separation and injection parameters were the same as in Figure 6. Structures corresponding to peaks are listed in Table 4.
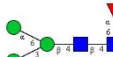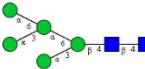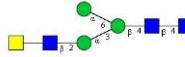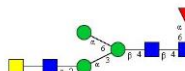
Table 4. Identified glycan structures from native PSA and glycan sequencing.

Glycan origin	Peak No.	Migration time (min)	GU	Glycan name	Glycan structure
Native PSA	1	9.82	4.24	A3G(4)3S(6,6,3,6)4	
	2	9.91	4.35	A3G(4)3S(3,6,3,6)4	
	3	9.96	4.41	A3G3(6,6,6)S3	
	4	10.03	4.51	A3G3(6,6,3)S3	
	5	10.21	4.73	A2G2(6,6)S2	
	6	10.25	4.79	A1[6]G(4)1(6)S1	
	7	10.30	4.85	A2G1NAG[6]1(6,6)S2*	
	8	10.34	4.90	A2G2(3,6)S2	
	9	10.41	4.99	F(6)A2G2(6,6)S2	
	10	10.50	5.11	F(6)A2G1NAG[6]1(6,6)S2*	
	11	10.54	5.18	F(6)A2G2(3,6)S2	
	12	10.63	5.30	F(6)A2G1NAG[6]1(3,6)S2*	
	13	10.71	5.41	F(6)A2G2(3,3)S2	
	14	10.82	5.56	F(6)A2G1NAG[6]1(3,3)S2*	
	15	10.92	5.71	A3G3(6,6)S2	

16	10.99	5.80	F(6)A2[6]G(4)1(6)S1	
17	11.04	5.87	F(6)A2[3]G(4)1(6)S1	
18	11.15	6.03	M5A1G1(6)S1	
19	11.23	6.16	A2G2(6)S1	
20	11.27	6.21	A2G1NAG1(6)S1*	
21	11.33	6.31	A3G3(3,3)S2	
22	11.37	6.36	M5A1G1(3)S1	
23	11.48	6.53	A2G2(3)S1	
24	11.53	6.60	A2G1NAG1(3)S1*	
25	11.65	6.78	F(6)A2G2(6)S1	
26	11.69	6.85	F(6)A2BG2S(6)1	
27	11.76	6.96	F(6)A2G1NAG1(6)S1*	
28	11.84	7.08	F(6)A2G2(3)S1	
29	11.89	7.16	F(6)A2BG2S(3)1	
30	12.04	7.39	F(6)A2G1NAG1(3)S1*	

Sequencing	31	11.67	6.82	A1G1	
	32	12.29	7.79	A2[6]G1	
	33	12.56	8.22	F(6)A1[3]G1	

34	13.12	9.11	F(6)A2[3]G1 + M5A1G1

35	13.17	9.20	A2G2

36	13.39	9.54	F(6)A2BG1

37	13.49	9.70	A2G1NAG1*

38	13.77	10.14	F(6)A2G2

39	14.01	10.52	F(6)A2BG2

40	14.06	10.60	F(6)A2G1NAG1*

41	14.28	10.96	A3[6]G3

42	14.52	11.35	A3[3]G3

43	11.02	5.86	A1

44	11.60	6.72	A2

45	12.21	7.67	F(6)A2

46	12.27	7.77	M5A1

47	12.40	7.97	A3

48	12.80	8.61	A2NAG1*

49	13.38	9.53	F(6)A2NAG1*

50	10.33	4.89	M3	
51	10.84	5.60	F(6)M3	
52	11.66	6.81	M5	
53	12.26	7.75	A1NAG1*	
54	12.81	8.63	F(6)A1NAG1*	

5.3   *N*-Glycan profiles of diluted semen and concentrated urine

Though, serum PSA test is one of the most common medical examination for PCa screening, the very low PSA concentration in blood allows only quantitative analysis and makes qualitative analysis rather challenging. In contrast, semen contains the highest PSA count, as PSA is one of the most abundant glycoproteins in semen [143], so it could be a beneficial source for glycan analysis, if the changes in PSA's glycan structures were reliably detectable in the total semen glycan profile. To ensure an ideal protein and salt concentration during sample preparation semen was diluted 5 times (Figure 8, trace b) and 50 times (Figure 8, trace c) with HEPES buffer. Both analyses resulted in similar *N*-glycan profiles with several individual sugar structures. Unfortunately, typical PSA glycan characteristics (Figure 8, trace a) were not recognizable from the profile, moreover, the peak intensities were minimal in the migration time frame, where PSA glycan peaks usually show maximum intensity.

Urine is the second most PSA-rich body fluid. Though, PSA concentration is too low for direct analysis, it can be viable after pre-concentration, as unlike in semen, the concentration of other potentially interfering glycoproteins is also limited. Initially, in the experiments, urine was concentrated by simple evaporation, but later the method was changed to spinfilter microfilters for reasons including 1) concentrating by evaporation requires elevated temperature, which can damage sensitive glycan structures, 2) increase the salt concentration in the sample, which can interfere with the rest of the sample preparation and also leads to precipitations.

Comparing the results of concentrated urine (Figure 8, trace d) to those obtained from diluted semen a bit higher peak intensity was obtained in the migration time frame of PSA glycans, though neither the urine nor the semen results did not match the standard PSA profile. In addition, both raw body fluid samples contained high concentration of small sugars (e.g., glucose), which could interfere with the sample preparation by reacting the labeling dye and displacing glycans from the magnetic beads during the step of washing off the remaining labeling dye.
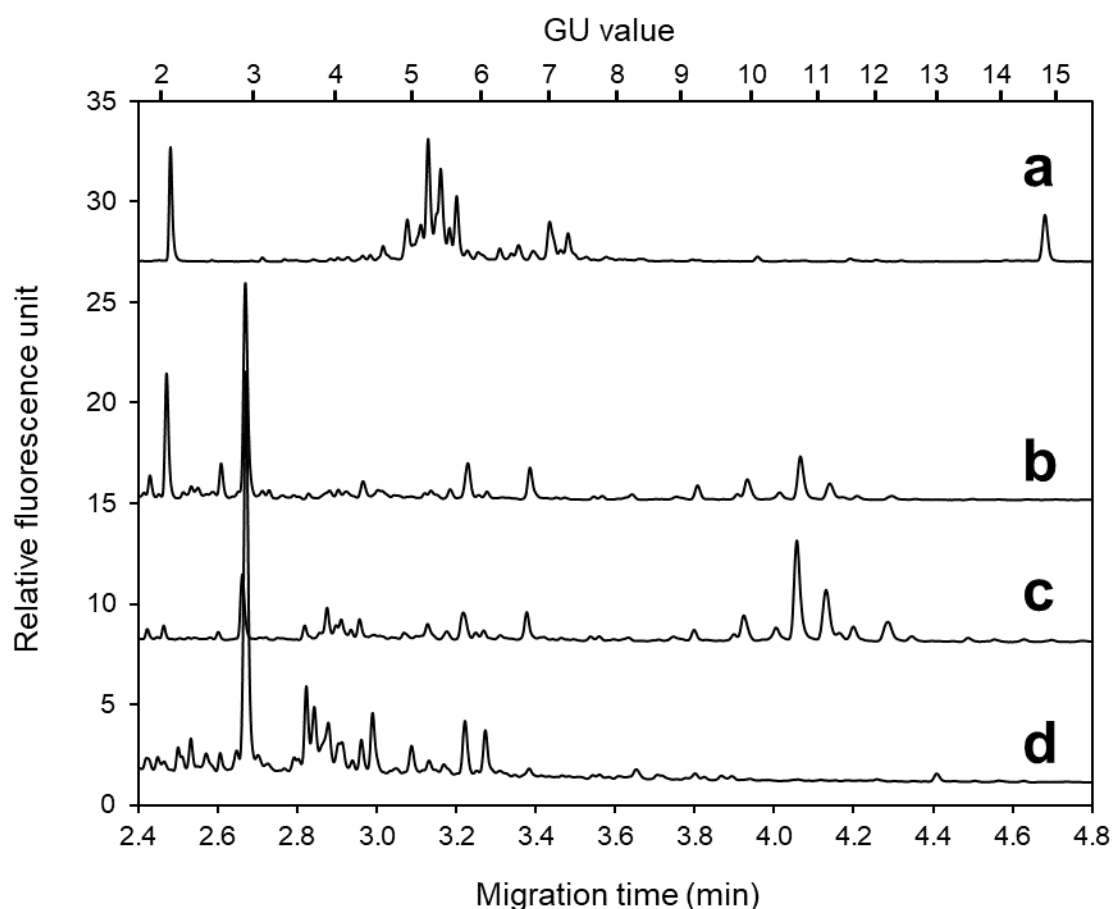
Figure 9. CE-LIF *N*-glycome analysis of standard PSA (a); 5 times diluted human semen (b); 50 times diluted human semen (c); 50 times concentrated human male urine (d); Separation conditions: 30 cm total (20 cm effective) length, 50 μm i.d. bare fused silica capillary with HR-NCHO gel buffer. Voltage: 30 kV (0.5 min ramp); Temperature: 25°C; Injection: 5 psi/5 sec water pre-injection followed by 2 kV/2 sec sample.

## 5.4 Selective urinary PSA capture and *N*-glycan analysis

All the drawbacks listed above implied the need for a selective procedure to analyze PSA from any biological matrices. To resolve this difficulty a complex multi-step procedure

was developed based on existing IP methods. The workflow started with the immobilization of the capturing agents to a surface, continued by the introduction of the sample containing the analyte, following by washing and/or elution steps and ending with the analysis of the target molecule. However, some specific modifications were required to fit the needs of the task.

First, the volume of the process had to be adjusted to the cross-section scale of both the available biological samples and the sample preparation for CE-LIF analysis. As the concentration of PSA is very limited in certain body fluids, high amount of sample is required to reach the limit of detection in the concentrated sample. The realization of IP could be challenging, that how to effectively introduce all the sample to the immobilized antibodies. Also, due to their high cost, the amount of applied capturing agent is also limited. To find a solution, microcolumns were taken into consideration, which fit perfectly between the microliter-milliliter scale. The beds were preliminary filled into 1 ml standard pipette tips, which also made the introduction of any solution to the surface very simple: the tips were fitted to an automated pipette and the required solution was continuously aspirated and dispensed through the tip.

The other innovation was the application of sdAbs over the traditional mAbs as capture agents. Nanobodies could be produced inhouse, which greatly increased their availability. Importantly, they were tagged with a 6-histidine linker to facilitate their immobilization to the surface of Ni-IMAC microcolumns. Combining these upgrades with evaporative labeling sample preparation process and the CE analysis a new 9-step workflow was created (Figure 9).
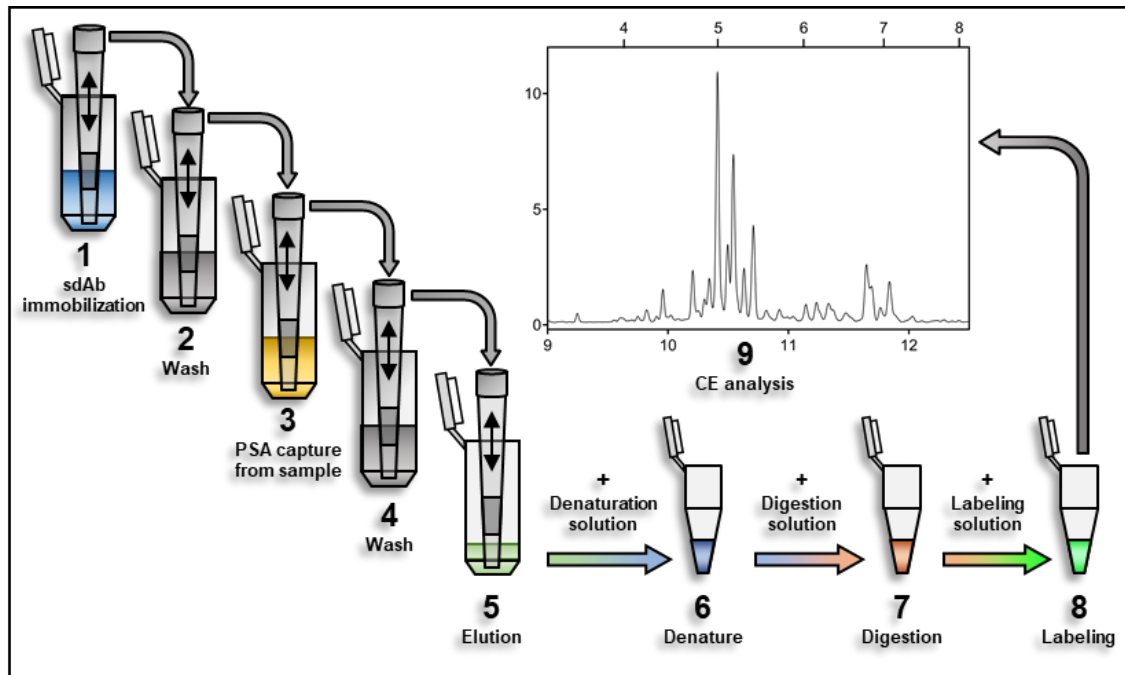
Figure 10. sdAb-based PSA capture and analysis workflow. 1) Immobilization of aPSA sdAbs to Ni-IMAC column; 2) Wash of excess sdAb; 3) PSA capture from sample; 4) Wash of sample residue; 5) Elution of antibody-PSA complex; 6) Denaturation of PSA; 7) *N*-glycan release by PNgase F digestion; 8) Fluorescent glycan labeling; 9) CE-LIF analysis.

5.4.1   Expression and purification of aPSA sdAbs

Saerens et. al. reported, that to provide sufficient PSA-binding agent, several aPSA single domain antibody sequences were selected by phage display using a variant library prepared from the variable domain of the heavy-chain antibody of dromedary immunized with PSA [139]. In order to be able to collect PSA even from low concentration body fluids, the two strongest PSA binder variants were chosen from the reported sequences, namely N7 ($K_d = 0.16$ nM) and C9 ($K_d = 4.7$ nM) (Figure 10). The sdAbs were expressed with fused histidine linkers to facilitate easy immobilization for affinity-based PSA capture.

C9 and N7 aPSA variants contain 2 and 4 cysteines, respectively, which makes proper protein folding less effective in the cytoplasm of standard *E. coli* strains (i.e. BL21 DE3 and its derivatives). Additionally, two cysteines from the N7 variant are located in the variable regions and supposedly form a stabilizing disulfide bond on the surface of the molecule. Periplasmic expression, which had been applied also for different aPSA variants [139], while supporting disulfide bond formation, usually results in lower protein yields. For this reason, Shuffle T7 Express cells were used for protein expression, which was an engineered *E. coli* B strain capable to promote disulfide bond formation in the

cytoplasm. These cells can express the disulfide bond isomerase DsbC, which promoted the correction of mis-oxidized proteins into their correct form [144,145]. As a result of applying an optimized in-house production protocol, typical yield for the aPSA variants was 8-12 mg/L culture.
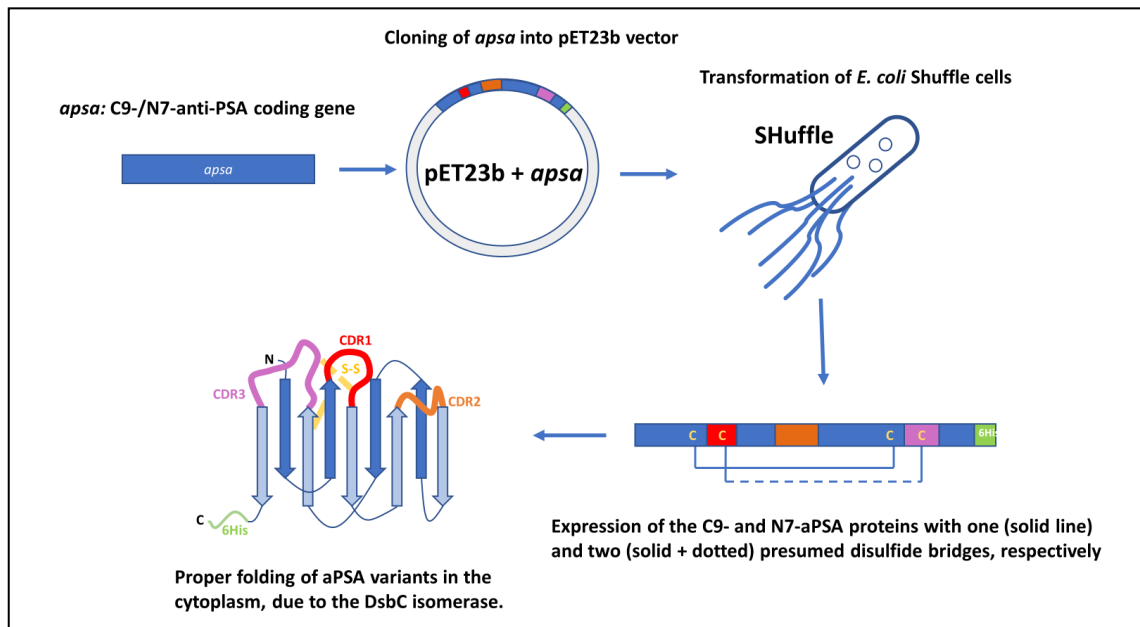

Figure 11. Schematic of the single domain anti-PSA production. Genes of strong PSA binder N7 and C9 SdAb aPSA variants were incorporated into the pET23b expression vector and the proteins produced in SHuffle T7 Express E. coli cells. SHuffle ensured the proper formation of disulfide bonds, thus appropriate folding of aPSA, resulting in soluble and functional antibody for selective capture of PSA from body fluids.

5.4.2 Immobilization of anti-PSA sdAbs

The first step of the PSA IP was the immobilization the nanobodies to the applied surface of microcolumns. The imidazole side-chain of histidine forms strong coordination complex with Ni (II) or Cu (II) ions [146], thus Ni-IMAC columns are widely applied tools for the cleaning of 6-His tagged recombinant proteins [147]. 50 mM of imidazole is usually added to avoid non-specific bond by serving as a competitive agent and repel proteins even with high histidine content. 6-His tag can bind strong enough to not to be affected by the presence of such low concentration inhibiting agent, but in higher concentration imidazole can be used for the removal of sdAb-PSA complexes from the surface in the elution step following the protein capture.

To find out if the sdAb could bind to the surface and the bound sdAb was able to capture PSA (the orientation was good) the applied solutions were analyzed by slab-gel electrophoresis (SGE). As Figure 11 shows, the initial nanobody solution had a high sdAb

concentration (A), which decreased steeply after the immobilization (B), but also found in high concentration in the eluted sample (C). When standard PSA solution (D) was flowed through the nanobody containing column, the PSA concentration level was examined (E), while both sdAb and PSA appeared in the elution (F). The results showed that even when bound to the surface, the nanobody was able to bind the PSA effectively, and, after that, the complex could be removed from the column.
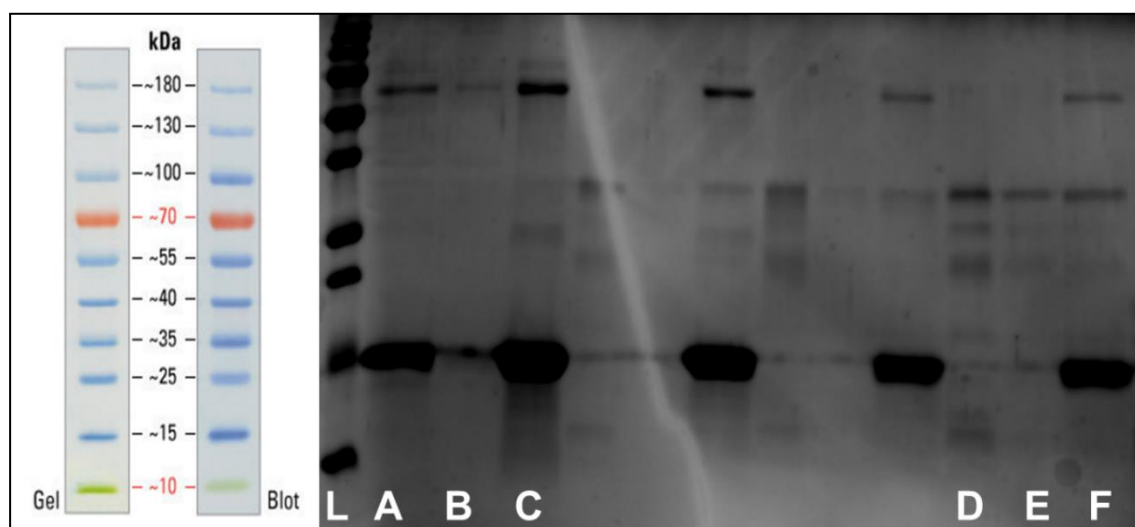

Figure 12. anti-PSA sdAb anchoring and PSA capture. L – ladder; A – anti-PSA sdAb solution before anchoring; B – washing buffer after anchoring; C – eluted anti-PSA sdAb; D – PSA standard solution; E – washing buffer after PSA capture; F – eluted PSA and anti-PSA sdAb.

To optimize the immobilization step, the nanobody concentration was monitored by a microvolume spectrophotometer. The results proved that the immobilization was very fast, after 5 minutes the concentration did not change significantly in the nanobody solution, the column was considered saturated, and only 50 µg/ml sdAb in 100 µl buffer was required to achieve that steadily. The washing buffer (containing 50 mM imidazole) did not remove significant amount of nanobody even in higher volumes (up to 1 ml), longer washing time (up to 30 min) or after several washing steps (up to 5 steps). On the other hand, even 100 µl of eluting buffer (containing 500 mM imidazole) was enough to remove all of the sdAbs from the column in less than 5 min. Notably, both C9 and N7 variants were tested, and they showed no difference in the immobilization tests.

5.4.3 Optimizing the elution

The captured glycoproteins had to be eluted from the column afterward the IP to be able to get analyzed. In recombinant protein cleaning processes, EDTA is a widely used
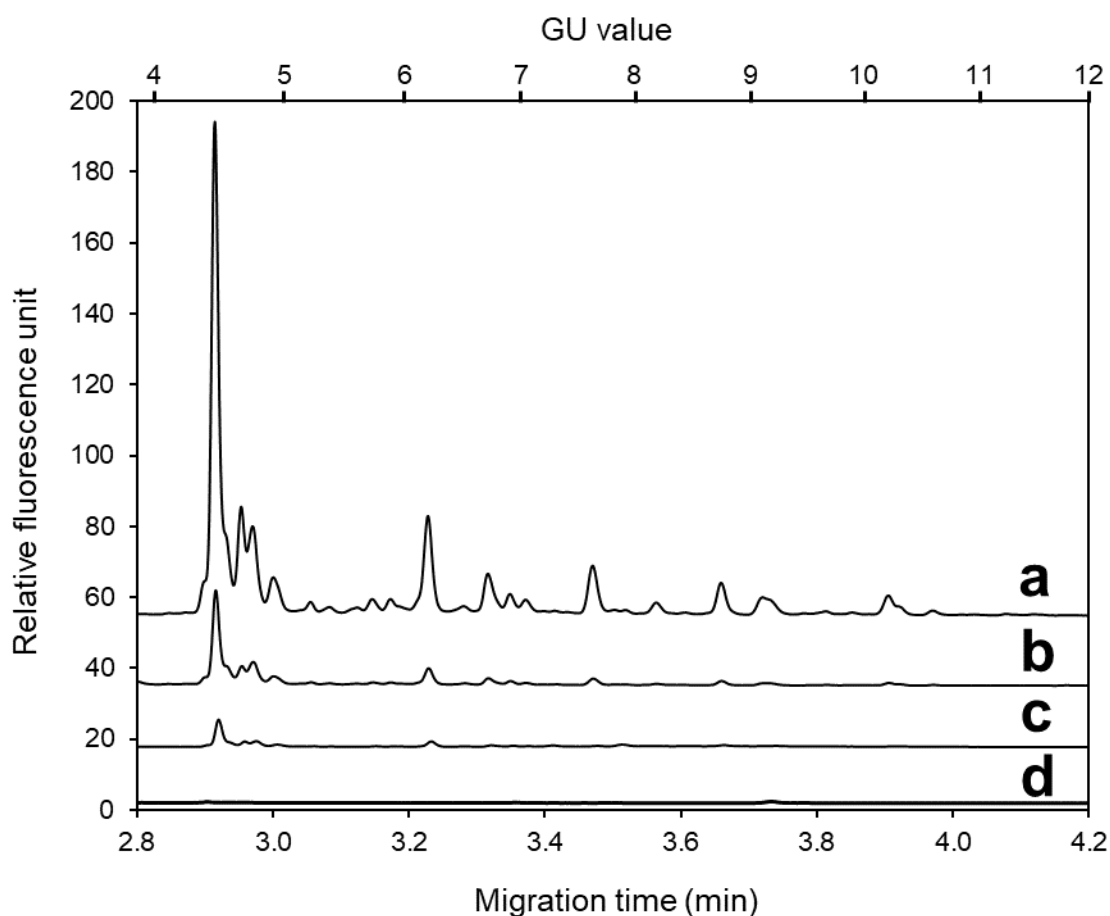
Figure 13. Comparison of the effect of different eluents on the sample preparation. 50x diluted human serum in H2O (a); Buffer 'A' (b); 50mM EDTA in H2O (c), 500mM EDTA in H2O (d); Separation and injection parameters were the same as in Figure 8.

chelation ligand with a high affinity constant to form metal-EDTA complexes, enabling to strip the column of nickel ions, which leads to breaking the linkage between the column and the 6-his tag of sdAbs. Initial tests showed that 500 mM EDTA removed both aPSA nanobody variants almost instantly from the column, but afterwards the PSA IP attempts resulted no detectable glycan peaks. It was suspected that the presence of EDTA might have an inhibiting effect on glycan labeling. To prove the theory four parallel sample preparations were initiated from human serum diluted 50 times by 500 mM EDTA (Figure 12, trace d), 50 mM EDTA (Figure 12, trace c), buffer 'A' (Figure 12, trace b) and water (Figure 12, trace a) for control. Both samples diluted by EDTA resulted in drastically reduced peak intensities compared to the control, proving that indeed EDTA disrupt the sample preparation process. As 50 mM concentration of EDTA showed some improvement to the 500 mM, a dilution series was prepared to define the limit of EDTA

in the sample, which no longer interfered with the analysis. The same test was repeated with EDTA concentrations of 50 mM, 2.4 mM, 113 µM, 5 µM and water for control. 113 µM or less EDTA had no effect on the results, resulting in the same peak intensity as of the control in Figure 12. Unfortunately, EDTA in that concentration was not able to reliably remove the nanobodies from the Ni-IMAC columns.

Buffer 'A' diluted sample outperformed both 50 and 500 mM EDTA samples but it was still below the control results. During the buffer 'A' sample preparation at the step of washing off the remaining labeling dye due to the addition of acetonitrile formation of second liquid phases were experienced. It was suspected that the high salt concentration can cause this effect by inhibiting the miscibility of aqueous and organic phases. In the next step if both phases were removed no glycan peaks were detected afterwards, if the aqueous phase remained the excess dye could not be removed effectively from the sample. The explanation to this can be that both labeled glycans and the remaining dye remained in the aqueous phase instead of the glycans adsorbed to the magnetic beads and the dye dissolved by the acetonitrile. Imidazole was tested in higher concentration (500 mM in water and as buffer 'B') and proved to be able to remove the nanobodies from the column but interfered with the sample preparation afterwards in every instance.

As the first step of the sample preparation was to denature the glycoprotein, that implied the idea, that it can be used for breaking the PSA-antiPSA complex without the necessity of removing the nanobodies from the column. By combining the two steps not just the workflow become simpler but the previous problems with EDTA and imidazole can be eliminated. For the implementation in a heating block 60 µl of denaturation solution was heated up to 80°C then the Ni-IMAC column pipette tip was immersed and the heated solution was aspirated and dispensed through the tip. The procedure successfully removed the PSA and also the majority of the nanobodies from the tip (checked via both NanoDrop and SGE). Unfortunately, the high volume denaturation solution interfered with the enzymatic cleavage of the glycans as it probably denatured even the somewhat resilient PNGase F enzyme as well. The amount of denaturation solution could not be lowered due to the limitations of the volume of the pipette and column. To avoid the negative effect on the digestion, the denatured sample was diluted by water. Several attempts were tried but unfortunately, it did not really solve the problem and also a significant amount of sample concentration was lost in the process.

Another solution was found by the application of centrifugal microfilters. With 10 kDa cut-off spinfilters the denaturation solution could be filtered from the sample. Washing it thoroughly by water removed the solution completely and from then on it did not interfere with digestion. Also, to continue the sample preparation, two approaches were tried. In the first, the enzymatic glycan digestion was executed on the filter, then the digested sugars (as they were <10 kDa) were filtered off from the proteins. This could be beneficial because denatured proteins in high concentration can form precipitates, which might adsorb glycans on their surface. Unfortunately, the digestion on the filter was not effective enough and only very limited results were obtained. On the other hand, recovering the sample from the filter, transfer it to a new vial and continue the sample preparation proved to be much better resulting in significantly higher analytical signals.
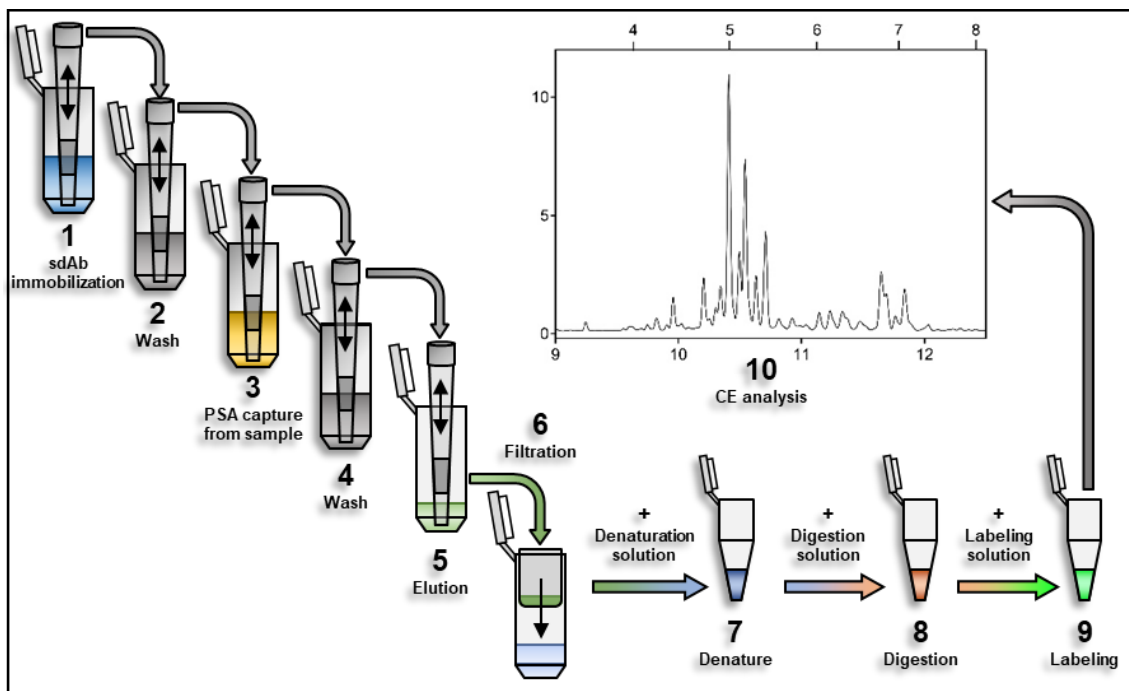
Figure 14. Capture and analysis workflow with filtration. 1) Immobilization of aPSA sdAbs to Ni-IMAC column; 2) Wash of excess sdAb; 3) PSA capture from sample; 4) Wash of sample residue; 5) Elution of antibody-PSA complex; 6) Filtration; 7) Denaturation of PSA; 8) *N*-glycan release by PNgase F digestion; 9) Fluorescent glycan labeling; 10) CE-LIF analysis.

The application of spinfilter opened a new window for the previous elution techniques as well, as it can be used to remove the unwanted EDTA, imidazole and other salts from the sample. Filtering, then recovering the eluted samples solved the interference problem with the rest of the sample preparation and resulted in similarly good results as of the method with denaturation. The same outcome was experienced when buffer 'B' was also

tested as eluting agent. As all three approaches worked broadly equally effective, finally the elution with buffer 'B' was selected, because it had a simpler setup, than the elution by denaturation and were closer in characteristic to the washing solution (buffer 'A'), than EDTA, therefore lowering the possibility of any interference by not adding a new component. The filtering added one plus step to the previous, initial workflow (Figure 13).

5.4.4   Immunoprecipitation of IgA by Z(IgA1)

As the availability of standard PSA was very limited the initial development of IP procedure had to utilize a more affordable glycoprotein target. For this purpose, IgA was selected because a stable amount was at hand as well as 6-His-tagged anti-IgA nanobodies (Z(IgA1)) were also available. Z(IgA1) is a specific IgA binding protein derived from the Z-domain of Protein A [148]. Notably, IgA is also in focus of current studies aiming to exploit its potential as a biomarker in different diseases [149].

In the initial experiments, Z(IgA1) was tested if it can be anchored similarly to aPSA and the results showed that both of the nanobodies behave in the same way during immobilization, the washing steps and the elution. Testing the capturing potential of Z(IgA1), at first, to avoid any possible matrix effect standard IgA in 0.2 mg/ml concentration dissolved in buffer 'A' was applied (Figure 14, trace b). For control the same sample was used, without the preliminary anchoring of the nanobodies to the microcolumn (Figure 14, trace d). From the CE analysis the same glycanprofile was obtained from the IgA capture as from the standard IgA (Figure 14, trace a) and no glycans were detected from the control. The results indicated that the nanobodies can preconcentrate the IgA from the diluted sample, while no non-specific interaction occurred between the column and IgA.

Next, testing possible matrix effects, male urine was spiked with IgA and the same IP was carried out. To avoid non-specific bindings, 50 mM imidazole was added to the urine as an inhibitor agent prior to the capture. Though, the analytical signal was lower than as at the capture from the buffer, the same glycanprofile was obtained without any visible interference from the matrix (Figure 14, trace c). In both instances, the IgA specific glycan peaks were identifiable, comparing to IgA standard control, and no additional sugar peaks appeared in the electropherogram.
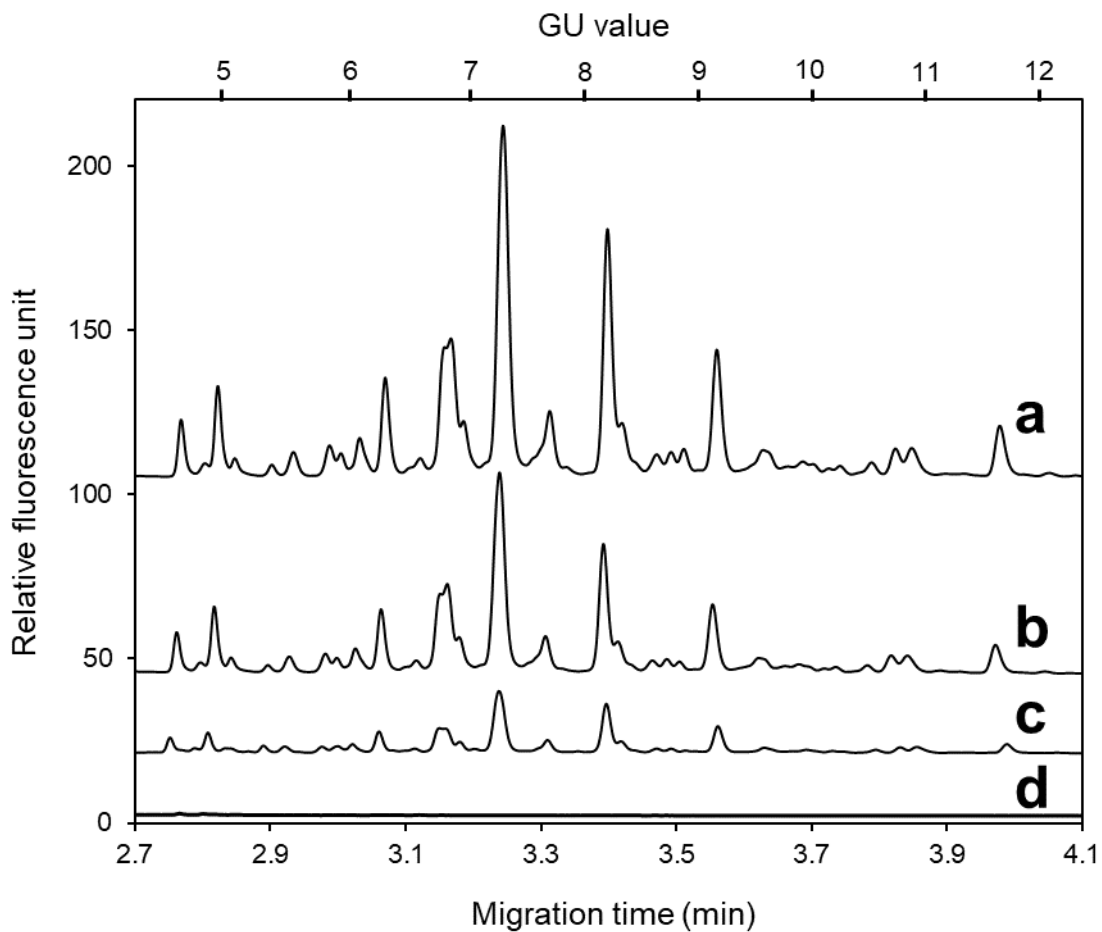
Figure 15. *N*-Glycan profile of standard IgA (2 mg/ml) (a), captured IgA from 0.2 mg/ml in buffer 'A' (b), captured IgA from 0.2 mg/ml spiked into urine (c) and control IP from 0.2 mg/ml in buffer 'A' without Z(IgA1) (d). Separation and injection parameters were the same as in Figure 8.

In the following step, the IgA IP was applied with more complex biological samples. The average IgA concentration in human serum is ~1,5 mg/ml [150], which makes IP possible, and serum also has a strong matrix effect from the high amount of other glycoproteins. To test the capability of the method two parallel captures ware initiated from human serum 50 times diluted with buffer 'A' and human serum was used for control. As the results show in Figure 15, the glycanprofile of the IgA captures were different from the ones from model test with standard IgA. Moreover, a similar glycanprofile, but at certain peaks with lower intensity was obtained using the control serum, which could indicate that other glycoprotein(s) could bind to the column non-specifically and then get eluted along with the Z(IgA1)-IgA complex.
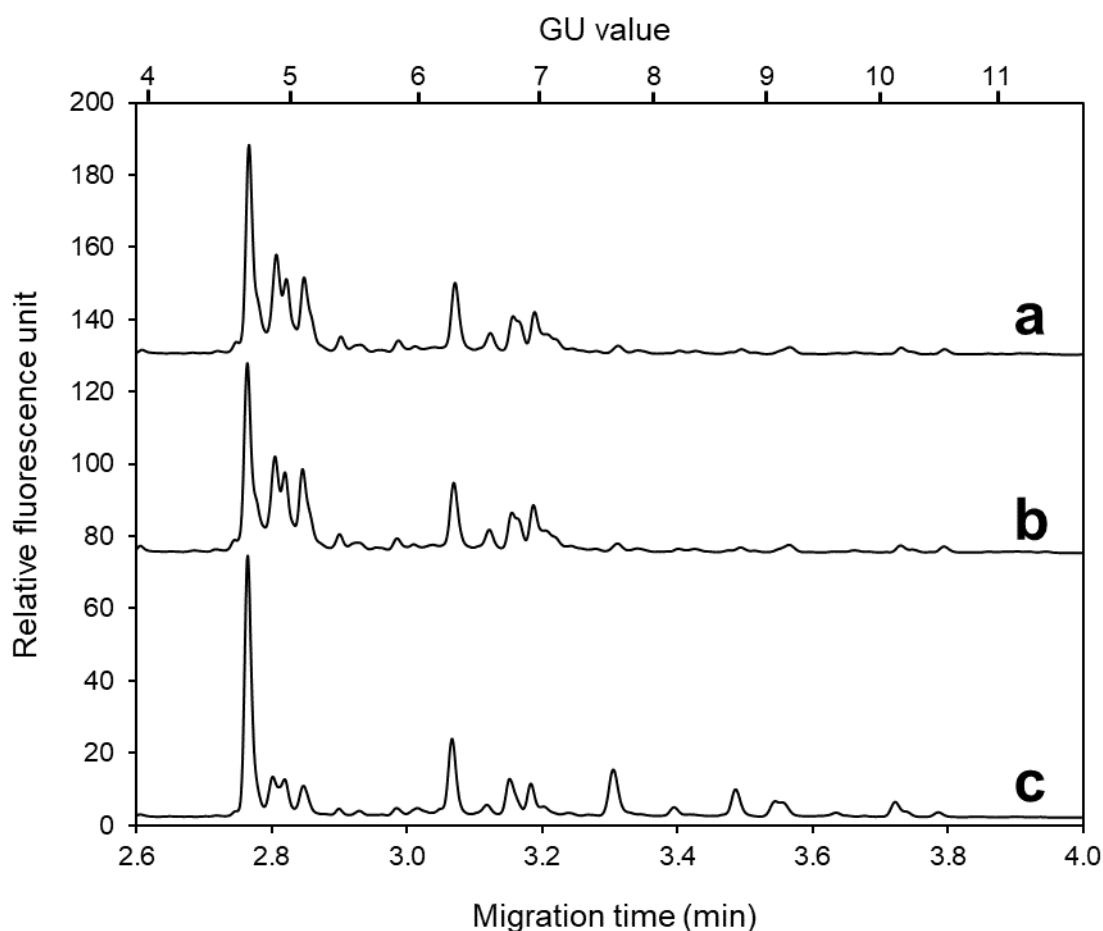
Figure 16. Glycanprofile of two parallels IgA IP from human serum (a and b) and human serum for control (c). Separation and injection parameters were the same as in Figure 8.

To discover the reason a new test was initiated in which an IgA IP from human serum 50 times diluted with buffer 'A' was realized but without Z(IgA1) immobilization (Figure 16, trace b). For comparison, human serum was used again (Figure 16, trace a). The glycan profiles showed that some glycoprotein could bind to the Ni-IMAC column despite of the 50 mM imidazole content of the diluting buffer. To try if the nanobodies has an effect on non-specific binding, the test was repeated with the replacement of Z(IgA1) by C9 antiPSA sdAb but there was no substantial difference comparing to the previous results.
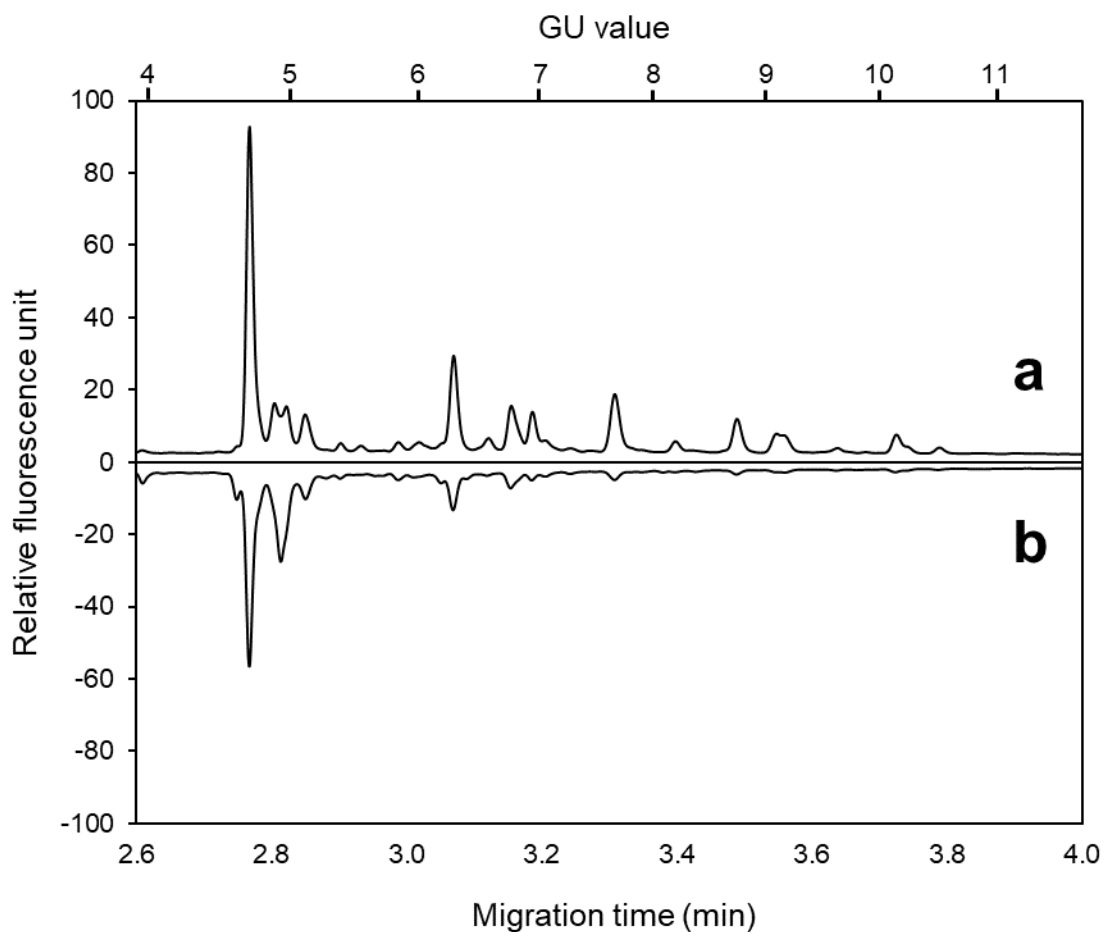
Figure 17. *N*-Glycan profile of serum capture with bare IMAC-Ni column (without Z(IgA1) immobilization) and serum control Separation and injection parameters were the same as in Figure 8.

This can be a limiting factor for the application of the column, therefore, it is always necessary to analyze the matrix effect otherwise it can lead to false results. Fortunately, there are several possible solutions to prevent non-specific bindings. Either increase the concentration or strength of the inhibiting agent (notably, the binding strength of the sdAb is a limiting factor for that), or masking the column surface with an inert but potent adsorbing agent, or change the column surface and the linker tags of the nanobodies to support more specific binding, which is not as sensitive for the matrix or changes of biological sample source with lower concentration of disturbing ingredients.

5.4.5 Avoid nonspecific binding

Several attempts were initiated to avoid the capture of undesirable glycoproteins from the sample matrix. One approach was to mask the surface of the Ni-IMAC column the other to add inhibiting agents to the sample to prevent unwanted bindings. The former was

implemented by pre-washing the column with a good adsorbent or complexing agent. For this purpose, traditionally cheap proteins with high availability and strong biding affinity are applied, like bovine serum albumin or milk proteins [151], but any potential glycan source can interfere with the analysis, thus, glycoproteins have to be excluded.
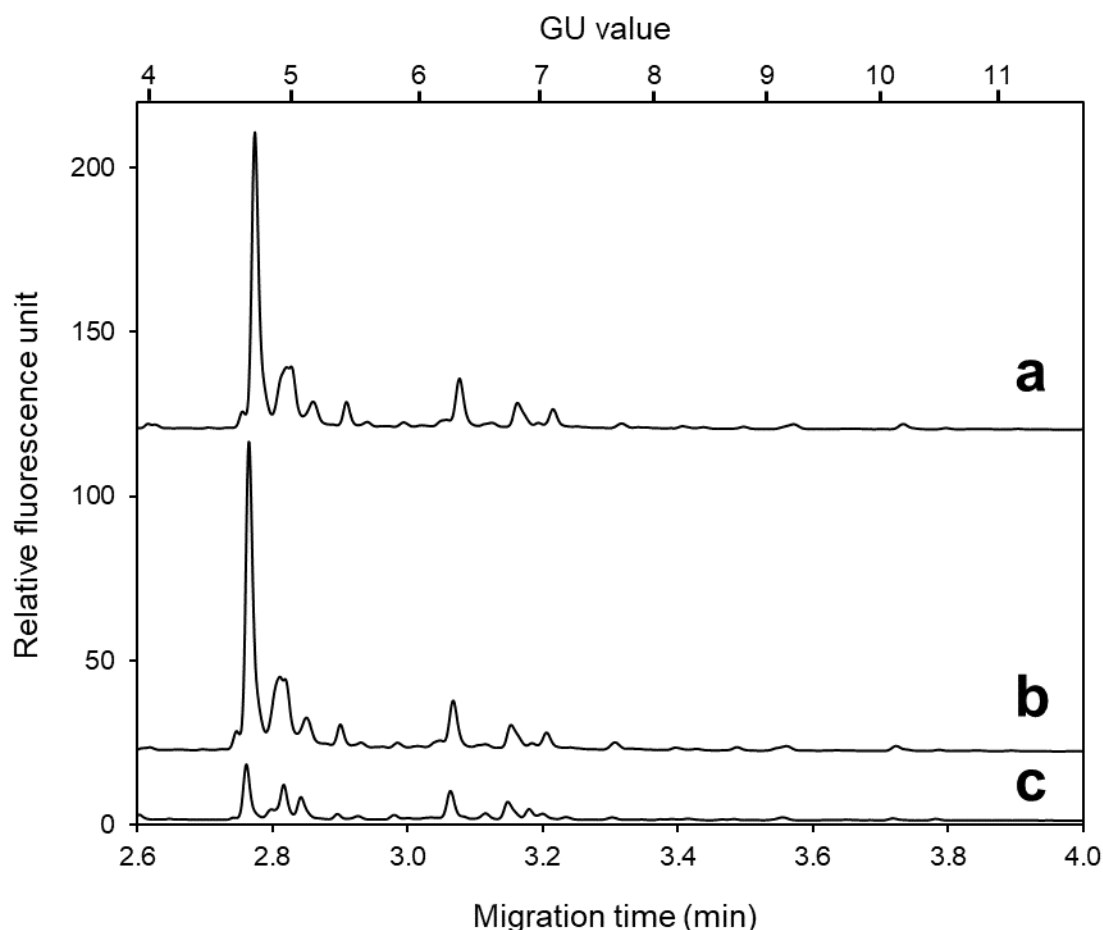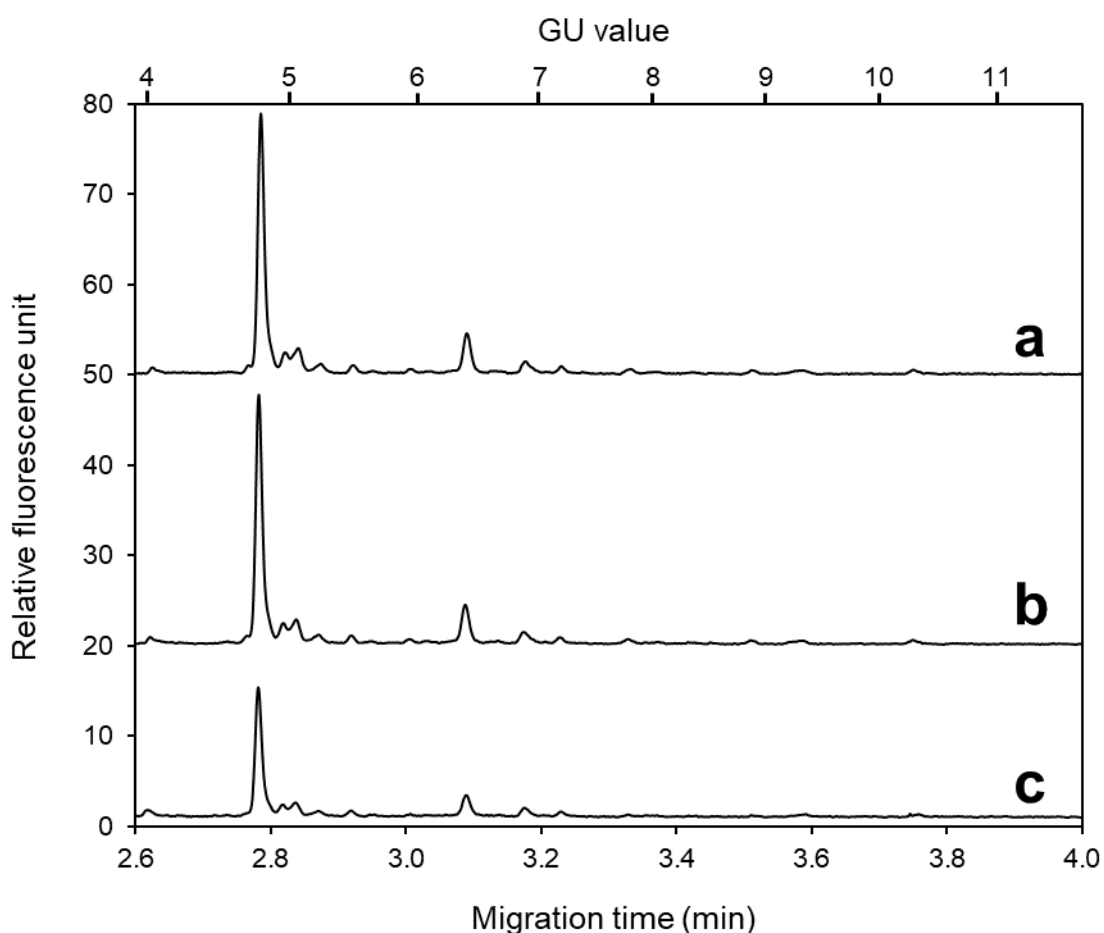

Figure 18. Blank IMAC-Ni column tests with serum capture without prewash for control (a); prewash with 25mg/ml PEG (MW:6000)(b); prewash with 50mM EDTA (c). Sequence: buffer 'A' wash → Prewash → buffer 'A' wash → capture from diluted human serum → buffer 'A' wash → elution with buffer 'B'. Separation and injection parameters were the same as in Figure 8.

Polyethylene glycol 6000 and EDTA were chosen instead in a concentration of 25 mg/ml and 50 mM respectively. In both instances a sdAb-free column was pretreated with 500 µl of masking agent, washed by 500 µl of buffer 'A', then the 50 times diluted human serum was introduced and the analysis continued as of the IgA capture without Z(IgA1) immobilization in point 5.4.4. As a control, the same process was used without the prewash. From the results in Figure 17 it can be seen that the PEG pretreatment (Trace b)

had no effect, while EDTA (Trace c) lowered and could not prevent totally the non-specific binding.

The other approach was the addition of inhibiting agents to the serum. 2-merkaptoethanol and surface-active ingredients, namely Triton X 100 and NP-40 were selected for this purpose. Three parallel capture experiments were initiated (all of them without sdAb immobilization), one from serum 50 times diluted by buffer 'A', plus 1% Triton X 100, plus 1 mM 2-merkaptoetanol (Figure 18, trace a), one from serum 50 times diluted by buffer 'A', plus 1% NP-40, plus 1 mM 2-merkaptoetanol (Figure 18, trace b) and one from serum 50 times diluted by buffer 'A' for control (Figure 18, trace c). In the results, oddly, an increase in peak intensity was observed due to the addition of inhibiting agents in both instances compared to the control.


Figure 19. Blank IMAC-Ni column tests with 50 times diluted serum with the addition of inhibiting agents: 1% Triton X 100, 1 mM 2-merkaptoetanol (a); 1% NP-40, 1 mM 2-merkaptoetanol (b) and no inhibiting agent for control (c). Separation and injection parameters were the same as in Figure 8.

Our results suggested that traditional masking or inhibiting methods were not effective to counter the non-specific bindings of certain serum glycoproteins on the Ni-IMAC surface. This effect can limit the application of the method to body fluids other than human blood. However, it should be noted, this can be a problem also when urine is used as a PSA source if some blood could mix with the sample, as the coherence of cancerous tissues are often corrupted, blood can leak into the urinary system. This problem was occurred when the PSA capturing procedure was tried on urine originated from a patient with advanced PCa cancer (data not showed). To overcome this issue further experiments should be done to find a suitable inhibiting agent or, as another approach, the Ni-IMAC – 6-His surface – linker tag pair should be changed to any surface with lower adsorbing potential.

5.4.6   Alternate sdAb immobilization

To avoid non-specific bindings from the biological matrix a different surface and immobilization method was investigated whether it can prevent the unwanted negative effect. Glass surface was chosen for that purpose as it has a lesser adsorbing potential compared to the chelating Ni-IMAC. As no specific linker tag was available for glass a slightly more complex covalent linkage formation was required to properly anchor the aPSA sdAbs [152]. First, glass beads were treated by (3-aminopropyl)triethoxysilane, which is a commonly used in the process of silanization, the functionalization of surfaces with alkoxysilane molecules. Then the activated surface was reacted with glutaraldehyde and finally the nanobodies were attached by reductive amination in the presence of 2-picoline-borane complex. The covalent link was beneficial to allow more intense washing processes between the steps of the capture because there was no risk of unintentionally losing the sdAbs during them. Notably, for the elution of the nanobody-antigen complex after the capture, no simple method was available either. Therefore, denaturation was applied to break the complex and elute only the target protein. It should be pointed out, if the denaturation is reversible for the nanobodies, this procedure could allow the reapplication of the sdAb coated beads over and over again, greatly reducing the binding agent requirements. In our experiments, both C9 and N7 variants were tested on urine and semen as well by mixing the glass beads into the matrixes. For control, untreated beads were applied, and standard PSA was used as reference. As the results show (Figure 19), unfortunately, the PSA glycan profile was not recognizable in any of the samples and
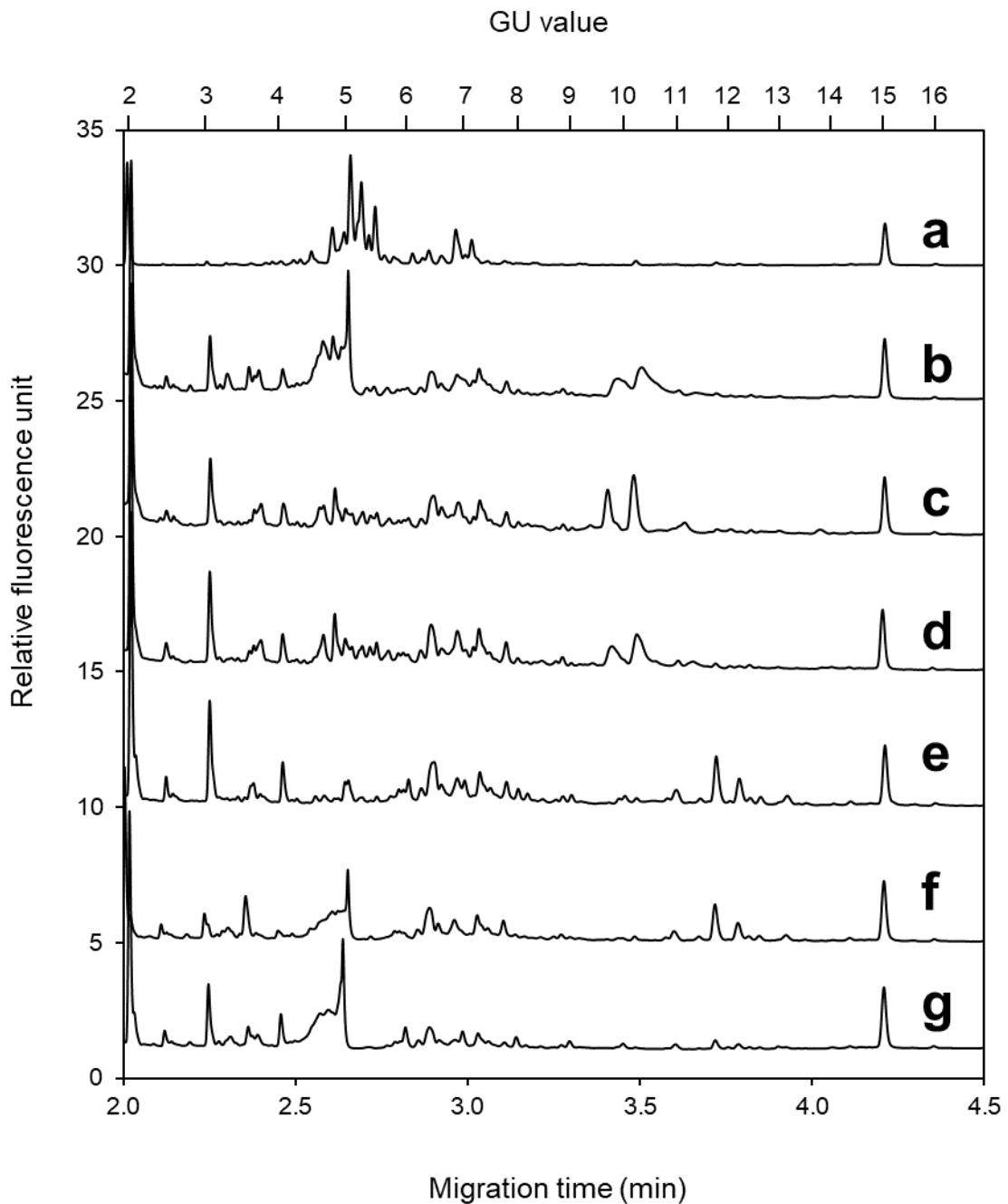
Figure 20. Glycan profiles of PSA IPs by sdAb immobilized to glass beads. Standard PSA for control (a); capture from urine with C9 sdAbs (b); capture from urine with N7 sdAbs (c); capture from urine without sdAbs for control (d); capture from semen with C9 sdAbs (e); capture from semen with N7 sdAbs (f); capture from semen without sdAbs for control (g). Separation and injection parameters were the same as in Figure 8.

there was no significant difference between the sdAb treated and control beads. The reason could be the decrease of the surface area. The special internal structural design of

the microcolumns provides a huge surface area, on the contrary, the solid glass beads do not possess hollowed structures, which lowers its surface area leading to a possible lower nanobody count. This effect could be counterbalanced by either decreasing the size of the beads to increase the specific surface area, or increasing the amount of beads applied or concentrating the sample to increase the effectiveness of the IP.

5.4.7   PSA immunoprecipitation from concentrated urine

Preliminary experiments suggested that the LoD was approximately 500 ng of standard PSA in 10 µl sample for the CE analysis of released *N*-glycans. Taking the LoD value into consideration for selecting the optimal biological sample source, blood had to be excluded due to its very low PSA concentration. Standard PSA-ELISA tests of our urine samples resulted in an average concentration of 60 ng/ml with a maximum of 120 ng/ml and a minimum of 30 ng/ml, which was slightly lower comparing to literature data [13]. Results varied on a high scale between the samples from different test subjects as well as from the same test subject but different sampling dates. The PSA-ELISA method was developed for testing blood PSA level, thus a female urine sample was also processed as negative control, resulting in 0 ng/ml PSA. Female urine was also spiked with standard PSA for positive control, resulting in the expected concentration. Control results suggested that the urine matrix did not affect the accuracy of PSA-ELISA tests. Considering the lowest concentration, a minimum requirement was 150 ml of urine to reliably obtain sufficient quantity of PSA for IP and analysis.

In order to effectively introduce all of the required urine to the column, its volume had to be reduced to the 1 ml scale (i.e., to fit in a 1000 µL pipette tip based affinity columns). Simple evaporation of the water content of the samples was problematic as precipitation was experienced and also the higher temperature could lead to possible loss of sensitive sialylated sugar structures. Therefore, 10 kDa cut-off value filters were utilized (Figure 20/1b), which could retain PSA effectively, while letting through the solvent and small contaminants (e.g., sugars). Then the filtrate was washed by then suspended in buffer 'A' and transferred into a new vial. Changing the urinary matrix to buffer was beneficial in multiple levels. It contributed to avoid any possible undesirable effect on the sdAb IP due to the variable urinary pH as well as introduced imidazole as an inhibiting agent to prevent non-specific bindings of remaining (>10 kDa) urine components.
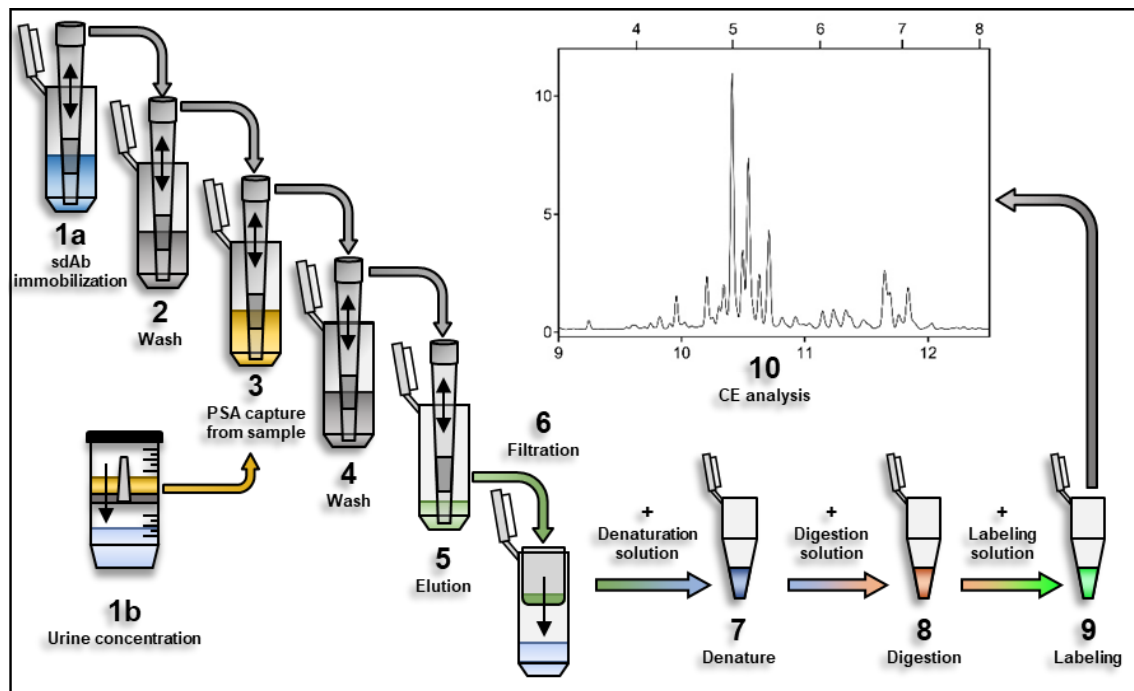
Figure 21. Urinary PSA analysis workflow. 1a) Immobilization of aPSA sdAbs to Ni-IMAC column; 1b) Concentration of urine via spinfilters; 2) Buffer wash 3) PSA capture from urinary matrix; 4) Buffer wash 5) Elution of antibody-PSA complex; 6) Desalting and concentration; 7) Denaturation of PSA; 8) *N*-glycan release by PNgase F digestion; 9) Fluorescent glycan labeling; 10) CE-LIF analysis

Similarly to IgA, the initial test of the PSA IP was facilitated with standard PSA spiked into buffer 'A'. The glycan profile of captured PSA (Figure 21, trace a) was corresponding to the standard PSA profile. To evaluate the matrix effect of urine, standard PSA was also spiked into and then captured from female urine, resulting similar yields in analytical signal compared to the spiked buffer, as well as, similar glycan profile (Figure 21, trace b) as of the standard PSA, suggesting that as in case of Z(IgA1), aPSA sdAbs were neither negatively affected by the matrix. The results of concentrated and immunoprecipitated male urine were also corresponding with both spiked variants (Figure 21, trace c). To verify that all the resulted glycans were originated from urinary or spiked PSA, unspiked female urine was used as a control (Figure 21, trace d), in which case no glycan related peaks were detected. From concentrated and immunoprecipitated male urine 19 corresponding structures were identified and their peak area distribution was also similar to the standard. Please note, 20 cm effective length capillary was utilized for the separation of the captured urinary PSA glycans as the development was aimed of a fast, high-throughput method, which can be readily adapted into the clinic. No desialylated glycans were found, proving that both the analytical tool and the selective capture procedure provided sufficiently mild conditions to preserve sensitive sugar

structures, e.g., sialic acids. As with the standard PSA, the α2,3- and α2,6-sialylated isomers were separated on both mono- and multi-sialylated structures, as well as, the core fucosylated or bisecting structures.
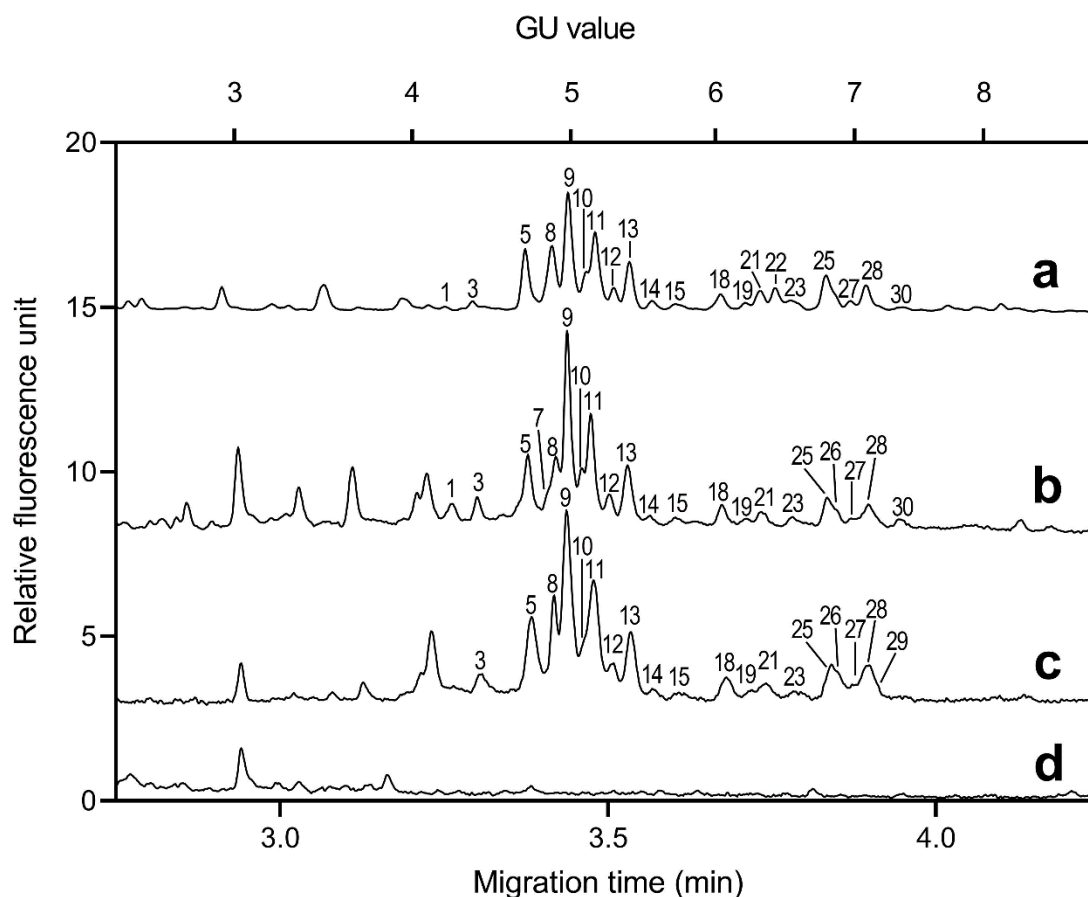
Figure 22. CE of the immunoprecipitated standard PSA spiked into buffer (a), immunoprecipitated standard PSA spiked into female urine (b), immunoprecipitated male urinary PSA *N*-glycome (c) and female urine control (d). Separation and injection parameters were the same as in Figure 8. Structures corresponding to peaks are listed in Table 4.

Relatively few studies investigated urinary PSA *N*-glycosylation. In one of them [70], a RP-ESI-MS based method was applied for the analysis of chymotrypsin digested PSA glycopeptides from pooled semen and urine. From the pooled urine samples, 8 different glycan structures were identified. Another, previously reported CE-LIF based urinary protein *N*-glycosylation analysis study identified 11 different structures [80], but none of them was sialylated as the sample preparation applied enzymatic de-sialylation. Also, without selective isolation of PSA, the entire urinary *N*-glycome was analyzed including other secreted glycoproteins. In another recent report [87], a similar nanobody-based capturing technique was reported for the IP of PSA, followed by CE-ESI-MS analysis. In

this study, several glycan structures were identified, including sialylated or also NAG-containing ones and the differentiation of $\alpha2,3$- and $\alpha2,6$-sialylated isomers were also realized. The reported structural information was remarkable, but translation of the method into a possible diagnostic tool was limited due to the complex analytical process, expensive equipment requirement and the relatively high separation time (60 min).

6   Conclusions

Prostate cancer is the most common cancer and the third-leading cause of cancer-death in men. Serum PSA tests greatly reduced fatal cases. However, because of the current PSA test is not PCa specific, the false positive rates and concomitantly unnecessary treatments increased. The unreliability of PSA assay more and more often questions the viability of this assay and represents an urgent need for alternative or complementary tests. Several new biomarker candidates were discovered in the past decades and among them, PSA *N*-glycosylation showed high potential to enhance the specificity and selectivity of this widely used test. Significant alterations were discovered in PSA glycosylation as a result of PCa, which can help to distinguish healthy samples from benign and malicious transformations. Characterization of these changes can be a challenging analytical task in many instances as PSA had to be partitioned from highly complex biological samples, like serum or urine.

During my doctoral curse a new workflow was developed to isolate PSA from urine samples by immobilized antiPSA nanobodies on IMAC-Ni microcolumns. The sdAbs were produced in-house and were engineered with a special linker tag to help their anchoring to the column matrix. The usage of sdAbs over mAbs may facilitate extension of the application in future clinical tests as their production even at larger quantities is possible with lower costs. The selective capturing procedure contributed both to remove other glycoprotein contaminants from the biological matrix and pre-concentrating the PSA content. The optimized, reductive amination based carbohydrate labeling, utilizing a novel, open vial based fluorophore tagging approach lead to higher detection signal, while still preserving the sensitive structures. The CE-LIF analysis of the released glycans from urinary PSA resulted in 19 structures out of the 30 obtained from standard PSA. Each identified glycan structure originated from native PSA was sialylated, suggesting that the mild conditions of both the capture and analysis procedure truly preserved labile sugar residues, e.g., sialic acids. Due to the high resolving power of CE, both the fucosylated and non-fucosylated structures as well as the α2,3- and α2,6-sialylated isomers were separated. Since the most common cancer related alterations are reportedly associated with these structures, it was key for any diagnostic application to reliably detect any possible changes in these residues. Furthermore, as not only glycan types but individual structures were identified more complex alterations could be discovered, which occurs in certain glycans only. My results showed that the developed workflow

was suitable for comprehensive *N*-glycan analysis of urinary PSA and could be a basis for future endeavors aiming to detect the alterations in PSA glycosylation caused by certain diseases like prostate cancer or benign prostatic hyperplasia.

7   Theses

Thesis 1. – Evaporative labeling

I developed a new sample preparation technique for the CE-LIF analysis of carbohydrates. The fluorescent labeling was executed in a novel open vial format, which greatly enhanced the reaction speed mediated by the continuously evaporating solvent. The reaction conditions, e.g. reaction time, temperature and reaction volumes were optimized and the results were compared by the derivatization yields, reaction time and the preservation of sensitive sugar structures. Yield maximalization was achieved by an overnight method suitable for research to obtain the highest amount of analytical information. An optimized 1-hour-method was also presented, which could promote a future diagnostical application. The evaporative labeling also enabled the addition of extra THF to the reaction mixture, which highly facilitated the even distribution of reaction mixture on the sample, while not effecting the reaction conditions.

Thesis 2. – Identification of standard PSA glycosylate

I fully mapped the *N*-glycan profile of standard PSA by CE-LIF, identifying 30 individual glycan structures by the application of both exoglycosidase glycan sequencing and the comparison of calculated GU values to literature data. Each glycan was sialylated, proving that the applied technique can preserve sensitive glycan structures, as well as α2,3 and α2,6 sialylation was differentiated to increase the value of diagnostical information.

Thesis 3. – Selective urinary PSA capture and glycan analysis

I developed, optimized and implemented a novel workflow for selective urinary PSA IP and analysis. Urinary PSA was immunoprecipitated from concentrated male urine by antiPSA sdAbs, which was preliminary expressed and purified, also with the addition of 6-His linker tag to facilitate the immobilization. The nanobodies were immobilized onto the microcolumns and the PSA capture was realized by flowing the concentrated urine through the column. The following elution and washing steps were optimized and the previously presented CE-LIF sample preparation steps were connected to the workflow. From male urine, 19 corresponding structures were identified compared to the standard.

8 Publications

Publications related to theses

Articles

B. Reider, E. Gacsi, H. Jankovics, F. Vonderviszt, T, Szarvas, A. Guttman, G. Jarvas, Integrated workflow for urinary prostate specific antigen *N*-glycosylation analysis using sdAb partitioning and downstream capillary electrophoresis separation, Anal Chim Acta, 1184:338892, 1 November 2021

B. Reider, G. Jarvas, A. Guttman, Separation based characterization methods for the *N*-glycosylation analysis of prostate specific antigen, J Pharm Biomed Anal, 194:113797, 5 February 2021

B. Reider, M. Szigeti, A. Guttman, Evaporative fluorophore labeling of carbohydrates via reductive amination, TALANTA 185: pp. 365-369. (2018)

Presentations

B.Reider, Prostate-specific antigen (PSA) immobilization from biological samples for capillary electrophoresis (CE) analysis, CECE, Veszprém, Hungary, October 11, 2017

B.Reider, Capillary electrophoresis (CE) based analysis of the possible alterations in prostate-specific antigen (PSA) glycoforms caused by prostate cancer, MKN, Veszprém, Hungary, April 27, 2017

Posters

B. Reider, D. Sárközy, H. Jankovics, G. Járvás, F. Vonderviszt, A. Guttman, Preconcentration of prostate-specific antigen (PSA) as a potential biomarker for prostate cancer from low-concentration medias for capillary electrophoresis (CE) analysis, MEDPECS, Pécs, Hungary, November 9, 2019

B. Reider, M. Szigeti, A. Guttman, High efficiency evaporative fluorophore labeling of glycans, CE Pharm, San Francisco, CA, USA, September 9-12, 2018

B. Reider, M. Szigeti, A. Domokos, A. Guttman, Evaporative fluorophore labeling, an effective novel tool in glycosylation analysis, AT Europe 2018, Barcelona, Spain, March 6-9, 2018

Publications not related to theses

Articles

B.Reider, H. Shao, G. Jarvas, A. Guttman; Z. Jiang, M. Taverna, N. T. Tran, On-line enrichment of N-glycans by immobilized metal-affinity monolith for capillary electrophoresis analysis, Analytica Chimica Acta, Volume 1134, 16 October 2020, Pages 1-9

Komaromy, B. Reider, G. Jarvas, A. Guttman, Glycoprotein biomarkers and analysis in chronic obstructive pulmonary disease and lung cancer with special focus on serum immunoglobulin G, Clinica Chimica Acta, Volume 506, Pages 204-213 (2020)

Presentations

B.Reider, Capillary electrophoresis based glycan analysis of tryptic digested serum proteins separated by hydrophilic interaction liquid chromatography, CECE, Gdansk, Poland, September 26, 2019

Posters

R. Farsang, B. Reider, G. Jarvas, A. Guttman, Preconcentration strategies for APTS labeled carbohydrate CE-LIF analysis, CECE, Brno, Czech Republic, October 15-17, 2018

L. Hajba, B. Reider, B. Borza, A. Guttman, High throughput glycan an alysis: the C100HT multicapillary electrophoresis system, CECE, Brno, Czech Republic, October 15-17, 2018

B. Reider, Zs. Kovács, B. Döncző, S. Dániel, C. Ruel, M. Taverna, T. Tran, A. Guttman, N-glycosylation modification analysis of several important serum glycoproteins in alzheimer's disease, Francia-Magyar Tudományos Kutatói Fórum, Budapest, Hungary, September 28, 2018

9   Acknowledgements

10 References

[1]   D. Thomas, A.K. Rathinavel, P. Radhakrishnan, Altered glycosylation in cancer: A promising target for biomarkers and therapeutics, Biochim. Biophys. Acta - Rev. Cancer. 1875 (2021) 188464. https://doi.org/10.1016/j.bbcan.2020.188464.

[2]   WHO Internetional Agency for Research on Cancer, (n.d.). https://www.iarc.who.int/.

[3]   R.D. Loberg, C.J. Logothetis, E.T. Keller, K.J. Pienta, Pathogenesis and treatment of prostate cancer bone metastases: targeting the lethal phenotype, J. Clin. Oncol. 23 (2005) 8232–8241. https://doi.org/10.1200/JCO.2005.03.0841.

[4]   J. Romero Otero, B. Garcia Gomez, F. Campos Juanatey, K.A. Touijer, Prostate cancer biomarkers: An update, Urol. Oncol. Semin. Orig. Investig. (2014). https://doi.org/10.1016/j.urolonc.2013.09.017.

[5]   M.J. Duffy, Biomarkers for prostate cancer: Prostate-specific antigen and beyond, Clin. Chem. Lab. Med. 58 (2020) 326–339. https://doi.org/10.1515/CCLM-2019-0693/PDF.

[6]   S. Saini, PSA and beyond: alternative prostate cancer biomarkers, Cell. Oncol. (Dordr). 39 (2016) 97–106. https://doi.org/10.1007/S13402-016-0268-6.

[7]   G.M. Yousef, E.P. Diamandis, The new human tissue kallikrein gene family: Structure, function, and association to disease, Endocr. Rev. (2001). https://doi.org/10.1210/er.22.2.184.

[8]   C.Y.F. Young, P.E. Andrews, B.T. Montgomery, D.J. Tindall, Tissue-specific and hormonal regulation of human prostate-specific glandular kallikrein, Biochemistry. (1992). https://doi.org/10.1021/bi00118a026.

[9]   D.A. Armbruster, Prostate-specific antigen: Biochemistry, analytical methods, and clinical application, Clin. Chem. (1993). https://doi.org/10.1093/clinchem/39.2.181.

[10]   A. CHRISTENSSON, H. LILJA, Complex formation between protein C inhibitor and prostate-specific antigen in vitro and in human semen, Eur. J. Biochem. (1994). https://doi.org/10.1111/j.1432-1033.1994.tb18597.x.

[11]   S.P. Balk, Y.J. Ko, G.J. Bubley, Biology of prostate-specific antigen, J. Clin. Oncol. (2003). https://doi.org/10.1200/JCO.2003.02.083.

[12]   C.M. Lynne, T.C. Aballa, T.J. Wang, H.G. Rittenhouse, S.M. Ferrell, N.L. Brackett, Serum and semen prostate specific antigen concentrations are different in young spinal cord injured men compared to normal controls, J. Urol. 162 (1999) 89–91. https://doi.org/10.1097/00005392-199907000-00022.

[13]   S. Bolduc, L. Lacombe, A. Naud, M. Grégoire, Y. Fradet, R.R. Tremblay, Urinary PSA: A potential useful marker when serum PSA is between 2.5 ng/ml and 10 ng/ml, J. Can. Urol. Assoc. 1 (2007) 377–381. https://doi.org/10.5489/cuaj.444.

[14]   S.E. Ilyin, S.M. Belkowski, C.R. Plata-Salamán, Biomarker discovery and validation: technologies and integrative approaches, Trends Biotechnol. 22 (2004) 411–416. https://doi.org/10.1016/J.TIBTECH.2004.06.005.

[15] A. Shoaibi, G.A. Rao, B. Cai, J. Rawl, K.S. Haddock, J.R. Hébert, Prostate specific antigen-growth curve model to predict high-risk prostate cancer., Prostate. 77 (2017) 173–184. https://doi.org/10.1002/pros.23258.

[16] A. Matoso, J.I. Epstein, Defining clinically significant prostate cancer on the basis of pathological findings., Histopathology. 74 (2019) 135–145. https://doi.org/10.1111/his.13712.

[17] W.J. Catalona, A.W. Partin, K.M. Slawin, M.K. Brawer, R.C. Flanigan, A. Patel, J.P. Richie, J.B. DeKernion, P.C. Walsh, P.T. Scardino, P.H. Lange, E.N. Subong, R.E. Parson, G.H. Gasior, K.G. Loveland, P.C. Southwick, Use of the percentage of free prostate-specific antigen to enhance differentiation of prostate cancer from benign prostatic disease: a prospective multicenter clinical trial., JAMA. 279 (1998) 1542–7. https://doi.org/10.1001/jama.279.19.1542.

[18] E.I. Canto, H. Singh, S.F. Shariat, D.J. Lamb, S.D. Mikolajczyk, H.J. Linton, H.G. Rittenhouse, D. Kadmon, B.J. Miles, K.M. Slawin, Serum BPSA outperforms both total PSA and free PSA as a predictor of prostatic enlargement in men without prostate cancer, Urology. 63 (2004) 905–910. https://doi.org/10.1016/J.UROLOGY.2003.12.037.

[19] B. V. Le, C.R. Griffin, S. Loeb, G.F. Carvalhal, D. Kan, N.A. Baumann, W.J. Catalona, [−2] pro-psa is more accurate than total and free psa in differentiating prostate cancer from benign disease in a prospective prostate cancer screening study, J. Urol. 183 (2010) 1355. https://doi.org/10.1016/J.JURO.2009.12.056.

[20] S. Loeb, M.G. Sanda, D.L. Broyles, S.S. Shin, C.H. Bangma, J.T. Wei, A.W. Partin, G.G. Klee, K.M. Slawin, L.S. Marks, R.H.N. van Schaik, D.W. Chan, L.J. Sokoll, A.B. Cruz, I.A. Mizrahi, W.J. Catalona, The prostate health index selectively identifies clinically significant prostate cancer., J. Urol. 193 (2015) 1163–9. https://doi.org/10.1016/j.juro.2014.10.121.

[21] D.J. Parekh, S. Punnen, D.D. Sjoberg, S.W. Asroff, J.L. Bailen, J.S. Cochran, R. Concepcion, R.D. David, K.B. Deck, I. Dumbadze, M. Gambla, M.S. Grable, R.J. Henderson, L. Karsh, E.B. Krisch, T.D. Langford, D.W. Lin, S.M. McGee, J.J. Munoz, C.M. Pieczonka, K. Rieger-Christ, D.R. Saltzstein, J.W. Scott, N.D. Shore, P.R. Sieber, T.M. Waldmann, F.N. Wolk, S.M. Zappala, A multi-institutional prospective trial in the USA confirms that the 4Kscore accurately identifies men with high-grade prostate cancer., Eur. Urol. 68 (2015) 464–70. https://doi.org/10.1016/j.eururo.2014.10.021.

[22] Z. Yang, L. Yu, Z. Wang, PCA3 and TMPRSS2-ERG gene fusions as diagnostic biomarkers for prostate cancer, Chin. J. Cancer Res. 28 (2016) 65–71. https://doi.org/10.3978/J.ISSN.1000-9604.2016.01.05.

[23] C. Song, H. Chen, Predictive significance of TMRPSS2-ERG fusion in prostate cancer: A meta-analysis, Cancer Cell Int. 18 (2018) 1–12. https://doi.org/10.1186/S12935-018-0672-2/FIGURES/5.

[24] S.A. Tomlins, J.R. Day, R.J. Lonigro, D.H. Hovelson, J. Siddiqui, L.P. Kunju, R.L. Dunn, S. Meyer, P. Hodge, J. Groskopf, J.T. Wei, A.M. Chinnaiyan, Urine TMPRSS2:ERG Plus PCA3 for Individualized Prostate Cancer Risk Assessment, Eur. Urol. 70 (2016) 45–53. https://doi.org/10.1016/J.EURURO.2015.04.039.

[25]   L. Van Neste, A.W. Partin, G.D. Stewart, J.I. Epstein, D.J. Harrison, W. Van
       Criekinge, Risk score predicts high-grade prostate cancer in DNA-methylation
       positive, histopathologically negative biopsies, Prostate. 76 (2016) 1078–1087.
       https://doi.org/10.1002/PROS.23191.

[26]   M.J. Donovan, M. Noerholm, S. Bentink, S. Belzer, J. Skog, V. O'Neill, J.S.
       Cochran, G.A. Brown, A molecular signature of PCA3 and ERG exosomal RNA
       from non-DRE urine is predictive of initial prostate biopsy result, Prostate Cancer
       Prostatic Dis. 2015 184. 18 (2015) 370–375. https://doi.org/10.1038/pcan.2015.40.

[27]   A. Sreekumar, L.M. Poisson, T.M. Rajendiran, A.P. Khan, Q. Cao, J. Yu, B.
       Laxman, R. Mehra, R.J. Lonigro, Y. Li, M.K. Nyati, A. Ahsan, S. Kalyana-
       Sundaram, B. Han, X. Cao, J. Byun, G.S. Omenn, D. Ghosh, S. Pennathur, D.C.
       Alexander, A. Berger, J.R. Shuster, J.T. Wei, S. Varambally, C. Beecher, A.M.
       Chinnaiyan, Metabolomic profiles delineate potential role for sarcosine in prostate
       cancer   progression,   Nature.   457   (2009)   910–914.
       https://doi.org/10.1038/NATURE07762.

[28]   I. Kohaar, G. Petrovics, S. Srivastava, A Rich Array of Prostate Cancer Molecular
       Biomarkers: Opportunities and Challenges, Int. J. Mol. Sci. 20 (2019).
       https://doi.org/10.3390/IJMS20081813.

[29]   P. Porzycki, E. Ciszkowicz, Modern biomarkers in prostate cancer diagnosis, Cent.
       Eur. J. Urol. 73 (2020) 300. https://doi.org/10.5173/CEJU.2020.0067R.

[30]   P. Blume-Jensen, D.M. Berman, D.L. Rimm, M. Shipitsin, M. Putzi, T.P. Nifong,
       C. Small, S. Choudhury, T. Capela, L. Coupal, C. Ernst, A. Hurley, A. Kaprelyants,
       H. Chang, E. Giladi, J. Nardone, J. Dunyak, M. Loda, E.A. Klein, C. Magi-
       Galluzzi, M. Latour, J.I. Epstein, P. Kantoff, F. Saad, Development and clinical
       validation of an in situ biopsy-based multimarker assay for risk stratification in
       prostate   cancer,   Clin.   Cancer   Res.   21   (2015)   2591–2600.
       https://doi.org/10.1158/1078-0432.CCR-14-2603.

[31]   A. Nevo, A. Navaratnam, P. Andrews, Prostate cancer and the role of biomarkers,
       Abdom.   Radiol.   (New   York).   45   (2020)   2120–2132.
       https://doi.org/10.1007/S00261-019-02305-8.

[32]   I. Häuselmann, L. Borsig, Altered tumor-cell glycosylation promotes metastasis,
       Front. Oncol. 4 (2014). https://doi.org/10.3389/FONC.2014.00028.

[33]   J. Munkley, D.J. Elliott, Hallmarks of glycosylation in cancer, Oncotarget. 7
       (2016) 35478–35489. https://doi.org/10.18632/ONCOTARGET.8155.

[34]   A. Kałuża, J. Szczykutowicz, M. Ferens-Sieczkowska, Glycosylation: Rising
       Potential for Prostate Cancer Evaluation, Cancers (Basel). 13 (2021).
       https://doi.org/10.3390/CANCERS13153726.

[35]   P.M. dos Santos Silva, P.B.S. Albuquerque, W.F. de Oliveira, L.C.B.B. Coelho,
       M.T. dos Santos Correia, Glycosylation products in prostate diseases, Clin. Chim.
       Acta. (2019). https://doi.org/10.1016/j.cca.2019.08.003.

[36]   B. Reider, G. Jarvas, J. Krenkova, A. Guttman, Separation based characterization
       methods for the *N*-glycosylation analysis of prostate-specific antigen, J. Pharm.
       Biomed. Anal. (2020) 113797. https://doi.org/10.1016/j.jpba.2020.113797.

[37] K. Mariño, J. Bones, J.J. Kattla, P.M. Rudd, A systematic approach to protein glycosylation analysis: A path through the maze, Nat. Chem. Biol. (2010). https://doi.org/10.1038/nchembio.437.

[38] M. Szigeti, A. Guttman, Automated *N*-glycosylation sequencing of biopharmaceuticals by capillary electrophoresis, Sci. Rep. 7 (2017). https://doi.org/10.1038/s41598-017-11493-6.

[39] A. Guttman, K.W. Ulfelder, Exoglycosidase matrix-mediated sequencing of a complex glycan pool by capillary electrophoresis, in: J. Chromatogr. A, J Chromatogr A, 1997: pp. 547–554. https://doi.org/10.1016/S0021-9673(97)00724-3.

[40] Y.E.M. van der Burgt, K.M. Siliakus, C.M. Cobbaert, L.R. Ruhaak, HILIC–MRM–MS for linkage-specific separation of sialylated glycopeptides to quantify prostate-specific antigen proteoforms, J. Proteome Res. (2020). https://doi.org/10.1021/acs.jproteome.0c00050.

[41] S. Ahuja, 1 Overview of HPLC method development for pharmaceuticals, Sep. Sci. Technol. (2007). https://doi.org/10.1016/S0149-6395(07)80007-9.

[42] L. Veillon, Y. Huang, W. Peng, X. Dong, B.G. Cho, Y. Mechref, Characterization of isomeric glycan structures by LC-MS/MS, Electrophoresis. 38 (2017) 2100–2114. https://doi.org/10.1002/elps.201700042.

[43] L.R. Ruhaak, G. Zauner, C. Huhn, C. Bruggink, A.M. Deelder, M. Wuhrer, Glycan labeling strategies and their use in identification and quantification, Anal. Bioanal. Chem. (2010). https://doi.org/10.1007/s00216-010-3532-z.

[44] C. Ashwood, B. Pratt, B.X. Maclean, R.L. Gundry, N.H. Packer, Standardization of PGC-LC-MS-based glycomics for sample specific glycotyping, Analyst. (2019). https://doi.org/10.1039/c9an00486f.

[45] S. Zhou, X. Dong, L. Veillon, Y. Huang, Y. Mechref, LC-MS/MS analysis of permethylated *N*-glycans facilitating isomeric characterization, Anal. Bioanal. Chem. (2017). https://doi.org/10.1007/s00216-016-9996-8.

[46] F. Higel, U. Demelbauer, A. Seidl, W. Friess, F. Sörgel, Reversed-phase liquid-chromatographic mass spectrometric *N*-glycan analysis of biopharmaceuticals, Anal. Bioanal. Chem. (2013). https://doi.org/10.1007/s00216-012-6690-3.

[47] P.J. Domann, A.C. Pardos-Pardos, D.L. Fernandes, D.I.R. Spencer, C.M. Radcliffe, L. Royle, R.A. Dwek, P.M. Rudd, Separation-based glycoprofiling approaches using fluorescent labels, Proteomics - Pract. Proteomics. (2007). https://doi.org/10.1002/pmic.200700640.

[48] K.Y. White, L. Rodemich, J.O. Nyalwidhe, M.A. Comunale, M.A. Clements, R.S. Lance, P.F. Schehhammer, A.S. Mehta, O.J. Semmes, R.R. Drake, Glycomic characterization of prostate-specific antigen and prostatic acid phosphatase in prostate cancer and benign disease seminal plasma fluids, J. Proteome Res. (2009). https://doi.org/10.1021/pr8007545.

[49] G.R. Guile, P.M. Rudd, D.R. Wing, S.B. Prime, R.A. Dwek, A rapid high-resolution high-performance liquid chromatographic method for separating glycan mixtures and analyzing oligosaccharide profiles, Anal. Biochem. (1996).

https://doi.org/10.1006/abio.1996.0351.

[50]   J.O. Nyalwidhe, L.R. Betesh, T.W. Powers, E.E. Jones, K.Y. White, T.C. Burch, J. Brooks, M.T. Watson, R.S. Lance, D.A. Troyer, O.J. Semmes, A. Mehta, R.R. Drake, Increased bisecting *N*-acetylglucosamine and decreased branched chain glycans of *N*-linked glycoproteins in expressed prostatic secretions associated with prostate cancer progression, Proteomics - Clin. Appl. (2013). https://doi.org/10.1002/prca.201200134.

[51]   T.M. Block, M.A. Comunale, M. Lowman, L.F. Steel, P.R. Romano, C. Fimmel, B.C. Tennant, W.T. London, A.A. Evans, B.S. Blumberg, R.A. Dwek, T.S. Mattu, A.S. Mehta, Use of targeted glycoproteomics to identify serum glycoproteins that correlate with liver cancer in woodchucks and humans, Proc. Natl. Acad. Sci. U. S. A. (2005). https://doi.org/10.1073/pnas.0408928102.

[52]   T. Yoneyama, C. Ohyama, S. Hatakeyama, S. Narita, T. Habuchi, T. Koie, K. Mori, K.I.P.J. Hidari, M. Yamaguchi, T. Suzuki, Y. Tobisawa, Measurement of aberrant glycosylation of prostate specific antigen can improve specificity in early detection of prostate cancer, Biochem. Biophys. Res. Commun. (2014). https://doi.org/10.1016/j.bbrc.2014.04.107.

[53]   R. Saldova, Y. Fan, J.M. Fitzpatrick, R.W.G. Watson, P.M. Rudd, Core fucosylation and α2-3 sialylation in serum *N*-glycome is significantly increased in prostate cancer comparing to benign prostate hyperplasia, Glycobiology. (2011). https://doi.org/10.1093/glycob/cwq147.

[54]   E. Llop, M. Ferrer-Batallé, S. Barrabés, P.E. Guerrero, M. Ramírez, R. Saldova, P.M. Rudd, R.N. Aleixandre, J. Comet, R. de Llorens, R. Peracaula, Improvement of prostate cancer diagnosis by detecting PSA glycosylation-specific changes, Theranostics. (2016). https://doi.org/10.7150/thno.15226.

[55]   A. Sarrats, R. Saldova, J. Comet, N. O'Donoghue, R. De Llorens, P.M. Rudd, R. Peracaula, Glycan characterization of PSA 2-DE subforms from serum and seminal plasma, Omi. A J. Integr. Biol. (2010). https://doi.org/10.1089/omi.2010.0050.

[56]   A. Sarrats, J. Comet, G. Tabarés, M. Ramírez, R.N. Aleixandre, R. De Llorens, R. Peracaula, Differential percentage of serum prostate-specific antigen subforms suggests a new way to improve prostate cancer diagnosis, Prostate. (2010). https://doi.org/10.1002/pros.21031.

[57]   X. Chen, G.C. Flynn, Analysis of *N*-glycans from recombinant immunoglobulin G by on-line reversed-phase high-performance liquid chromatography/mass spectrometry, Anal. Biochem. (2007). https://doi.org/10.1016/j.ab.2007.08.012.

[58]   J. Amano, T. Nishikaze, F. Tougasaki, H. Jinmei, I. Sugimoto, S.I. Sugawara, M. Fujita, K. Osumi, M. Mizuno, Derivatization with 1-pyrenyldiazomethane enhances ionization of glycopeptides but not peptides in matrix-assisted laser desorption/ionization mass spectrometry, Anal. Chem. (2010). https://doi.org/10.1021/ac101555a.

[59]   H.N. Behnken, A. Ruthenbeck, J.M. Schulz, B. Meyer, Glycan analysis of prostate specific antigen (PSA) directly from the intact glycoprotein by HR-ESI/TOF-MS, J. Proteome Res. (2014). https://doi.org/10.1021/pr400999y.

[60] A. Ács, O. Ozohanics, K. Vékey, L. Drahos, L. Turiák, Distinguishing core and antenna fucosylated glycopeptides based on low-energy tandem mass spectra, Anal. Chem. (2018). https://doi.org/10.1021/acs.analchem.8b03140.

[61] A. Toyama, H. Nakagawa, K. Matsuda, T.A. Sato, Y. Nakamura, K. Ueda, Quantitative structural characterization of local *N*-glycan microheterogeneity in therapeutic antibodies by energy-resolved oxonium ion monitoring, Anal. Chem. (2012). https://doi.org/10.1021/ac3023372.

[62] Y. Haga, M. Uemura, S. Baba, K. Inamura, K. Takeuchi, N. Nonomura, K. Ueda, Identification of multisialylated lacdiNAc structures as highly prostate cancer specific glycan signatures on PSA, Anal. Chem. (2019). https://doi.org/10.1021/acs.analchem.8b04829.

[63] R. Lang, A. Leinenbach, J. Karl, M. Swiatek-de Lange, U. Kobold, M. Vogeser, An endoglycosidase-assisted LC-MS/MS-based strategy for the analysis of site-specific core-fucosylation of low-concentrated glycoproteins in human serum using prostate-specific antigen (PSA) as example, Clin. Chim. Acta. (2018). https://doi.org/10.1016/j.cca.2018.01.040.

[64] R. Lang, V. Rolny, A. Leinenbach, J. Karl, M. Swiatek-de Lange, U. Kobold, M. Schrader, H. Krause, M. Mueller, M. Vogeser, Investigation on core-fucosylated prostate-specific antigen as a refined biomarker for differentiation of benign prostate hyperplasia and prostate cancer of different aggressiveness, Tumor Biol. (2019). https://doi.org/10.1177/1010428319827223.

[65] J. Zhou, W. Yang, Y. Hu, N. Höti, Y. Liu, P. Shah, S. Sun, D. Clark, S. Thomas, H. Zhang, Site-specific fucosylation analysis identifying glycoproteins associated with aggressive prostate cancer cell lines using tandem affinity enrichments of intact glycopeptides followed by mass spectrometry, Anal. Chem. (2017). https://doi.org/10.1021/acs.analchem.7b01493.

[66] Y. Li, Y. Tian, T. Rezai, A. Prakash, M.F. Lopez, D.W. Chan, H. Zhang, Simultaneous analysis of glycosylated and sialylated prostate-specific antigen revealing differential distribution of glycosylated prostate-specific antigen isoforms in prostate cancer tissues, Anal. Chem. (2011). https://doi.org/10.1021/ac102319g.

[67] A.Y. Liu, H. Zhang, C.M. Sorensen, D.L. Diamond, Analysis of prostate cancer by proteomics using tissue specimens, J. Urol. (2005). https://doi.org/10.1097/01.ju.0000146543.33543.a3.

[68] H. Zhang, X. jun Li, D.B. Martin, R. Aebersold, Identification and quantification of *N*-linked glycoproteins using hydrazide chemistry, stable isotope labeling and mass spectrometry, Nat. Biotechnol. (2003). https://doi.org/10.1038/nbt827.

[69] R. Kawahara, F. Ortega, L. Rosa-Fernandes, V. Guimarães, D. Quina, W. Nahas, V. Schwämmle, M. Srougi, K.R.M. Leite, M. Thaysen-Andersen, M.R. Larsen, G. Palmisano, Distinct urinary glycoprotein signatures in prostate cancer patients, Oncotarget. (2018). https://doi.org/10.18632/oncotarget.26005.

[70] C.J. Hsiao, T.S. Tzai, C.H. Chen, W.H. Yang, C.H. Chen, Analysis of Urinary Prostate-specific antigen glycoforms in samples of prostate cancer and benign prostate hyperplasia, dis. markers. (2016). https://doi.org/10.1155/2016/8915809.

[71] W. Morelle, J.C. Michalski, Analysis of protein glycosylation by mass spectrometry, Nat. Protoc. (2007). https://doi.org/10.1038/nprot.2007.227.

[72] I. Van Den Broek, F.P.H.T.M. Romijn, J. Nouta, A. Van Der Laarse, J.W. Drijfhout, N.P.M. Smit, Y.E.M. Van Der Burgt, C.M. Cobbaert, Automated multiplex LC-MS/MS assay for quantifying serum apolipoproteins A-I, B, C-I, C-II, C-III, and E with qualitative apolipoprotein E phenotyping, Clin. Chem. (2016). https://doi.org/10.1373/clinchem.2015.246702.

[73] G. Jia, Z. Dong, C. Sun, F. Wen, H. Wang, H. Guo, X. Gao, C. Xu, C. Yang, Y. Sun, Alterations in expressed prostate secretion-urine PSA *N*-glycosylation discriminate prostate cancer from benign prostate hyperplasia, Oncotarget. (2017). https://doi.org/10.18632/oncotarget.20299.

[74] K. Khatri, J.A. Klein, J.R. Haserick, D.R. Leon, C.E. Costello, M.E. McComb, J. Zaia, Microfluidic capillary electrophoresis-mass spectrometry for analysis of monosaccharides, oligosaccharides, and glycopeptides, Anal. Chem. (2017). https://doi.org/10.1021/acs.analchem.7b00875.

[75] X. Yang, M.G. Bartlett, Glycan analysis for protein therapeutics, J. Chromatogr. B Anal. Technol. Biomed. Life Sci. 1120 (2019) 29–40. https://doi.org/10.1016/j.jchromb.2019.04.031.

[76] B.C. Durney, C.L. Crihfield, L.A. Holland, Capillary electrophoresis applied to DNA: Determining and harnessing sequence and structure to advance bioanalyses (2009-2014), Anal. Bioanal. Chem. (2017). https://doi.org/10.1007/s00216-015-8703-5.

[77] P.G. Righetti, R. Sebastiano, A. Citterio, Capillary electrophoresis and isoelectric focusing in peptide and protein analysis, Proteomics. (2013). https://doi.org/10.1002/pmic.201200378.

[78] V. Mantovani, F. Galeotti, F. Maccari, N. Volpi, Recent advances in capillary electrophoresis separation of monosaccharides, oligosaccharides, and polysaccharides, Electrophoresis. (2018). https://doi.org/10.1002/elps.201700290.

[79] A. Guttman, F.T.A. Chen, R.A. Evangelista, N. Cooke, High-resolution capillary gel electrophoresis of reducing oligosaccharides labeled with 1 -aminopyrene-3,6,8-trisulfonate, Anal. Biochem. (1996). https://doi.org/10.1006/abio.1996.0034.

[80] T. Vermassen, C. Van Praet, D. Vanderschaeghe, T. Maenhout, N. Lumen, N. Callewaert, P. Hoebeke, S. Van Belle, S. Rottey, J. Delanghe, Capillary electrophoresis of urinary prostate glycoproteins assists in the diagnosis of prostate cancer, Electrophoresis. (2014). https://doi.org/10.1002/elps.201300332.

[81] G. Tabarés, C.M. Radcliffe, S. Barrabés, M. Ramírez, N. Aleixandre, W. Hoesel, R.A. Dwek, P.M. Rudd, R. Peracaula, R. de Llorens, Different glycan structures in prostate-specific antigen from prostate cancer sera in relation to seminal plasma PSA, Glycobiology. (2006). https://doi.org/10.1093/glycob/cwj042.

[82] Y. Mechref, M. V. Novotny, Glycomic analysis by capillary electrophoresis-mass spectrometry, Mass Spectrom. Rev. (2009). https://doi.org/10.1002/mas.20196.

[83] A. Stolz, K. Jooß, O. Höcker, J. Römer, J. Schlecht, C. Neusüß, Recent advances

in capillary electrophoresis-mass spectrometry: Instrumentation, methodology and applications, Electrophoresis. 40 (2019) 79–112. https://doi.org/10.1002/elps.201800331.

[84] F.P. Gomes, J.R. Yates, Recent trends of capillary electrophoresis-mass spectrometry in proteomics research, Mass Spectrom. Rev. 38 (2019) 445–460. https://doi.org/10.1002/mas.21599.

[85] M.R. Santos, C.K. Ratnayake, D.M. Horn, B.L. Karger, A.R. Ivanov, R. Viner, Separation and analysis of intact prostate specific antigen (PSA) and its proteoforms by CESI-MS under native and denaturing conditions, (2015) RUO-MKT-02-2331-A.

[86] G.S.M. Kammeijer, B.C. Jansen, I. Kohler, A.A.M. Heemskerk, O.A. Mayboroda, P.J. Hensbergen, J. Schappler, M. Wuhrer, Sialic acid linkage differentiation of glycopeptides using capillary electrophoresis - electrospray ionization - mass spectrometry, Sci. Rep. (2017). https://doi.org/10.1038/s41598-017-03838-y.

[87] G.S.M. Kammeijer, J. Nouta, J.J.M.C.H. De La Rosette, T.M. De Reijke, M. Wuhrer, An in-depth glycosylation assay for urinary prostate-specific antigen, Anal. Chem. (2018). https://doi.org/10.1021/acs.analchem.7b04281.

[88] Q. Zhang, Z. Li, Y. Wang, Q. Zheng, J. Li, Mass spectrometry for protein sialoglycosylation, Mass Spectrom. Rev. (2018). https://doi.org/10.1002/mas.21555.

[89] C.S. Ho, C.W.K. Lam, M.H.M. Chan, R.C.K. Cheung, L.K. Law, L.C.W. Lit, K.F. Ng, M.W.M. Suen, H.L. Tai, Electrospray ionisation mass spectrometry: principles and clinical applications., Clin. Biochem. Rev. (2003).

[90] N. Leymarie, P.J. Griffin, K. Jonscher, D. Kolarich, R. Orlando, M. McComb, J. Zaia, J. Aguilan, W.R. Alley, F. Altmann, L.E. Ball, L. Basumallick, C.R. Bazemore-Walker, H. Behnken, M.A. Blank, K.J. Brown, S.C. Bunz, C.W. Cairo, J.F. Cipollo, R. Daneshfar, H. Desaire, R.R. Drake, E.P. Go, R. Goldman, C. Gruber, A. Halim, Y. Hathout, P.J. Hensbergen, D.M. Horn, D. Hurum, W. Jabs, G. Larson, M. Ly, B.F. Mann, K. Marx, Y. Mechref, B. Meyer, U. Möginger, C. Neusüß, J. Nilsson, M. V. Novotny, J.O. Nyalwidhe, N.H. Packer, P. Pompach, B. Reiz, A. Resemann, J.S. Rohrer, A. Ruthenbeck, M. Sanda, J.M. Schulz, U. Schweiger-Hufnagel, C. Sihlbom, E. Song, G.O. Staples, D. Suckau, H. Tang, M. Thaysen-Andersen, R.I. Viner, Y. An, L. Valmu, Y. Wada, M. Watson, M. Windwarder, R. Whittal, M. Wuhrer, Y. Zhu, C. Zou, Interlaboratory study on differential analysis of protein glycosylation by mass spectrometry: The ABRF glycoprotein research multi-institutional study 2012, Mol. Cell. Proteomics. (2013). https://doi.org/10.1074/mcp.M113.030643.

[91] E. Song, A. Mayampurath, C.Y. Yu, H. Tang, Y. Mechref, Glycoproteomics: Identifying the glycosylation of prostate specific antigen at normal and high isoelectric points by LC-MS/MS, J. Proteome Res. (2014). https://doi.org/10.1021/pr500575r.

[92] C. Lee, C.K. Ni, Soft Matrix–Assisted Laser Desorption/Ionization for Labile Glycoconjugates, J. Am. Soc. Mass Spectrom. (2019). https://doi.org/10.1007/s13361-019-02208-4.

[93] M.L.A. De Leoz, H.J. An, S. Kronewitter, J. Kim, S. Beecroft, R. Vinall, S. Miyamoto, R. De Vere White, K.S. Lam, C. Lebrilla, Glycomic approach for potential biomarkers on prostate cancer: Profiling of *N*-linked glycans in human sera and pRNS cell lines, Dis. Markers. (2008). https://doi.org/10.1155/2008/515318.

[94] M. Tajiri, C. Ohyama, Y. Wada, Oligosaccharide profiles of the prostate specific antigen in free and complexed forms from the prostate cancer patient serum and in seminal plasma: A glycopeptide approach, Glycobiology. (2008). https://doi.org/10.1093/glycob/cwm117.

[95] T.W. Powers, B.A. Neely, Y. Shao, H. Tang, D.A. Troyer, A.S. Mehta, B.B. Haab, R.R. Drake, MALDI imaging mass spectrometry profiling of *N*-glycans in formalin-fixed paraffin embedded clinical tissue blocks and tissue microarrays, PLoS One. (2014). https://doi.org/10.1371/journal.pone.0106255.

[96] J. Hirabayashi, M. Yamada, A. Kuno, H. Tateno, Lectin microarrays: Concept, principle and applications, Chem. Soc. Rev. (2013). https://doi.org/10.1039/c3cs35419a.

[97] Š. Belický, J. Katrlík, J. Tkáč, Glycan and lectin biosensors, Essays Biochem. (2016). https://doi.org/10.1042/EBC20150005.

[98] J. Tkac, V. Gajdosova, S. Hroncekova, T. Bertok, M. Hires, E. Jane, L. Lorencova, P. Kasak, Prostate-specific antigen glycoprofiling as diagnostic and prognostic biomarker of prostate cancer, Interface Focus. (2019). https://doi.org/10.1098/rsfs.2018.0077.

[99] R.K. Scopes, Separation by precipitation, in: protein purif., Springer New York, New York, NY, 1987: pp. 41–71. https://doi.org/10.1007/978-1-4757-1957-4_3.

[100] C.M. Gabe, S.J. Brookes, J. Kirkham, Preparative SDS PAGE as an Alternative to His-Tag Purification of Recombinant Amelogenin, Front. Physiol. 8 (2017). https://doi.org/10.3389/fphys.2017.00424.

[101] C. Dennison, R. Lovrien, Three phase partitioning: concentration and purification of proteins, protein expr. purif. 11 (1997) 149–161. https://doi.org/10.1006/prep.1997.0779.

[102] W.-C. Lee, K.H. Lee, Applications of affinity chromatography in proteomics, Anal. Biochem. 324 (2004) 1–10. https://doi.org/10.1016/j.ab.2003.08.031.

[103] J.P.D. Goldring, Methods to concentrate proteins for protein isolation, Proteomic, and Peptidomic Evaluation, in: 2015: pp. 5–18. https://doi.org/10.1007/978-1-4939-2718-0_2.

[104] J. DeCaprio, T.O. Kohl, Immunoprecipation, Cold Spring Harb. Protoc. 2017 (2017) pdb.prot098640. https://doi.org/10.1101/pdb.prot098640.

[105] P. Yaciuk, Co-Immunoprecipitation of Protein Complexes, in: 2007: pp. 103–111. https://doi.org/10.1007/978-1-59745-277-9_8.

[106] P. Collas, The current state of chromatin immunoprecipitation, Mol. Biotechnol. 45 (2010) 87–100. https://doi.org/10.1007/s12033-009-9239-8.

[107] M.Q. Hassan, J.A.R. Gordon, J.B. Lian, A.J. van Wijnen, J.L. Stein, G.S. Stein,

Ribonucleoprotein immunoprecipitation (RNP-IP): A direct in vivo analysis of microRNA-targets, J. Cell. Biochem. 110 (2010) 817–822. https://doi.org/10.1002/jcb.22562.

[108] B. Kaboord, M. Perr, Isolation of proteins and protein complexes by immunoprecipitation, in: 2008: pp. 349–364. https://doi.org/10.1007/978-1-60327-064-9_27.

[109] J. Ghiso, M. Calero, E. Matsubara, S. Governale, J. Chuba, R. Beavis, T. Wisniewski, B. Frangione, Alzheimer's soluble amyloid β is a normal component of human urine, FEBS Lett. 408 (1997) 105–108. https://doi.org/10.1016/S0014-5793(97)00400-6.

[110] S.K. Vashist, J.H.T. Luong, Antibody immobilization and surface functionalization chemistries for immunodiagnostics, in: Handb. Immunoass. Technol. Approaches, Performances, Appl., Elsevier, 2018: pp. 19–46. https://doi.org/10.1016/B978-0-12-811762-0.00002-5.

[111] M. Arbabi-Ghahroudi, Camelid single-domain antibodies: Historical perspective and future outlook, Front. Immunol. 8 (2017) 1589. https://doi.org/10.3389/fimmu.2017.01589.

[112] S. Muyldermans, Applications of nanobodies, Annu. Rev. Anim. Biosci. 9 (2021) 401–421. https://doi.org/10.1146/annurev-animal-021419-083831.

[113] W. Liu, H. Song, Q. Chen, J. Yu, M. Xian, R. Nian, D. Feng, Recent advances in the selection and identification of antigen-specific nanobodies, Mol. Immunol. 96 (2018) 37–47. https://doi.org/10.1016/j.molimm.2018.02.012.

[114] J.-P. Salvador, L. Vilaplana, M.-P. Marco, Nanobody: outstanding features for diagnostic and therapeutic applications, Anal. Bioanal. Chem. 411 (2019) 1703–1713. https://doi.org/10.1007/s00216-019-01633-4.

[115] G.K. Ehrlich, W. Berthold, P. Bailon, Phage display technology: affinity selection by biopanning, in: affin. chromatogr., Humana Press, New Jersey, n.d.: pp. 195–208. https://doi.org/10.1385/1-59259-041-1:195.

[116] S. Muyldermans, Nanobodies: natural single-domain antibodies, Annu. Rev. Biochem. 82 (2013) 775–797. https://doi.org/10.1146/annurev-biochem-063011-092449.

[117] H. Cai, H. Yao, T. Li, C.A.J. Hutter, Y. Li, Y. Tang, M.A. Seeger, D. Li, An improved fluorescent tag and its nanobodies for membrane protein expression, stability assay, and purification, Commun. Biol. 3 (2020) 753. https://doi.org/10.1038/s42003-020-01478-z.

[118] R.A. O'Neill, Enzymatic release of oligosaccharides from glycoproteins for chromatographic and electrophoretic analysis, J. Chromatogr. A. 720 (1996) 201–215. https://doi.org/10.1016/0021-9673(95)00502-1.

[119] H. Zhou, A.C. Briscoe, J.W. Froehlich, R.S. Lee, PNGase F catalyzes de-*N*-glycosylation in a domestic microwave, Anal. Biochem. 427 (2012) 33–35. https://doi.org/10.1016/j.ab.2012.04.011.

[120] Z. Szabo, A. Guttman, B.L. Karger, Rapid release of n-linked glycans from glycoproteins by pressure-cycling technology, Anal. Chem. 82 (2010) 2588–2593.

https://doi.org/10.1021/ac100098e.

[121] J. Krenkova, A. Szekrenyes, Z. Keresztessy, F. Foret, A. Guttman, Oriented immobilization of peptide-*N*-glycosidase F on a monolithic support for glycosylation analysis, J. Chromatogr. A. 1322 (2013) 54–61. https://doi.org/10.1016/j.chroma.2013.10.087.

[122] M. Szigeti, J. Bondar, D. Gjerde, Z. Keresztessy, A. Szekrenyes, A. Guttman, Rapid *N*-glycan release from glycoproteins using immobilized PNGase F microcolumns, J. Chromatogr. B. 1032 (2016) 139–143. https://doi.org/10.1016/j.jchromb.2016.02.006.

[123] J. You, X. Sheng, C. Ding, Z. Sun, Y. Suo, H. Wang, Y. Li, Detection of carbohydrates using new labeling reagent 1-(2-naphthyl)-3-methyl-5-pyrazolone by capillary zone electrophoresis with absorbance (UV), Anal. Chim. Acta. 609 (2008) 66–75. https://doi.org/10.1016/j.aca.2007.12.022.

[124] Y. Shinohara, H. Sota, M. Gotoh, M. Hasebe, M. Tosu, J. Nakao, Y. Hasegawa, M. Shiga, Bifunctional labeling reagent for oligosaccharides to incorporate both chromophore and biotin groups, Anal. Chem. 68 (1996) 2573–2579. https://doi.org/10.1021/ac960004f.

[125] J.C. Bigge, T.P. Patel, J.A. Bruce, P.N. Goulding, S.M. Charles, R.B. Parekh, Nonselective and efficient fluorescent labeling of glycans using 2-amino benzamide and anthranilic acid, Anal. Biochem. (1995). https://doi.org/10.1006/abio.1995.1468.

[126] D.S. Dalpathado, H. Jiang, M.A. Kater, H. Desaire, Reductive amination of carbohydrates using NaBH(OAc)3, Anal. Bioanal. Chem. 381 (2005) 1130–1137. https://doi.org/10.1007/s00216-004-3028-9.

[127] D. Locke, C.G. Bevans, L.-X. Wang, Y. Zhang, A.L. Harris, Y.C. Lee, Neutral, acidic, and basic derivatives of anthranilamide that confer different formal charge to reducing oligosaccharides, Carbohydr. Res. 339 (2004) 221–231. https://doi.org/10.1016/j.carres.2003.10.020.

[128] L.R. Ruhaak, E. Steenvoorden, C.A.M. Koeleman, A.M. Deelder, M. Wuhrer, 2-Picoline-borane: A non-toxic reducing agent for oligosaccharide labeling by reductive amination, Proteomics. 10 (2010) 2330–2336. https://doi.org/10.1002/pmic.200900804.

[129] Z. Kovács, G. Papp, H. Horváth, F. Joó, A. Guttman, A novel carbohydrate labeling method utilizing transfer hydrogenation-mediated reductive amination, J. Pharm. Biomed. Anal. 142 (2017) 324–327. https://doi.org/10.1016/j.jpba.2017.05.017.

[130] L.R. Ruhaak, R. Hennig, C. Huhn, M. Borowiak, R.J.E.M. Dolhain, A.M. Deelder, E. Rapp, M. Wuhrer, Optimized workflow for preparation of APTS-Labeled *N*-glycans allowing high-throughput analysis of human plasma glycomes using 48-channel multiplexed CGE-LIF, J. Proteome Res. 9 (2010) 6655–6664. https://doi.org/10.1021/pr100802f.

[131] R.A. Evangelista, A. Guttman, F.-T.A. Chen, Acid-catalyzed reductive amination of aldoses with 8-aminopyrene-1,3,6-trisulfonate, Electrophoresis. 17 (1996) 347–351. https://doi.org/10.1002/elps.1150170210.

[132] F.-T.A. Chen, T.S. Dobashi, R.A. Evangelista, Quantitative analysis of sugar constituents of glycoproteins by capillary electrophoresis, Glycobiology. 8 (1998) 1045–1052. https://doi.org/10.1093/glycob/8.11.1045.

[133] C. Chiesa, C. Horváth, Capillary zone electrophoresis of malto-oligosaccharides derivatized with 8-aminonaphthalene-1,3,6-trisulfonic acid, J. Chromatogr. A. 645 (1993) 337–352. https://doi.org/10.1016/0021-9673(93)83394-8.

[134] L. Royle, M.P. Campbell, C.M. Radcliffe, D.M. White, D.J. Harvey, J.L. Abrahams, Y.-G. Kim, G.W. Henry, N.A. Shadick, M.E. Weinblatt, D.M. Lee, P.M. Rudd, R.A. Dwek, HPLC-based analysis of serum *N*-glycans on a 96-well plate platform with dedicated database software, Anal. Biochem. 376 (2008) 1–12. https://doi.org/10.1016/j.ab.2007.12.012.

[135] H. Suzuki, O. Müller, A. Guttman, B.L. Karger, Analysis of 1-aminopyrene-3,6,8-trisulfonate-derivatized oligosaccharides by capillary electrophoresis with matrix-assisted laser desorption/ionization time-of-flight mass spectrometry, Anal. Chem. 69 (1997) 4554–4559. https://doi.org/10.1021/ac970090z.

[136] F.-T.A. Chen, R.A. Evangelista, Profiling glycoprotein *N*-linked oligosaccharide by capillary electrophoresis, Electrophoresis. 19 (1998) 2639–2644. https://doi.org/10.1002/elps.1150191512.

[137] C. Váradi, C. Lew, A. Guttman, Rapid magnetic bead based sample preparation for automated and high throughput *N*-glycan analysis of therapeutic antibodies, Anal. Chem. 86 (2014) 5682–5687. https://doi.org/10.1021/ac501573g.

[138] M. Szigeti, C. Lew, K. Roby, A. Guttman, Fully automated sample preparation for ultrafast *N*-glycosylation analysis of antibody therapeutics, J. Lab. Autom. 21 (2016) 281–286. https://doi.org/10.1177/2211068215608767.

[139] D. Saerens, J. Kinne, E. Bosmans, U. Wernery, S. Muyldermans, K. Conrath, Single domain antibodies derived from dromedary lymph node and peripheral blood lymphocytes sensing conformational variants of prostate-specific antigen, J. Biol. Chem. (2004). https://doi.org/10.1074/jbc.M409292200.

[140] E. Gasteiger, C. Hoogland, A. Gattiker, S. Duvaud, M.R. Wilkins, R.D. Appel, A. Bairoch, Protein identification and analysis tools on the ExPASy server, in: Proteomics Protoc. Handb., 2005. https://doi.org/10.1385/1-59259-890-0:571.

[141] B. Mészáros, G. Járvás, A. Farkas, M. Szigeti, Z. Kovács, R. Kun, M. Szabó, E. Csánky, A. Guttman, Comparative analysis of the human serum *N*-glycome in lung cancer, COPD and their comorbidity using capillary electrophoresis, J. Chromatogr. B Anal. Technol. Biomed. Life Sci. (2020). https://doi.org/10.1016/j.jchromb.2019.121913.

[142] A. Orita, G. Uehara, K. Miwa, J. Otera, Rate acceleration of organic reaction by immediate solvent evaporation, Chem. Commun. (2006) 4729. https://doi.org/10.1039/b609567d.

[143] R. Sharma, A. Agarwal, G. Mohanty, R. Jesudasan, B. Gopalan, B. Willard, S.P. Yadav, E. Sabanegh, Functional proteomic analysis of seminal plasma proteins in men with various semen parameters, Reprod. Biol. Endocrinol. 2013 111. 11 (2013) 1–20. https://doi.org/10.1186/1477-7827-11-38.

[144] P.H. Bessette, F. Åslund, J. Beckwith, G. Georgiou, Efficient folding of proteins with multiple disulfide bonds in the Escherichia coli cytoplasm, Proc. Natl. Acad. Sci. U. S. A. (1999). https://doi.org/10.1073/pnas.96.24.13703.

[145] R. Levy, R. Weiss, G. Chen, B.L. Iverson, G. Georgiou, Production of correctly folded fab antibody fragment in the cytoplasm of Escherichia coli trxB gor mutants via the coexpression of molecular chaperones, Protein Expr. Purif. (2001). https://doi.org/10.1006/prep.2001.1520.

[146] T. Sakurai, A. Nakahara, Interaction of copper(II) and nickel(II) with L-histidine and glycylglycyl-L-histidine as an albumin model, Inorg. Chem. 19 (1980) 847–853. https://doi.org/10.1021/ic50206a012.

[147] Z. Rashid, H. Naeimi, A.-H. Zarnani, M. Nazari, M.-R. Nejadmoghaddam, R. Ghahremanzadeh, Fast and highly efficient purification of 6×histidine-tagged recombinant proteins by Ni-decorated MnFe 2 O 4 @SiO 2 @NH 2 @2AB as novel and efficient affinity adsorbent magnetic nanoparticles, RSC Adv. 6 (2016) 36840–36848. https://doi.org/10.1039/C5RA25949E.

[148] J. Rönnmark, H. Grönlund, M. Uhlén, P.-Å. Nygren, Human immunoglobulin A (IgA)-specific ligands from combinatorial engineering of protein A, Eur. J. Biochem. 269 (2002) 2647–2655. https://doi.org/10.1046/j.1432-1033.2002.02926.x.

[149] E. Gebri, Z. Kovács, B. Mészáros, F. Tóth, Á. Simon, H. Jankovics, F. Vonderviszt, A. Kiss, A. Guttman, T. Hortobágyi, N-glycosylation alteration of serum and salivary immunoglobulin a is a possible biomarker in oral mucositis, J. Clin. Med. 9 (2020) 1747. https://doi.org/10.3390/jcm9061747.

[150] J.T. Cassidy, G.L. Nordby, Human serum immunoglobulin concentrations: Prevalence of immunoglobulin deficiencies, J. Allergy Clin. Immunol. 55 (1975) 35–48. https://doi.org/10.1016/S0091-6749(75)80006-6.

[151] B.A. Baldo, E.R. Tovey, S.A. Ford, Comparison of different blocking agents and nitrocelluloses in the solid phase detection of proteins by labelled antisera and protein A, J. Biochem. Biophys. Methods. 12 (1986) 271–279. https://doi.org/10.1016/0165-022X(86)90063-1.

[152] G. Járvás, T. Varga, M. Szigeti, L. Hajba, P. Fürjes, I. Rajta, A. Guttman, Tilted pillar array fabrication by the combination of proton beam writing and soft lithography for microfluidic cell capture Part 2: Image sequence analysis based evaluation and biological application, Electrophoresis. 39 (2018) 534–539. https://doi.org/10.1002/elps.201700268.